

# Coastal Marine Institute

**University of Alaska**

## **Assessment of the Direction and Rate of Alongshore Transport of Sand and Gravel in the Prudhoe Bay Region, North Arctic Alaska**

A. Sathy Naidu  
Principal Investigator

John J. Kelley  
Orson P. Smith  
Co-Principal Investigators

Additional Researchers:  
Zygmunt Kowalik  
William J. Lee  
Martin C. Miller  
Thomas M. Ravens

Final Report  
OCS Study BOEMRE 2011-038

July 2011

**Bureau of Ocean Energy Management, Regulation and Enforcement  
Department of the Interior**

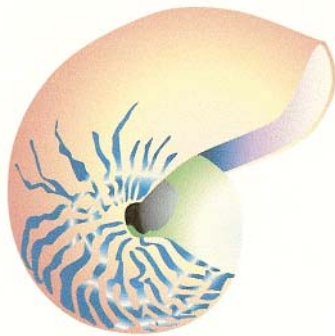
and the

**School of Fisheries & Ocean Sciences  
University of Alaska Fairbanks**

This study was funded in part by the U.S. Department of the Interior, Bureau of Ocean Energy Management, Regulation and Enforcement (BOEMRE) through Cooperative Agreement No. 1435-01-02-CA-85294, Task Order No. 39380 between BOEMRE, Alaska Outer Continental Shelf Region, and the University of Alaska Fairbanks.

This report, OCS Study BOEMRE 2011-038, is available from the Coastal Marine Institute (CMI), School of Fisheries and Ocean Sciences, University of Alaska, PO Box 757220, Fairbanks, AK 99775-7220. Electronic copies can be downloaded from the BOEMRE website at [www.alaska.boemre.gov/alaska/ref/akpubs.htm](http://www.alaska.boemre.gov/alaska/ref/akpubs.htm). Hard copies are available free of charge, as long as the supply lasts, from the above address. Requests may be placed with Ms. Sharice Walker, CMI, by phone (907) 474-7208, by fax (907) 474-7204, or by email at [skwalker@alaska.edu](mailto:skwalker@alaska.edu). Once the limited supply is gone, copies will be available from the National Technical Information Service, Springfield, Virginia 22161, or may be inspected at selected Federal Depository Libraries.

The views and conclusions contained in this document are those of the authors and should not be interpreted as representing the opinions or policies of the U.S. Government. Mention of trade names or commercial products does not constitute their endorsement by the U.S. Government.



# Coastal Marine Institute

University of Alaska

## **Assessment of the Direction and Rate of Alongshore Transport of Sand and Gravel in the Prudhoe Bay Region, North Arctic Alaska**

A. Sathy Naidu  
Principal Investigator

John J. Kelley  
Orson P. Smith  
Co-Principal Investigators

Additional Researchers:  
Zygmunt Kowalik  
William J. Lee  
Martin C. Miller  
Thomas M. Ravens

Final Report  
OCS Study BOEMRE 2011-038

July 2011

**Bureau of Ocean Energy Management, Regulation and Enforcement  
Department of the Interior**

and the

**School of Fisheries & Ocean Sciences  
University of Alaska Fairbanks**

**Contact information**

email: [skwalker@alaska.edu](mailto:skwalker@alaska.edu)

phone: 907.474.7208

fax: 907.474.7204

Coastal Marine Institute

School of Fisheries and Ocean Sciences

University of Alaska Fairbanks

P. O. Box 757220

Fairbanks, AK 99775-7220

## TABLE OF CONTENTS

<b>TABLE OF CONTENTS</b> .....	<b>2</b>
<b>LIST OF FIGURES</b> .....	<b>3</b>
<b>LIST OF PLATES</b> .....	<b>4</b>
<b>LIST OF TABLES</b> .....	<b>5</b>
<b>LIST OF APPENDICES</b> .....	<b>5</b>
<b>ABSTRACT</b> .....	<b>6</b>
<b>BACKGROUND/RELEVANCE TO FRAMEWORK ISSUES</b> .....	<b>7</b>
<b>OBJECTIVES/HYPOTHESIS</b> .....	<b>11</b>
<b>STUDY AREA/REGIONAL SETTING</b> .....	<b>12</b>
<b>METHODS</b> .....	<b>16</b>
Field Activities .....	16
Topographic surveys .....	16
GIS analysis of historical shorelines .....	18
Deployment of the Acoustic Doppler Current Profiler (ADCP) .....	19
Beach experiments to assess sediment transport .....	20
Storm-surge model development .....	26
<b>RESULTS</b> .....	<b>26</b>
Beach Profiles, and Historical Changes in Narwhal Island Geomorphology .....	26
Time-series changes on the wave climate and wind statistics .....	31
Time-interval surveys of alongshore movements of fluorescent-dyed sands and PIT-tagged gravel particles on Narwhal Island .....	33
Results of the storm-surge model .....	34
<b>DISCUSSION</b> .....	<b>34</b>
Dynamics of the Narwhal Island relief and morphology .....	34
Empirical and theoretical investigations on alongshore sand and gravel transport on Narwhal Island: challenges, scope and assessment .....	36
Storm surge model and potential sediment mass transport .....	37
Computation of the alongshore transport rate of sand on Narwhal Island .....	38
Selection of the Longshore Transport Model .....	37
Estimates of Sediment Transport at Narwhal Island, Summer 2007 .....	45
<b>CONCLUSIONS</b> .....	<b>54</b>
Presentations .....	55
Acknowledgements .....	55
<b>REFERENCES</b> .....	<b>56</b>

## LIST OF FIGURES

<b>Figure 1.</b> Study area, showing location of Narwhal Island and adjacent nearshore and mainland coast in north Arctic Alaska. ....	10
<b>Figure 2.</b> Blown up map of the study area showing the location of the Narwhal Island located northeast of Endicott Causeway, North Slope region of Arctic Alaska. ...	11
<b>Figure 3.</b> Locations of the transects for topographic surveys, and positions on the shoreline and berms where the dyed-sand and PIT-tagged gravel particles were injected. ....	17
<b>Figure 4.</b> Blown up of a prototype PIT tag encapsulated in glass. ....	22
<b>Figure 5.</b> A schematic illustrating the general principle of working of a typical PIT tag system. ....	22
<b>Figure 6.</b> Surface profiles from the Narwhal Island crest to seaward shoreline along eight transects, for summer 2006 and 2007. The dotted and solid lines depict the 2006 and 2007 profiles, respectively. ....	27
<b>Figure 7.</b> Historical changes in the morphology of Narwhal Island since 1955. ....	30
<b>Figure 8.</b> Results of the topographic surveys conducted in 2006 and 2007 showing short-term changes in the morphology of Narwhal Island with reference to the 1955 baseline. ....	31
<b>Figure 9.</b> Time-series of wave heights (cm) and wind speeds (m/s) in July-September, 2007, as recorded by the ADCP off Narwhal Island and at Deadhorse, respectively. ....	32
<b>Figure 10.</b> Significant wave heights determined each 2-hour interval during the ADCP deployment period from 24 July until 14 September 2007. ....	48
<b>Figure 11.</b> NOAA wind data recorded at Prudhoe Bay during the wave measurement interval of 24 July to 14 September 2007. ....	48
<b>Figure 12.</b> Comparison of measured wave height and breaking wave height during Storm 1. ....	49
<b>Figure 13.</b> NOAA-measured winds at Prudhoe Bay during the period of storm 1 (between dark vertical lines) from about 0900, 3 August to 1700, 7 August 2007 local time. ....	49
<b>Figure 14.</b> Comparison of measured wave height and breaking wave height during Storm 2. ....	50

<b>Figure 15.</b> NOAA-measured winds at Prudhoe Bay during the period of storm 2 (between dark vertical lines) from about 2000, 10 August to 0400, 14 August 2007 local time.....	<b>50</b>
<b>Figure 16.</b> Comparison of measured wave height and breaking wave height during Storm 3.....	<b>51</b>
<b>Figure 17.</b> NOAA-measured winds at Prudhoe Bay during the period of storm 3 (between dark vertical lines) from about 0900, 18 August to 1300, 22 August 2007 local time.....	<b>51</b>
<b>Figure 18.</b> Comparison of measured wave height and breaking wave height during Storm 4. The ADCP ceased recording on 14 September 2007.....	<b>52</b>
<b>Figure 19.</b> NOAA-measured winds at Prudhoe Bay during the period of storm 4 (between dark vertical lines) from about 0000, 13 September to 1000, 14 September 2007 local time.....	<b>52</b>
<b>Figure 20.</b> Estimated relative longshore transport rate for storms 1 – 3 plotted for each 2-hour interval of the storm. Note that each storm is of different duration.....	<b>53</b>
<b>Figure 21.</b> Estimated relative longshore transport rate for storms 4 plotted for each 2-hour interval of the storm. ....	<b>53</b>

## LIST OF PLATES

<b>Plate 1.</b> Typical landscape across Narwhal Island, and the mixed sand-gravel surficial deposits. ....	<b>13</b>
<b>Plate 2.</b> Typical relief and surficial deposits consisting of sand and gravel mixture found throughout the surface of the Narwhal Island.. ....	<b>13</b>
<b>Plate 3.</b> A gravel mound (up to ~3m high) found stranded at the seaward shoreline at late spring/early summer.....	<b>14</b>
<b>Plate 4.</b> An example illustrating the action of shorefast ice having pushed a pile of gravel into a mound at the seaward shoreline on Narwhal Island. ....	<b>14</b>
<b>Plate 5.</b> Scanning with the Reader for and locating PIT-tagged gravels on the seaward beach of Narwhal Island by Bill Streever of British Petroleum Co., and John Kelley and Mindy Krzykowsky of the University of Alaska Fairbanks. ....	<b>24</b>
<b>Plate 6.</b> Scanning the seaward beach for PIT-tagged gravel, adjacent to site 1A marker stake, using a rectangle grid sampling pattern.....	<b>25</b>

## LIST OF TABLES

<b>Table 1.</b> The coordinates for the locations of the baseline stations relating to the topographic surveys, and locations of beach (A-series) and berm (B-series) sites at which the dyed sand and PIT-tagged gravel particles were injected and the baseline stations. ....	<b>23</b>
<b>Table 2.</b> The time-interval distances (m) and annual rate (m/yr) of migration of the western tip of Narwhal Island. ....	<b>35</b>
<b>Table 3.</b> Total relative volume longshore transport during each of the storms for which waves were measured.....	<b>47</b>

## LIST OF APPENDICES

<b>Appendix 1.</b> Storm Surges and Sediment Transport Models in the Beaufort Sea by Zygmunt Kowalik.....	<b>60</b>
---	-----------

## ABSTRACT

Results are provided of a three-year (2005- 2008) study on the direction and rate of alongshore transport of coastal sediments at the mixed sand-gravel beach of Narwhal Island, a microtidal barrier located NE of Prudhoe Bay, North Arctic Alaska. Two approaches were followed addressing the study.

The first approach (empirical) used fluorescence-dyed sand and gravel tagged with 12mm long Passive Integrated Transponders (PIT) tags. On the seaward beach mid tide-level (MTL) two suites each of 13 kg of a sand mixture (6.5 kg of red or green fluorescent sand mixed with 6.5 kg of native raw sand) and 50 tagged gravel grains were point injected at two sites on 30 June, 2006 and at an additional two sites on 26 July, 2006. Fifteen tagged gravel particles were also placed at the base of the berms located adjacent to the beach sites and at the time coinciding with the injection of the beach tagged samples. A survey on the 26 July, 2006 indicated that 42% and 22% of the gravel injected in June at beach sites 1 and 2 respectively, were intercepted. These gravel particles had drifted east and west within 1m of the marker stakes. Of the 21 tagged gravels from site 1 three were intercepted at ~1 m subtidal zone. None of the tagged gravel particles were located on the beach in late August 2006. A survey on 25 July, 2007 of the beach located only one of the 200 tagged gravel particles originally injected. This gravel had drifted 29 m westward from the June 2006 point of injection. The fate of the rest of the tagged gravel particles is unknown. It is likely that during the 2006-2007 winter the tagged gravels were reworked by beach ice and emplaced under sand-gravel mounds at depths beyond the PIT reader's detection limit (~0.3m). The 2006 and 2007 surveys showed that the maximum displacements seaward on the beach of the tagged gravels from berm sites 1, 2, 3, and 4 were 6.6m, 2.46, 2.15m and 1.85m respectively. These relatively short displacements of the gravels were surprising considering that there was a few summer storm surges that extended up to the berm followed by backwash along the beach slope.

One month after injection most of the dyed sands were dispersed, presumably by high-tide and wave, into a beach-parallel, concentrated linear strand located 2.53m upbeach from MTL. At this time traces of the sand extended up to 10 m west and 2.6 m east of the injection point, while a minor portion was clumped in ~1 m subtidal zone. However, microscopic examination of the subsequent time-interval beach sand samples, collected east and west of the injected points, showed no dyed grains. It is likely that the dyed sands were either thoroughly diluted by untagged beach sands (reworked by ice) and/or lost to subtidal zone by backwash of storm surge, shorefast ice and melt water. Thus, in the Alaskan arctic the use of dyed sand has been unsuccessful for estimating alongshore sand transport.

The second approach (theoretical) consisted of measuring in June-September, 2007, the time-series of wave climate statistics at 10m depth of the ice-free zone north of Narwhal Island. This was achieved by a SonTek Acoustic Doppler Current Profiler (ADCP) and directional wave gauge moored in approximately 10m water depth and,

configured to make measurements at two-hour intervals. The purpose was to quantify the longshore wave energy flux (wave power). The volume rates ( $\text{m}^3$  per two-hour measurement interval) of potential longshore sand transport were computed based on the ADCP record, using of the SWAN wave propagation model, the CERC sand transport equations (Rosati et al., 2002) and wind data coinciding with the wave climate time-series. The total amount of material ( $\text{m}^3$ ) transported during each of the measured storms was 55.4, 81.2, 121.6 and 1191.6  $\text{m}^3$ , all of which were from east to west. The average transport rates for each storm were 0.52, 0.99, 1.24 and 33.1  $\text{m}^3/\text{hr}$  respectively. The ADCP failed during the final storm so the last rate reflects the average up until the instrument ceased recording.

Empirical studies in the Alaskan arctic beach indicate that use of PIT tags has a potential in assessing the direction and rate of alongshore transport of gravel only in summer. However, application of the marker for the rest of the year was frustrated by the inability to detect the tagged gravel particles that were buried under ice-pushed sand-gravel piles. Gravel transport in the Alaskan arctic beach can be three times more during ice-stressed months than during summer.

Studies of the time-intervals air photos, satellite images and historical maps of Narwhal Island and supplemental field surveys indicate occurrence since 1955 of several breaches in the island and regrouping of the islets. In the past 50 years, the western end of the island has migrated about 200 m to the west, which is consistent with the direction of the net annual sea-ice movement and easterly wind. Additionally, the island has retreated landward by  $\sim 5\text{m}/\text{year}$  during the past decade, which is consistent with the findings of others on North Slope barriers.

## **BACKGROUND/RELEVANCE TO FRAMEWORK ISSUES**

Understanding the fundamental principles that govern threshold of sediment movement, and processes of transport and deposition of particulates in fluids have been a major topic of research among geologists and engineers in attempting to address the relationship between coastal hydro- and sediment dynamics, particularly the processes prevailing on the shorelines (Komar, 1998; Komar and Inman, 1970; Middleton and Southard, 1978; Voropayev et al., 2001, 2003; da Silva et al., 2006; Kobayashi et al., 2007). The above basic research has numerous practical applications, for example, in the designing and maintaining of coastal engineering structures, predicting the fate of dredge and petroleum-related drill spoils and pollutants discharged into the nearshore, environmental problems relating to coastal erosion, beach nourishment, mining of placer minerals, and alteration in the natural mass balance of coastal sediments and coastal geomorphology resulting from some of the above anthropogenic activities, among many others.

Since the discovery of oil in 1968 in the Prudhoe Bay region, the coastal and nearshore regions of the North Slope have been subjected to increasing industrialization from activities relating to the exploration and exploitation of petroleum reserves. The

initial focus of activities was onshore, but more recently the direction has shifted to the offshore. Coastal and offshore industrial infrastructure (e.g., docks, causeways, offshore producing and drilling platforms, submerged marine pipelines) has been built, in support of the oil-related activities and sea floor dredging and offshore mining of gravel and sand fill material have been some of the additional geoenvironmental activities. These activities will continue to grow with the expansion of the current oil prospects and development of new tracts.

In North Arctic Alaska the possible cause-effect relationship between the industrial infrastructures and the natural nearshore sediment- and hydro-dynamic processes (wave, current and sea ice regimes, and storm surges), coastal geomorphology, barrier island stability, shoreline erosion, and littoral sediment drift are little known. The engineering structures built on the shoreline are bound to alter, to various extents, the natural regimes of wave-current-sea ice and sediment budget in the vicinity of the structures. For example, site-specific perturbations in the coastal circulation patterns and hydrography (salinity and temperature) have occurred subsequent to the construction of the West Dock Causeway, NE of Prudhoe Bay and near the Endicott Causeway east of the Bay (Envirosphere Company, 1987; Hale et al., 1989). Some of these alterations are likely to impact the nearshore bathymetry and mass balance of sediments and sedimentary processes, such as enhancement down-current in the coastal erosion and depositional rates, the direction and volume of littoral sediment drift, and shift in the transport trajectories of suspended sediment plumes (Barnes et al., 1977; Barnes and Minkler, 1982; Naidu et al., 1984; Hale et al., 1989). These perturbations, in turn, could have practical consequences to the industry, such as a destructive impact on existing (or future) man-made infrastructures such as those reported widely for shorelines of the world (Shepard, 1973). For example, submerged pipelines in the North Slope region can be overburdened with sediment blanket, navigational channels - especially in between the barrier islands and/or docks - can be shoaled by enhanced sediment accumulation (Hale et al., 1989), and coastal engineering structures (causeways, docks, offshore drilling platforms, breakwater, groins) down current can be severely disrupted by the modified wave-current action. The nearshore region of North Arctic Alaska is a highly dynamic environment, with continuous changes in the coastal geomorphology marked, for example, by large-scale (6-28 m/yr) migration rates of barrier islands and spits (Wiseman et al., 1973; Barnes and Reimnitz, 1974; Dygas and Burrell, 1976a; Miller and Gadd, 1983; Ravens et al., 2007) and drastic shifts in longshore sediment drift, especially during cataclysmic storms (Hume and Schalk, 1967). With the predicted global climate warming and attendant sea level rise and increased open water fetch resulting from sea ice retreat (IPCC, 2001) some of the above concerns can be exacerbated.

Some site-specific baseline information is available on wind-tide-wave-current and sediment movement along the coast and littoral zone of North arctic Alaska (Matthews, 1970; Wiseman et al., 1973; Short et al., 1974; Dygas and Burrell, 1976a and 1976b; Nummedal, 1979; Owens et al., 1980; Barnes and Reimnitz, 1982; Miller and Gadd, 1983; Naidu et al., 1984; Kozo, 1984; Envirosphere Co, 1987; Hale et al., 1987 and references therein). Results of the seabed drifter experiments and OCSEAP projects having possible bearing in the understanding of sediment transport, are synthesized in

Barnes and Reimnitz (1982) and Barnes et al. (1984), respectively. However, these sediment investigations, which were focused in the Point Barrow, Pingok and Flaxman Island regions, were conducted far away from the Colville Delta-Prudhoe Bay area where the petroleum-related activities are now concentrated in the North Slope.

In addition, all the estimates to-date on alongshore sediment drift in the North Slope are either based solely on theoretical deductions from wind-wave-current statistics (Dygas and Burrell, 1976a and 1976b; Nummedal, 1979) or study of historical charts and aerial photos ((Wiseman et al., 1973; Barnes and Reimnitz, 1974; Miller and Gadd, 1983; Ravens et al., 2007). These assessments, however, have not been verified by actual field measurements (empirical) of the alongshore drift using, for example, tracers such as dyed-sand and tagged-gravel. Additionally, it is likely that the outcome of some of the site-specific studies referred to above cannot be extrapolated across the entire North Slope shoreline such as the region east of the Colville Delta (including sites adjacent to Prudhoe Bay) where the environmental settings locally are different and, thus, are of limited use (Naidu, 1975; Jorgenson and Brown, 2003). A point illustrating this concern is the results of the studies conducted along the Point Barrow Spit (Nummedal, 1979), where the net west to east current-wave direction is opposite to that generally prevailing east of the Colville Delta-Prudhoe Bay region. Although studies of time-series maps and air photos of the North Slope have the potential to furnish valuable information on the net changes in the 2-dimensional geometry of shorelines and barriers and transport direction of alongshore sediment drifts, they cannot *per se* provide a quantitative estimate of the rate of motion.

Some may suggest that results of the investigations conducted at temperate beaches and numerical models of alongshore sediment transport developed there are applicable to the North Slope. The processes at lower latitudes especially pertaining to sandy beaches are relatively well understood. However, the models of beach processes and calculation of littoral sediment drift developed for the temperate latitudes are of limited practical use at northern high-latitude where the permafrost-dominated environment is strikingly different. In the Alaskan arctic, for example, unique regional factors govern coastal sediment and hydro-dynamics. Some of the salient features of the region are the coastal erosion rates among the highest in the world, 1-10m yr<sup>-1</sup> (Naidu et al., 1984; Reimnitz and Kempema, 1987), beaches generally comprised of very poorly-sorted mixture of sand and gravel and the beaches are subjected to highly oblique wave angles during the open water (three months ice-free) season, and for 8-9 months in a year ice action is pervasive both above and below the still water level. Therefore, in order to help scaling and calibration of numerical sediment transport models for the arctic shoreline it is essential that a comprehensive, integrated database on alongshore sediment transport be established there on a region-specific basis. Such basic information and fundamental understanding will be invaluable in the planning and selection of local sites and designing of coastal and offshore engineering infrastructure by the industry and will also help in effective management of the coastal region by the regulating governing agencies.

This report synthesizes the results of our investigations conducted during June 2006-September 2007, to assess the direction and potential rate of alongshore transport of sand and gravel along Narwhal Island, Prudhoe Bay region (Figs. 1 and 2). To meet this goal two approaches were followed. The first consisted of experiments conducted on the seaward beach of the island using two sediment tracers (fluorescent dyed-sand and gravel tagged with tiny (12 mm long) Passive Integrated Transponder (PIT). The second approach included theoretical computation of the direction and rate of volume transport of sand during open water season, based on the time-series climates of wave (to assess the energy flux or wave power) and contemporaneous time-series on wind (speed and direction). The study site is the Narwhal Island, a microtidal sand-gravel barrier island located NE of the Endicott Causeway and Prudhoe Bay adjacent to the Liberty Prospect on the North Slope of Alaska (Figs.1 and 2).

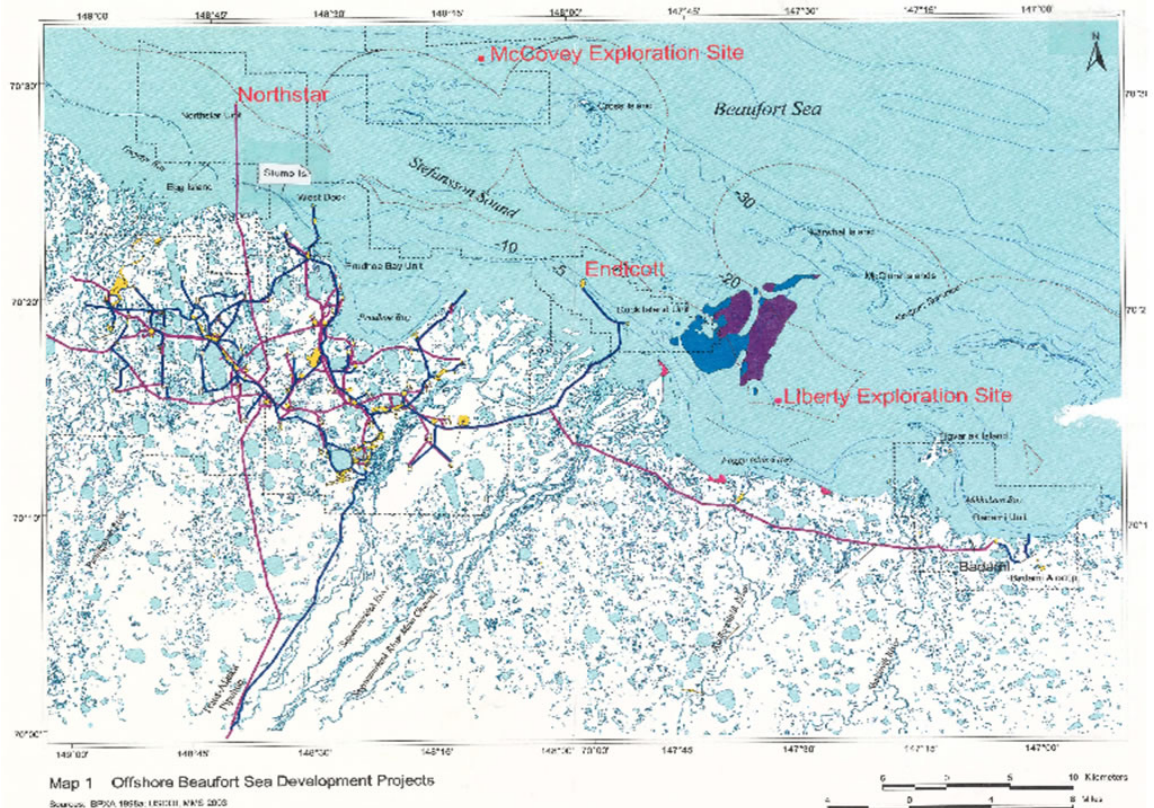


**Figure 1. Study area, showing location of Narwhal Island and adjacent nearshore and mainland coast in north Arctic Alaska.**

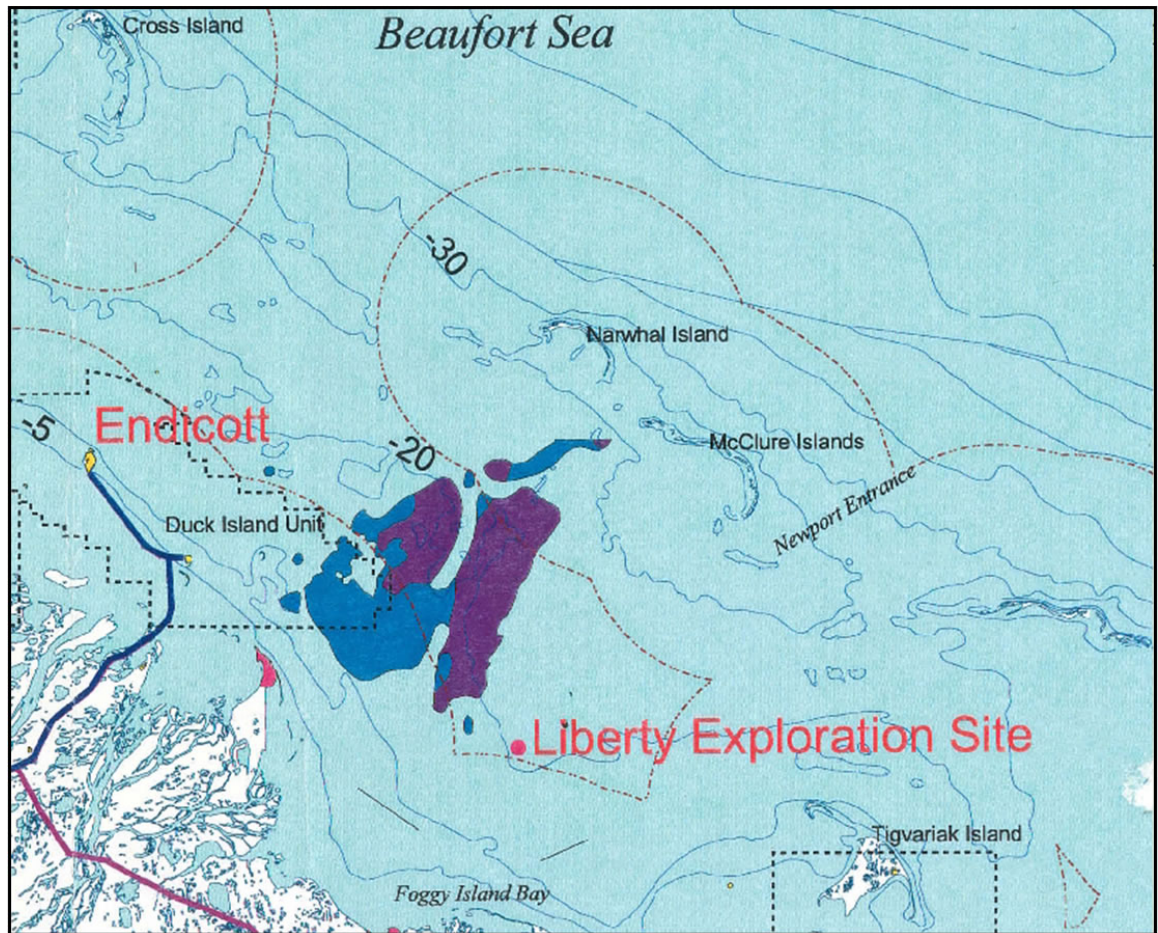


**Figure 2. Blown up map of the study area showing the location of the Narwhal Island located northeast of Endicott Causeway, North Slope region of Arctic Alaska.**

This project was conducted by a partnership of a multidisciplinary group, including investigators from the University of Alaska Fairbanks and Anchorage (UAF and UAA), the Pacific Northwest National (PNNL), Marine Sciences Laboratory (MSL) – Sequim, WA), and Coastal and Ocean Concept, LLC (Sequim, WA), with field logistics support provided by the British Petroleum Exploration (Alaska).

## **OBJECTIVES/HYPOTHESIS**

The overall objectives of the project were as follows:

1. To conduct a comprehensive survey of the literature and develop an annotated bibliography and listing of more recent investigations on alongshore sediment transport, with special reference to the north Alaskan Arctic coast.
2. To survey the beach during two summer time-intervals to record the beach relief.

3. Record the real time statistics of the wind (velocity and direction) and wave (height, direction of propagation using a ADCP moored system) in open water condition (summer) for the Narwhal Island region.
4. To determine the seasonal direction and volume of the transport of sand and gravel for a barrier island beach at the study site (Narwhal Island), applying two approaches: empirical [using fluorescent-dyed sands and Passive Integrated Transponder (PIT) tagged gravel particles] and theoretical computations (based on time-series climates of wave and wind and associated alongshore current), and
5. To reconfigure and downscale the existing wide-scale Beaufort Sea storm surge model, for application to the boundary conditions of the above nearshore, to generate basic database that would be useful to predict the impact of episodic storms on sediment drift.

The underlying hypothesis is that on Narwhal Island -- a mixed sand-gravel barrier in the North Slope region of Arctic Alaska -- the annual alongshore transport of sand and gravel particles is measurable, both by empirical and theoretical approaches, and that the barrier has a stable geomorphology.

## **STUDY AREA/REGIONAL SETTING**

The study area consists of Narwhal Island and the contiguous nearshore north of the island (Figs. 1 and 2). The arcuate barrier island is situated northeast of Prudhoe Bay and the Endicott Causeway in the Alaskan Beaufort Sea nearshore, and constitutes the western-most barrier of the McClure Island chain that is elongated roughly southeast-northwest to the mainland coast (Fig. 1 and 2). It is to be noted that all the islands located offshore of the North Slope of Alaska are not barrier islands in the true sense. The term barrier island, as per the accepted geological nomenclature (Schwartz, 1972), is restricted to islands that are resultant of recent or ongoing sediment accretion by littoral longshore currents. This definition, therefore, excludes, for example those offshore islands which are either rocky outcrops, subaerially exposed paleomoraines (such as in southeast Alaska) or islands which are literally cutoff remnants of a coastal plain (e.g., Pingok, Flaxman, Bodfish Islands off the North Alaskan arctic coast, Naidu et al., 1984). In the above context, the Narwhal Island is a true barrier island.

Wiseman et al., (1973), Naidu and Mowatt, (1975), Naidu et al. (1984), and Barnes et al. (1984) have enumerated the highlights of the nearshore environment that are generally representative for the Narwhal Island region and vicinity, including the seasonal processes characterizing the geological, hydrographic and ice regimes. The specifics for the Narwhal Island follow. The highest elevation of the island is about 4.2m above mean sea level (MSL). The crest of the island descends sharply to the narrow (~15-25m wide) beach with a well-defined berm in between at ~3.4m above MSL (Plate 1).

The Narwhal Island sediments are composed of a mixture of poorly-sorted sand and gravel/shingles (up to cobble size, ellipsoidal to discoidal shape Plates 2, 3 and 4), and of varied lithology including sedimentary, igneous and metamorphic rocks.



**Plate 1. Typical landscape across Narwhal Island, and the mixed sand-gravel surficial deposits.**



**Plate 2. Typical relief and surficial deposits consisting of sand and gravel mixture found throughout the surface of the Narwhal Island. Note the sand-gravel mounds at the shoreline and adjacent to remnants of shorefast ice at late spring/early summer. The gravel mounds were piled by shorefast ice push in winter.**



**Plate 3. A gravel mound (up to ~3m high) found stranded at the seaward shoreline at late spring/early summer. The mound was apparently pushed up the beach by shorefast ice in winter. Note the black glove on the mound top for scale.**



**Plate 4. An example illustrating the action of shorefast ice having pushed a pile of gravel into a mound at the seaward shoreline on Narwhal Island. Apparently, sand originally admixed with the gravel 'filters' down through the gravel pile with melt water action, leaving a mound of gravel lag.**

Presumably the gravel of Narwhal Island and other barriers of the North Slope have a mixed source, most of them derived from the local hinterland and a few from provenances as far as the Canadian Shield region due south of the Coronation Gulf in north Canada (Naidu and Mowatt, 1994). However, the mode and emplacement of the gravel deposits on the mainland beaches and barrier islands of the North Slope region, including Narwhal Island, is not well understood. Their concentrations at the shoreline remains an enigma, considering that for 8-9 months in a year the North Slope coastal region is covered with ice and thus not exposed to extended hydraulic sorting of sediment by wave-current. With the exception during occasional storm events, the barrier and nearshore vicinity is a relatively low-energy environment for rest of the year, characterized by low wave and tidal actions. The following explanation is suggested for the evolution of the gravel concentration on Narwhal Island and adjacent barriers and beaches. The permafrost-dominated tundra coastal plain of the North Slope has intercalation of gravels which probably are Pleistocene glacial marginal outwash and fluvial deposits. It is possible that thermo-erosion of these deposits and their subsequent hydraulic sorting result in lag gravel at the beach, nearshore and river bed. Presumably, the subsequent transport, emplacement and concentration of the lag gravel on the barrier islands is a cumulative result of actions by longshore currents, storm waves and ice. It is conceivable that some of the offshore gravel deposits were originally coarse lags left in place from paleoshorelines and which are currently being reworked by waves, currents and ice to emerge as barriers from submerged bars.

With a few patchy exceptions Narwhal Island is free of vegetation. The profiles of the surface relief recorded in summer 2006 and 2007 along eight transects extending from the island crest to seaward beach (Fig. 3), are displayed in Figure 3 (refer to the results section). The profiles have been smoothed by excluding minor variations in the relief. The entire Narwhal Island, like the rest of the North Slope barriers is exposed to ice action during the 8-9 months winter, but sediment reworking by shorefast ice is more pervasive along the lower beach. The reworking is marked by mass movement of material by ice gouging and bulldozing and subsequent piling of sediment into mounds up to one meter high (Plates 2, 3 and 4). The resulting micro-relief on the Narwhal Island beach is very similar to the ice-related features described as typical for arctic beaches (Greene, 1970). The tidal range for the Alaskan Beaufort Sea nearshore including the study area is typically low (~16cm, Matthews, 1970) and, therefore, the region is classified as a microtidal environment. However, the Narwhal Island crest can occasionally be subjected to overflow by storm surge, such as that observed during the September 2007 field season. During the cataclysmic storm events large-scale transport of sediments can occur across and along the beaches, similar to that described at Point Barrow shoreline (Hume and Schalk, 1967). The Narwhal Island is a dynamic environment inasmuch as the morphology of the island has been continually changing, which is marked by a net westward and landward migration and occasionally splitting into several fragments and then regrouping (refer below for further discussion on the subject).

Prior to the field study, two preliminary tasks were addressed. The first task was to collect and review recent literature related to arctic coastal sediment transport and

depositional processes with special reference to north Alaska, review of the tracer technologies as related to sediment alongshore transport, and papers on hydrodynamics of the study area. Papers available in the open literature and which existed in pdf format were favored. The survey product consists of 107 documents in the bibliography, 101 pdf files, and a short list of useful relevant web sites.

The second task consisted of all the project participants going through the tests conducted at the Alaska West Training Center and specified by the North Slope Training Center (NSTC) to satisfy the safety, emergency, security and badge requirements mandated by the British Petroleum (BP) for the field participants at their operational facilities in the North Slope.

## **METHODS**

### ***Field Activities***

Field activities were delineated into four major tasks: determination of the surface profiles of the Narwhal Island, deployment and retrieval of the Acoustic Doppler Current Profiler (ADCP) for recording the time-series of wave conditions, conducting beach experiments to assess the direction and rate of sediment transport, and surveying the island in order to understand the temporal changes in the island's geomorphology. Each of these tasks is enumerated in the following.

### ***Topographic surveys***

The goal of the topographic surveys conducted in 2006 and 2007 was to monitor the short-term changes (summer to winter cycle) in the island's relief. The profiles of the surface relief of Narwhal Island were determined along eight transects extending from the island crest to the seaward beach (Fig. 3). Relating to this task there were two trips made during 2006 to Narwhal Island. The first trip was on July 24 to 26, 2006, and the second trip was on September 22 to 26, 2006. Likewise, during 2007 two additional trips were made to the island, from 23 to 27 July 2007 and 11 to 15 September 2007. The July 2006 profiles were measured by means of a Wild differential level and Philadelphia rod. Elevations were measured from base line stations placed on the approximate beach crest and referenced to an arbitrary bench mark with an elevation of 100m (MSL). The July 2007 survey was used to reference the 2006 data to elevations derived from the July 2007 static GPS survey and the Geoid 06 model in Trimble's Geomatics Office, (Trimble Navigation Ltd. 2001). The July 2007 profiles were prepped by automated interpolation of the topographic surface generated by ESRI's Geostatistical Analyst using a global polynomial interpolation, (Environmental Systems Research Inc. 2007). The 2007 profiles were interpolated at approximately 0.5m intervals. The 2006 profiles were measured on the beach at irregular intervals of approximately 10 meters beginning at the benchmark and extending in the offshore direction. Because of the sparseness of the 2006 data it was necessary to spline the data to produce an estimate of the complete beach profile. The profiles were splined by either a cubic (e.g., Bezier), or composite Bezier

spline in Mathematica, (Wolfram, 2007) The spline that best matched the original data based on simple inspection was selected for the profile.

The consolidation of the survey data was accomplished as follows. The initial field survey was completed in an assumed coordinate system. The data was transferred to Trimble Geomatics Office, (TGO) and adjusted (Trimble Navigation Ltd. 2001). The adjusted coordinates were then exported to a text file. The surveyed GPS locations were used as control coordinates to complete a least squares adjusted four parameter transformation that referenced the survey to Universal Transverse Mercator Zone 6, (UTM Z6), coordinates in the World Geodetic Reference System of 1984, (WGS84). Elevations were derived by applying the geoid separation from the National Geodetic Survey geoid model of 2006, (Geoid06) to the GPS ellipsoid heights. An average of the differences between the GPS elevations and the assumed coordinate system elevations was used to correct the assumed coordinate system elevations to elevations referenced to Geoid06.

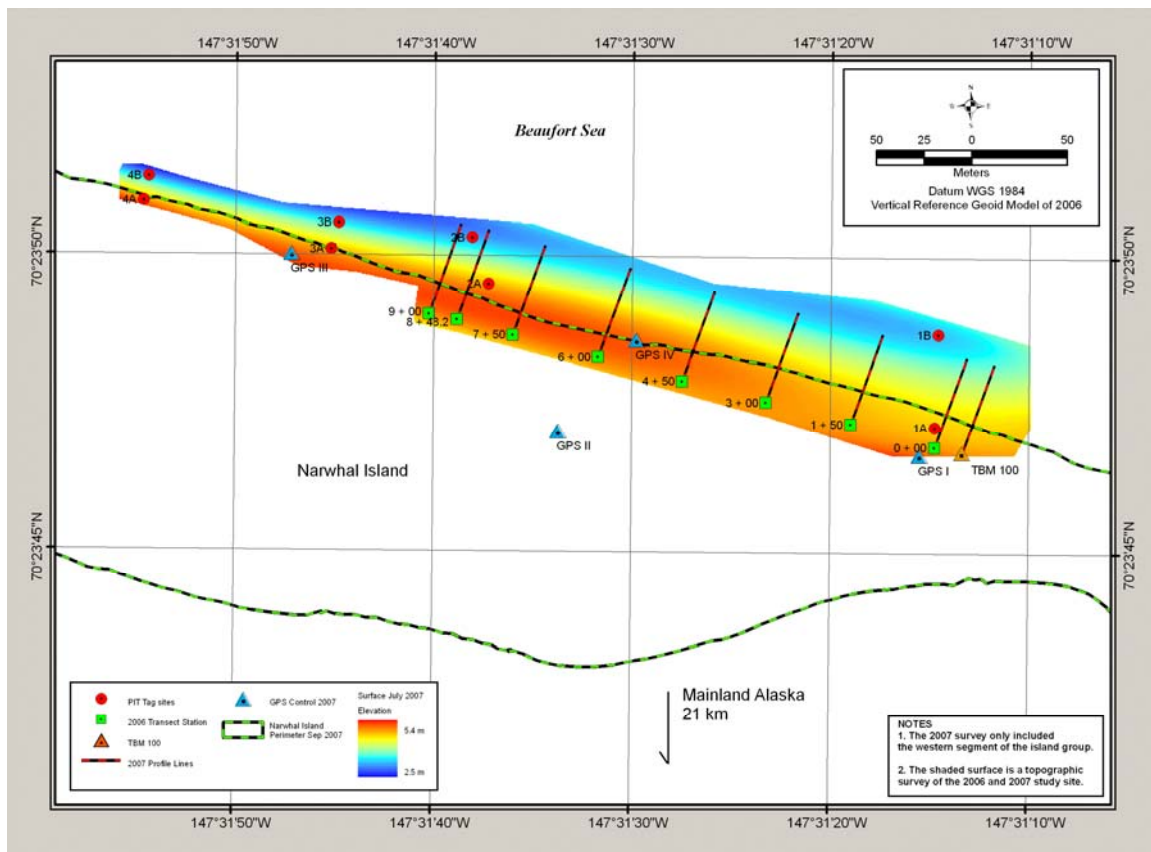


**Figure 3. Locations of the transects for topographic surveys, and positions on the shoreline and berms where the dyed-sand and PIT-tagged gravel particles were injected.**

The static survey data from the GPS units was transferred to TGO, (Trimble Navigation Ltd. 2001). Additional GPS data from three NGS continuously operating reference stations (CORS) were obtained from the National Geodetic Survey (2007). The three stations were located on the mainland at East Dock, (EDOC), the Prudhoe Bay Operations Center, (PBOC) and Drill Site L1, (DSL1). The average horizontal precision

at one standard deviation ( $1 \sigma$ ) for the static GPS positions was 0.006 m and 0.007 m for the northing and easting respectively. The average vertical precision for the static GPS positions was 0.128 m.

The transformed topographic survey data were transferred to ArcMap, (Environmental Systems Research Inc., 2007) and used to interpolate an elevation surface of the beach. Cross shore and along shore profiles of the beach were then interpolated from the generated beach elevation surface. The cross shore profiles were referenced to the stations used for the July 2006 survey. An additional six profiles to the west of station 9+00 were also added. The along shore profiles were parallel to the base line used for the July 2006 profile stations. One was placed along the base line and two successive profiles were placed at 25 and 50 meters seaward.

### ***GIS analysis of historical shorelines***

An analysis of the historical location of the Narwhal Island shore line was done using the United States Geological Survey (USGS) 15 minute topographic maps, (United States Army Map Service, 1955) and the National Oceanographic and Atmospheric Administration (NOAA), (National Oceanographic Service, 1990), nautical chart. This data was combined with the September 2007 perimeter survey done as part of the current study. The purpose of this was to quantify the changes in shape and extent of migration that the island has experienced over approximately four decades.

The Narwhal Island coast line was digitized from the USGS 15 minute topographic map Beechey Point B-1, (United States Army Map Service, 1955). The digitized shape file was then transformed to UTM Zone 6 WGS 84 coordinate system and datum, (Environmental Systems Research Inc., 2007). The Narwhal Island coastline was similarly digitized from the McClure and Stockton Islands and Vicinity nautical chart, (National Oceanographic Service, 1990; Environmental Systems Research Inc., 2007). The DGPS survey completed in September 2007 was then added to this historical data. This survey was done using a Trimble GeoExplorer III GPS. The data was post processed differentially corrected using Trimble's Path Finder Office, (Trimble Navigation Ltd., 2005). The shape files representing each of the time referenced coast lines were assembled in a single GIS. The extents of the Island's westward movement for different time-intervals was then estimated by on screen graphical measurement.

It is to be noted that during most of the three field days, 12-14 September, 2007 the weather was stormy, with up to 25 knot wind accompanied by high waves (average height of the breakers was 1.5-2 m), resulting in inundation of the four beach sites well into the surf zone and waves washing over the island ridge in several locations and almost completely obliterating the berm's sharp slope. There was significant wave run up with several locations of complete over wash of the island. The east side of the island was a smooth gentle sloping beach all the way around the tip to the south side. On this end of the island the largest waves would break and wash over to the south. On the west end of the island there were a few well defined wash over areas. There was one that crossed in the western third of the July 2007 topographic survey area. These waves would break and

wash over the crest of the island and drain into the pond. The pond in turn overflowed and drained to the south side of the island. At the western tip there was a continuous flowing breach which was approximately 20 m wide and 20 cm deep at the thalweg. In July 2007 there was a well formed vertical embankment approximately 1 meter high and oriented along shore. It extended along the western two thirds of the topographic survey area. It was noted during the 13 September, 2007 visit to the island that this feature was almost completely obliterated with the minor exception of severely eroded remnants in the western portion of the topographic survey area.

In addition, on 25 July, 2007 a survey of the northwest portion of the Narwhal Island beach was conducted. This survey included a topographic survey and placement of four survey control monuments. The topographic survey data was collected using a Trimble 5600 DR robotic total station. The GPS control was established by means of a static survey with Trimble LS 4200, and Trimble 5700 survey grade receivers. There were two LS 4200 GPS receivers and two Trimble 5700 GPS receivers. One of the Trimble 5700 GPS receivers was fitted with a Zephyr<sup>tm</sup> RTK antenna and the other had a Geodetic Zephyr<sup>tm</sup> antenna. Antenna heights were measured from the hook to the aluminum cap using the Trimble measuring tape provided for the LS 4200 GPS receivers. The antenna heights for the Zephyr<sup>tm</sup> antennas were measured from the notch using the Trimble measuring rod for these antennas. A single measurement was made for the RTK Zephyr antenna and the perimeter notch measurements were averaged for the Geodetic Zephyr antenna. All GPS receivers and the total station were provided by Trimble Navigation Ltd. Monuments constructed of 5/8" x 30" rebar and fitted with aluminum caps were driven flush at the locations of each GPS occupation. The cap was stamped with a Roman numeral signifying the occupation site number. Similar monuments were also set at the instrument and back site location. The monument caps at the instrument site and back sight were stamped "IN", and "BS" respectively.

### ***Deployment of the Acoustic Doppler Current Profiler (ADCP)***

Two approaches were used to determine the direction and rate of alongshore sediment transport. The first consisted of recording the time-series wave conditions and currents for the nearshore region north of Narwhal Island. The goal was to assess from the wave climate the theoretical wave energy flux (wave power), direction of wave propagation and associated alongshore currents, and from this database to compute the potential rate of alongshore transport of the volume of sand, using relatively simple sand transport equations (Rosati et al., 2002). The above wave measurements were made by a University of Alaska Anchorage SonTek 1.5 MHz ADCP, that was placed in a gimbal mount in a Barnacle<sup>tm</sup> (Ocean Science Inc.), trawl resistant mooring that was deployed on the sea floor. The ADCP was programmed to collect three dimensional current data and 2 dimensional wave spectra at two-hour intervals. Currents were recorded for the first two minutes followed by 17 minute of pressure measurements used to determine the wave conditions. Sampling frequency was set to 2 Hz. The unit hibernates between 2-hour duty cycles.

The first deployment of the ADCP on the sea floor was on 25 July, 2006 in 7.9 m water depth north of the Narwhal Island at 70° 24.0'N and 147° 28.4'W. The system was retrieved in September, 2006. Unfortunately, no data was recorded during the above period, because of instrument malfunction. The system was redeployed on 24 July, 2007 in 10 m of water, approximately 1.5 km north of the seaward beach study site on Narwhal Island. The location of the ADCP was at 70° 24' 33" N and 147° 31' 34" W. In the afternoon of 14 September, 2007 the instrument was retrieved with data recorded intact up to the morning of 14 September, 2007. The ADCP and wind data were downloaded and processed by the UAA team to get the wave and wind time-series. The resulting information was forwarded to Dr. M. C. Miller for calculating the rate of alongshore sediment transport volume. On both occasions the instrument was deployed from the Alaska Clean Seas (ACS) tender under contract to the British Petroleum Company (BP).

The potential volume rate ( $\text{m}^3/\text{hr}$ ) and direction of longshore sand transport were computed using the SWAN wave propagation model and the CERC sand transport equations (Rosati et al, 2002). The SWAN model is an advanced wave model developed by the Delft Institute of Technology specifically for nearshore applications. The model accounts for wave generation due to wind action, exchange of wave energy between different wave frequencies, wave shoaling, diffraction, and breaking. The model has been validated in the field (Ris *et al.*, 1999), and is currently in use in over 50 countries including extensive use in the United States (Work *et al.*, 2004; Li *et al.*, 2005). The SWAN model, when run in the quasi steady mode, calculates significant wave height and period at various locations in the Beaufort Sea as a function of bathymetry and as a function of wind speed and direction.

During a visit on the afternoon of 13 September 2007 to Narwhal Island a ADCP burst (sampling event) # 613 was recorded. This visit took place during a storm event when several observations were made. The dominant wind was from 070° magnetic. (099° True). It was estimated to be 8 to 12 knots. The observed waves were propagating from the east. The wave heights were estimated at 1.5 to 2 m. The period was ~5 seconds, and the wave length was approximately 20 m. The waves were breaking about 50 m offshore. The breaking azimuth was 273° magnetic (302° True). The interior angle formed by the shore line and the wave break was 15°.

To determine the correlation between wind and wave climate statistics, time-series data on the speed and direction of wind was obtained for the duration of time which coincided with the period of the Barnacle/ADCP deployment. The wind data was obtained from the NOAA's online database which was recorded at Deadhorse in Prudhoe Bay region, which was the nearest meteorological station for the study site.

### ***Beach experiments to assess sediment transport***

The empirical approach used to determine the direction and rate of alongshore transport of sand and gravel sized particles was based on the experiments conducted on Narwhal Island seaward beach using the fluorescent-dyed sand and the PIT tagged

gravel. Ingle (1966) has reviewed the types of tracers and instruments that have been used to assess alongshore transport of sand size particles. Likewise, Allen et al. (2006) have referred to the literature on the use of different techniques to estimate the transport of gravel-size clastics along beaches. The use of the Passive Integrated Transponder (PIT) tag technique is a relatively innovative approach inasmuch as it has not been applied *per se* to the study of beach gravel movement, except for a study in Oregon relating to cobble size gravel (Allan, et al., 2006). However, PIT tags have been used for tracking the movement in streams of coarse gravel (Lamarre et al., 2005; Gallagher, 2005, personal communication). The technique has been widely used, though, for monitoring movement and migration of fish, birds, mammals, reptiles and benthic organisms and to identify pets (e.g., Roussel et al., 2000; BIOMark web site (<http://biomark.com/reference.html>)). We believe that our beach experiment is the first application of the 12mm-long PIT tag to assess longshore gravel transport on a beach and the first application of the PIT tag technique in the Arctic.

Relating to our experiments, five 5-gallon buckets of a mixture of gravel and sand samples, native to the Narwhal Island, were collected in late October 2005. The purpose of procuring the samples specifically from the island was to ensure that the experiments conducted using the tracer particles would mimic as closely as possible the natural transport mode and hydrodynamics of the particles concerned (in context of particle size, shape and density). Following this collection, preliminary experiments were conducted jointly by Drs. Naidu, Kelley and Miller on the beach adjacent of the PNNL, MSL facility in Sequim, WA, to adapt a field procedure for the use of the PIT tags. For the Narwhal Island study 400 gravel particles (16-20 mm long) from the above sample suite were taken and individually drilled to make ~14 mm long holes to accommodate the 12mm tags. The tags were implanted into each of the gravel particles and the holes sealed with Epoxy. The particles were then coated with red fluorescent paint to facilitate their visual identification in the field.

The gravel particles were grouped into four suites, each consisting of 50 individuals, and bagged. Prior to the departure to the field the ID number, discrete tag code for each of the gravel particles in the individual suite, were identified (using the Biomark Destron Model FS2001 Reader). The Biomark® reader transmits a radio frequency (RF) signals at 134.2 kHz, which are intercepted one at a time by the antenna in the glass encapsulated tag (Fig. 4). The PIT tag relays its corresponding RFID number back via RF of 12.5 kHz to the reader where it is displayed digitally on a window screen (Fig. 5). In our case, experiments conducted through wet sand indicated the maximum distance of detection of the PIT tag by the reader was about 0.3 m. Additional details on the general principles governing the operation of the PIT tags are described in Allen et al. (2006).

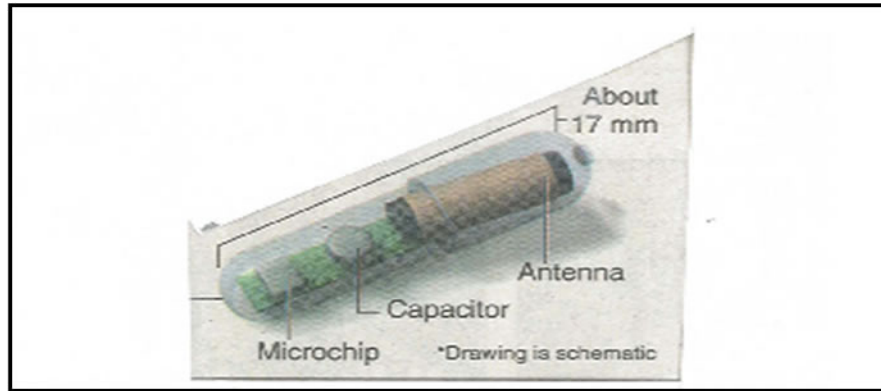


Figure 4. Blown up of a prototype PIT tag encapsulated in glass.

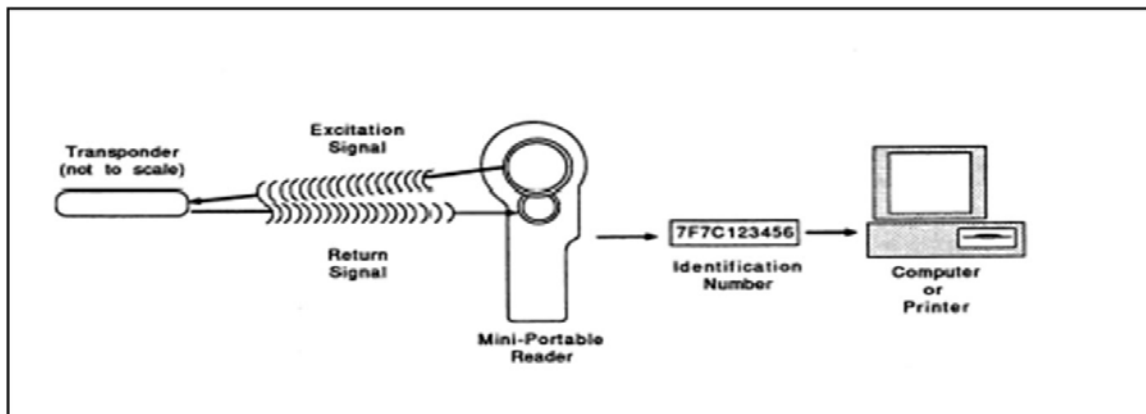


Figure 5. A schematic illustrating the general principle of working of a typical PIT tag system.

Four suites, each of 6.5 Kg, of sand samples collected from Narwhal Island were coated with a green or red fluorescent dye. Each suite of tagged gravel and dyed sand (mixed with equal proportion of raw native sand from the island resulting in total 13 kg) was point injected on the surface of four seaward beach sites (~100-150m apart) at mid-tide level (MTL) waterline. It is to be noted that the mean tidal range in the island region is ~16cm (Matthews, 1970). One set of the tagged sand and gravel was placed on 30 June, 2006 each at beach sites 1A and 2A and another two sets on 26 July, 2006 at beach sites 3A and 4A (Fig. 2). Coinciding with the above injections 15 tagged gravel particles were also discharged at the foot of the seaward berm on the Narwhal Island and located directly landward of each of the four waterline staked sites mentioned above. The purpose was to determine the impact of occasional storm surge on transport of gravel from the upper beach. The timing of injection of the tagged gravel particles at the individual berm sites coincided with that at the adjacent beach. The condition on 30 June, 2006 was about 9/10 floating ice cover and considerable ice override on the lower seaward beach. Photographs were taken to record beach ice conditions. The coordinates of the berm sites (1A, 2A, 3A and 4A) and beach sites (1B, 2B, 3B and 4B), which were established on 30 June, 2006 with a GPS and marked by steel rebar stakes driven into the beach, are indicated below in Table 1 and shown in Figure 3.

**Table 1. The coordinates for the locations of the baseline stations relating to the topographic surveys, and locations of beach (A-series) and berm (B-series) sites at which the dyed sand and PIT-tagged gravel particles were injected and the baseline stations.**

Description	Latitude	Longitude
Baseline Stations		
0 + 00	N 70° 23' 46.8"	W 147° 31' 14.7"
1 + 50	N 70° 23' 47.2"	W 147° 31' 18.9"
3 + 00	N 70° 23' 47.5"	W 147° 31' 23.2"
4 + 50	N 70° 23' 47.9"	W 147° 31' 27.4"
6 + 00	N 70° 23' 48.3"	W 147° 31' 31.6"
7 + 50	N70° 23' 48.3"	W 147° 31' 31.6"
8 + 48.2	N 70° 23' 48.9"	W 147° 31' 38.8"
9 + 00	N 70° 23' 49.0"	W 147° 31' 40.2"
PIT Tag Sites		
1A	N 70° 23' 47.1"	W 147° 31' 14.7"
1B	N 70° 23' 48.7"	W 147° 31' 14.5"
2A	N 70° 23' 49.5"	W 147° 31' 37.2"
2B	N 70° 23' 50.3"	W 147° 31' 38.0"
3A	N 70° 23' 50.1"	W 147° 31' 45.1"
3B	N 70° 23' 50.5"	W 147° 31' 44.7"
4A	N 70° 23' 50.9"	W 147° 31' 54.6"
4B	N 70° 23' 51.3"	W 147° 31' 54.3"

As an adjunct to the Narwhal Island study, experiments have also been conducted at the Sag Delta-1 site on the mainland coast (70° 20.467'N and 148° 06.362'W) to determine the direction and rate of gravel and sand movements at the site. The site is an abandoned oil drilling gravel pad which is currently in the process of being restored by the British Petroleum (BP) Exploration, Inc. to its pristine (tundra) state. On June 30, 2006 twenty-six PIT-tagged gravel particles and a sand mixture consisting of 6.5 Kg of fluorescence dyed sand and 6.5 kg of native raw sand (Total 13 kg) were placed on the surface at each of two locations about 10m east of the pad. The dyed sand was placed at the waterline in a circle of ~20 cm diameter around a rebar marker stake. The tagged gravel particles were lined up in arrays along two side by side rows of parallel transects (set 60 cm apart) laid across the beach from each marker. The gravel particles were laid on the surface at 30-cm intervals along each transect, which ran from the waterline to the berm foot. The ID number of each of the PIT-tagged gravel was recorded prior to its discharge. Subsequently, the site was surveyed on 26 July, 2007 and found little changes in the positions of the tagged gravel and the dyed sands.

On July 26, 2006 surveys were conducted around beach sites 1A and 2A, to determine the locations of the tagged gravel particles and dyed sands that were injected at the sites about a month previous (30 June, 2006). This survey was also extended to the subtidal zone up to ~1 m water depth in the vicinity of the 1A site, where a few PIT-tagged gravel particles were found. The identification of these submerged particles was made possible because the water was clear and the particles were identified with little difficulty as aided by the red dye on them. The identification of the individual red PIT-tagged gravel particles on the beach was by visual means and scanning the beach with the hand-held PIT tag reader (Plate 5). The survey was conducted at successively 1 X 1 meter grids, using a plastic frame that was moved across and along the beach starting from the original point of discharge of the tagged gravel (Plate 6).



**Plate 5. Scanning with the Reader for and locating PIT-tagged gravels on the seaward beach of Narwhal Island by Bill Streever of British Petroleum Exploration, Inc., and John Kelley and Mindy Krzykowski of the University of Alaska Fairbanks. Note the clump of red dyed-sand submerged in subtidal water and adjacent to the marker stake.**



**Plate 6. Scanning the seaward beach for PIT-tagged gravel, adjacent to site 1A marker stake, using a rectangle grid sampling pattern . Note the band of concentrated streak of red fluorescent-dyed sand along the beach stranded at the high-tide mark. The streak was elongated mostly to the west of the stake.**

The RFID code number of the tagged gravel detected was recorded and its location obtained. The location of the gravel was determined by measuring the distance by a tape and direction (using a Brunton compass) of its position relative to the beach stake. Thus, a map was generated for the beach limiting to the area around which tagged gravel particle were encountered. The surveys were also conducted at beach sites 1A, 2A, 3A and 4A (Fig. 2) on 15 August, and 13 October, 2006, and in the subsequent year around the four sites on 25 July, and 13 September, 2007. These surveys included visual observations and use of the PIT tag Reader. The Sag Delta-1 site on the mainland coast was also surveyed during the above periods.

Coinciding with the time-interval surveys to locate, identify and determine the positions of PIT-tagged gravel particles, the extent and distribution pattern of the dyed sands were also ascertained for the beach around the four marker stakes. The latter effort involved observations under a hand-held lens of random representative sand samples collected from the beach surface at 5-m intervals along two transects (3m apart) that ran parallel to the beach length and above the MTL. The individual beach sand samples thus collected around beach site 1A on 25 July, 2006 were bagged in labeled Whirlpack and shipped to the Fairbanks Laboratory for further observation under a binocular microscope. This examination was conducted in dark under exposure to ultraviolet light radiation which facilitates the detection of fluorescent-dyed sand.

## ***Storm-surge model development***

An effort was made toward understanding the potential impact of episodic storm events on hydrodynamics and alongshore sediment transport in the study area. In this context, a set of 2-D coupled ice-ocean models was developed for the Arctic Ocean, Canada Basin and the McClure Islands area with different spatial and temporal resolutions. The effort involved reconfiguration and downscaling of the existing wide-scale Beaufort Sea storm surge models (Kowalik, 1984; Proshutinsky, 1993), for application to the boundary conditions of the above nearshore and to investigate the impact of episodic storms on sediment drift. The models were calibrated and validated based on the data from coastal stations and taking into consideration relation between the observed and simulated sea levels.

Two major factors, potentially important for sediment transport were considered for analysis: permanent barotropic currents due to sea level gradient between the Pacific and Atlantic Ocean, and wind-driven circulation due to storm surges. The roles of the permanent currents and wind-driven circulations (counterclockwise and clockwise island-trapped patterns characterizing different regimes of sea level change around the McClure Islands) were investigated in details. A simple sediment transport semi-empirical model was applied as the first order approach to study the peculiarities of sediment motion around McClure Islands. A text enumerating details on the model development is submitted as Appendix 1.

## **RESULTS**

### ***Beach Profiles, and Historical Changes in Narwhal Island Geomorphology***

In Figure 6 are illustrated the beach profiles of summer 2006 and 2007 along eight transects extending from the Narwhal Island crest to the seaward shoreline (Fig. 3). The eastern most profile is at stations 0+00, and the western most profile is at station 9+00 (see Fig. 3). The profiles were generated from the measurements made during field surveys, and the minor undulations in the surface relief have been smoothed. The 2006 and 2007 profiles along each transect are represented by dotted and solid lines, respectively.

Comparison of the 2006 and 2007 profiles shows that the island is increasing in elevation toward the crest in the westward direction. This trend is more pronounced in the 2007 profiles than in the 2006 profiles. The profiles also show a slight increase in elevation toward the crest from 2006 to 2007. The increase in elevation appears to cease at a point approximately 30m seaward of the baseline. The 2007 profiles exhibit a remarkably stable elevation at 30m distance along the transect. The base line stations remained constant in elevation as well. Beyond 30m seaward the beach profile appears to be moving to lower elevation. This is particularly evident in the 2007 profiles. The results of the GIS analysis of historical changes in shorelines are displayed in Figures 7 and 8.

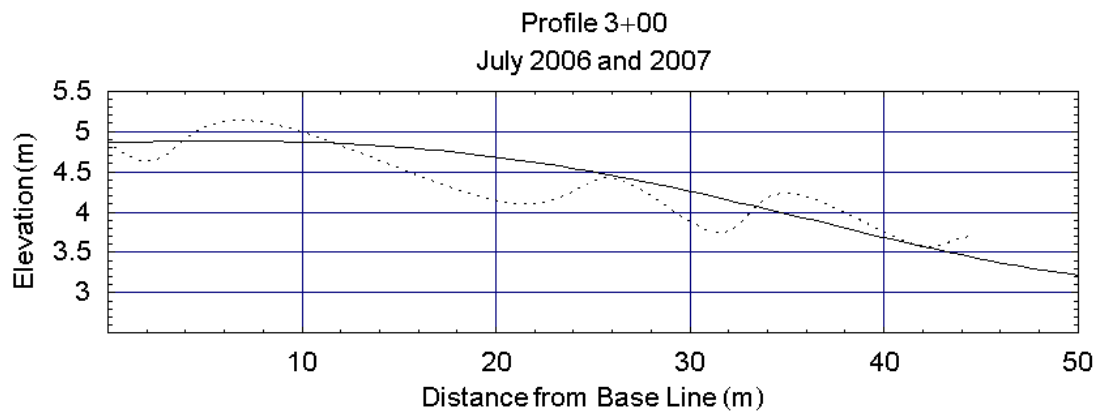
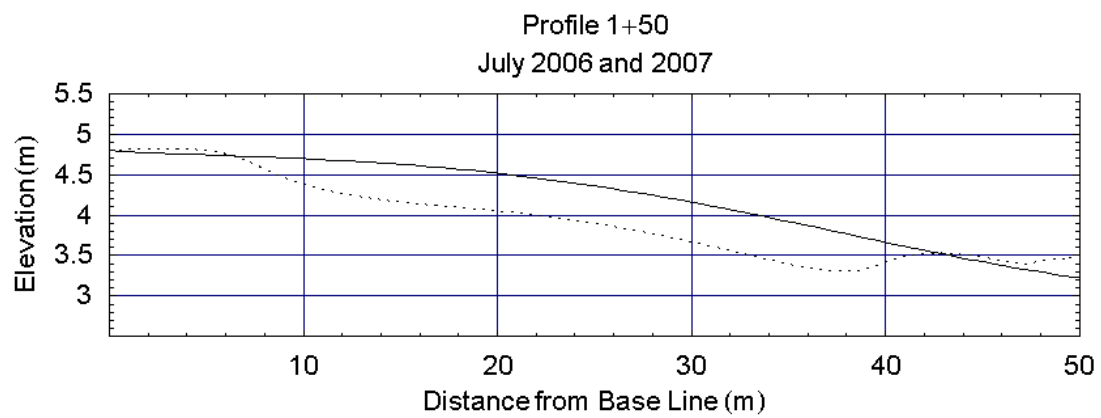
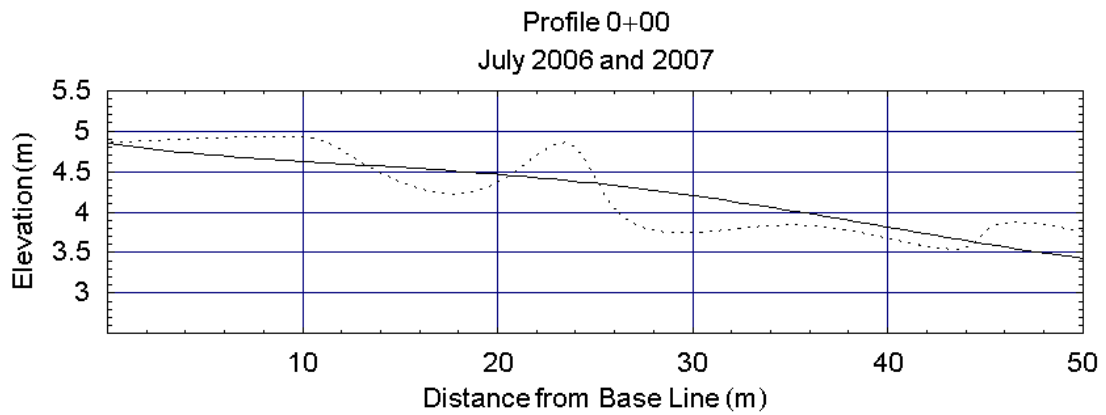


**Figure 6. Surface profiles from the Narwhal Island crest to seaward shoreline along eight transects, for summer 2006 and 2007. The dotted and solid lines depict the 2006 and 2007 profiles, respectively.**

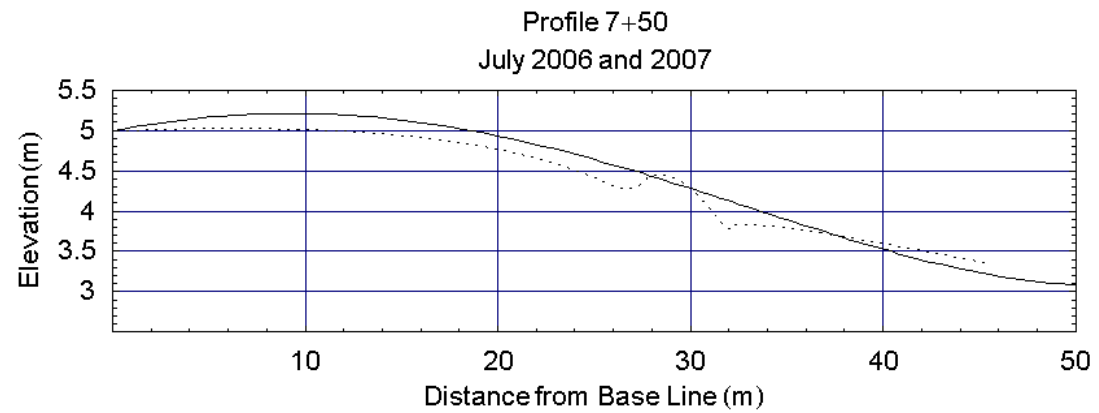
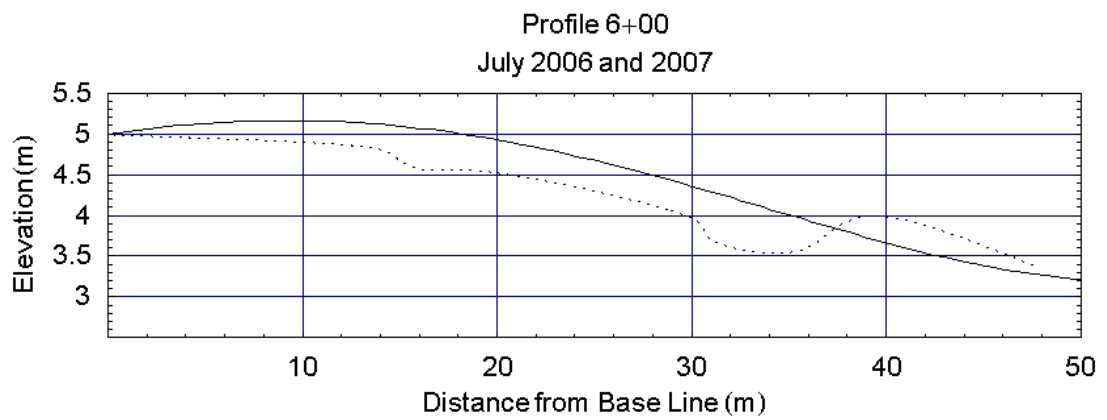
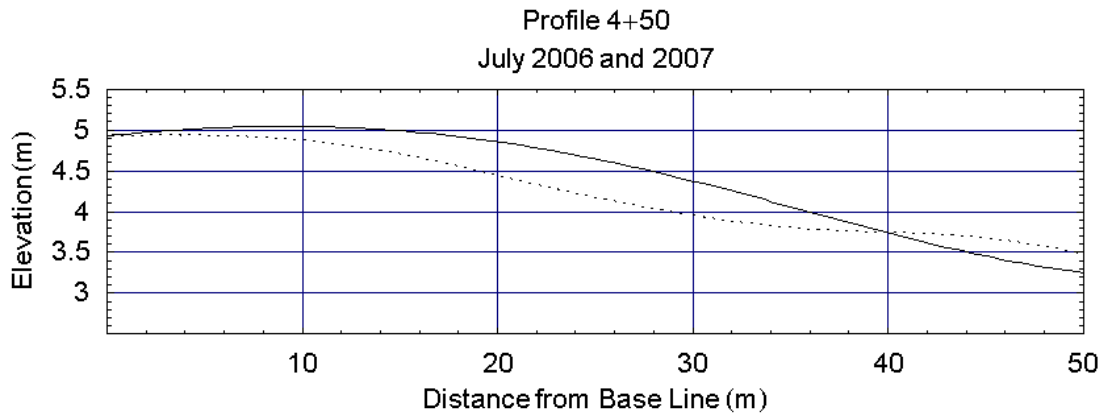


**Figure 6 (continued). Surface profiles from the Narwhal Island crest to seaward shoreline along eight transects, for summer 2006 and 2007. The dotted and solid lines depict the 2006 and 2007 profiles, respectively.**

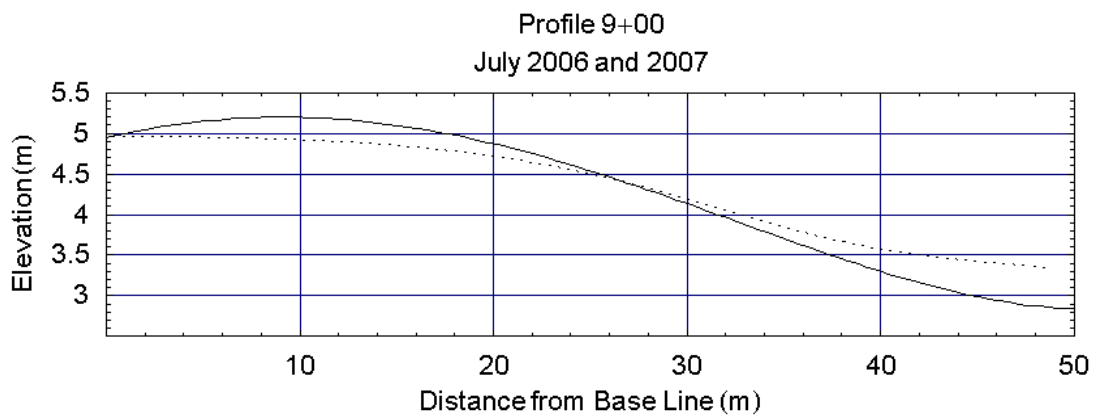
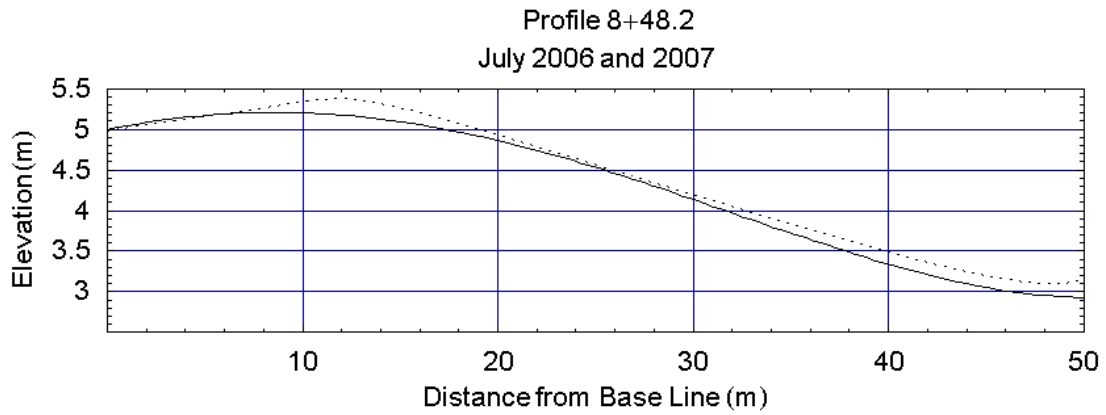


**Figure 6 (continued).** Surface profiles from the Narwhal Island crest to seaward shoreline along eight transects, for summer 2006 and 2007. The dotted and solid lines depict the 2006 and 2007 profiles, respectively.

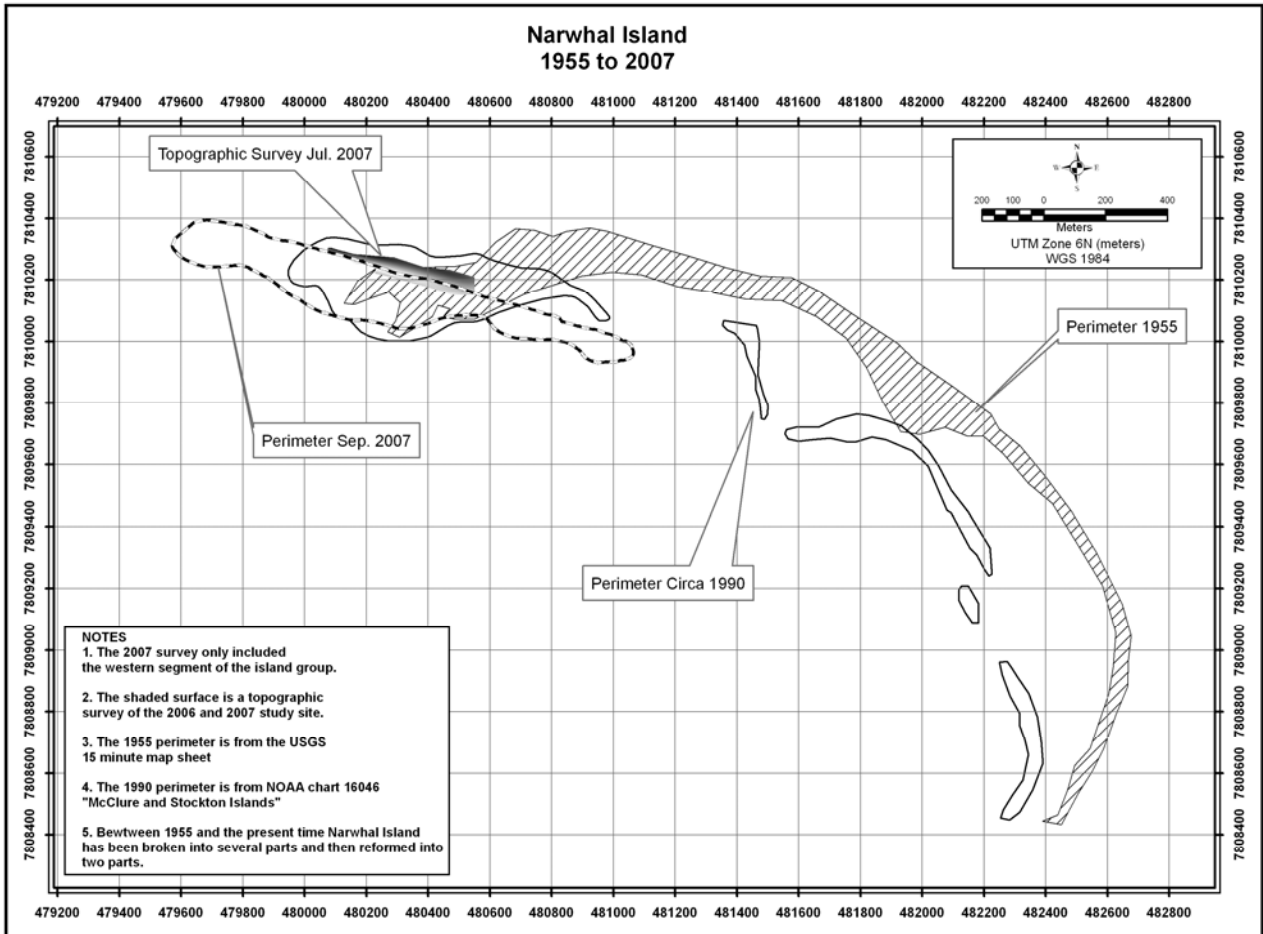


**Figure 7. Historical changes in the morphology of Narwhal Island since 1955.**

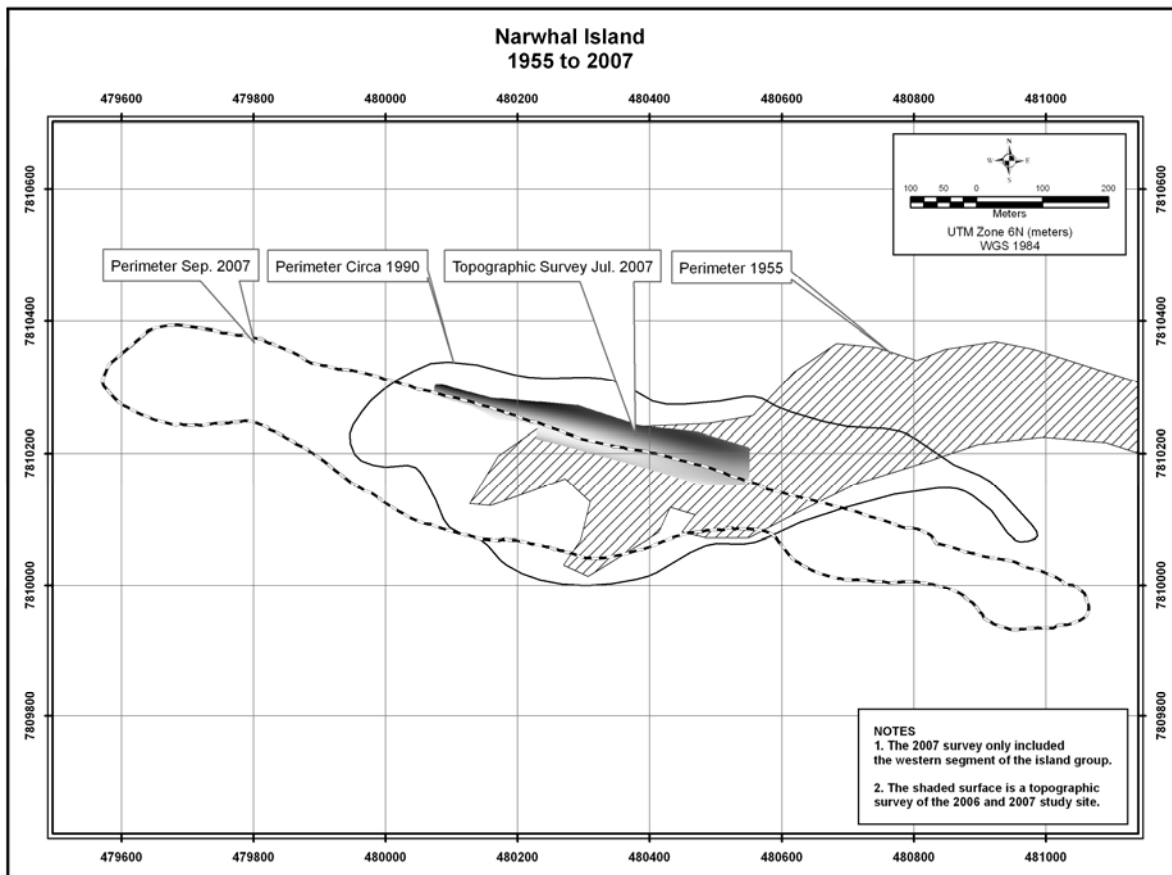
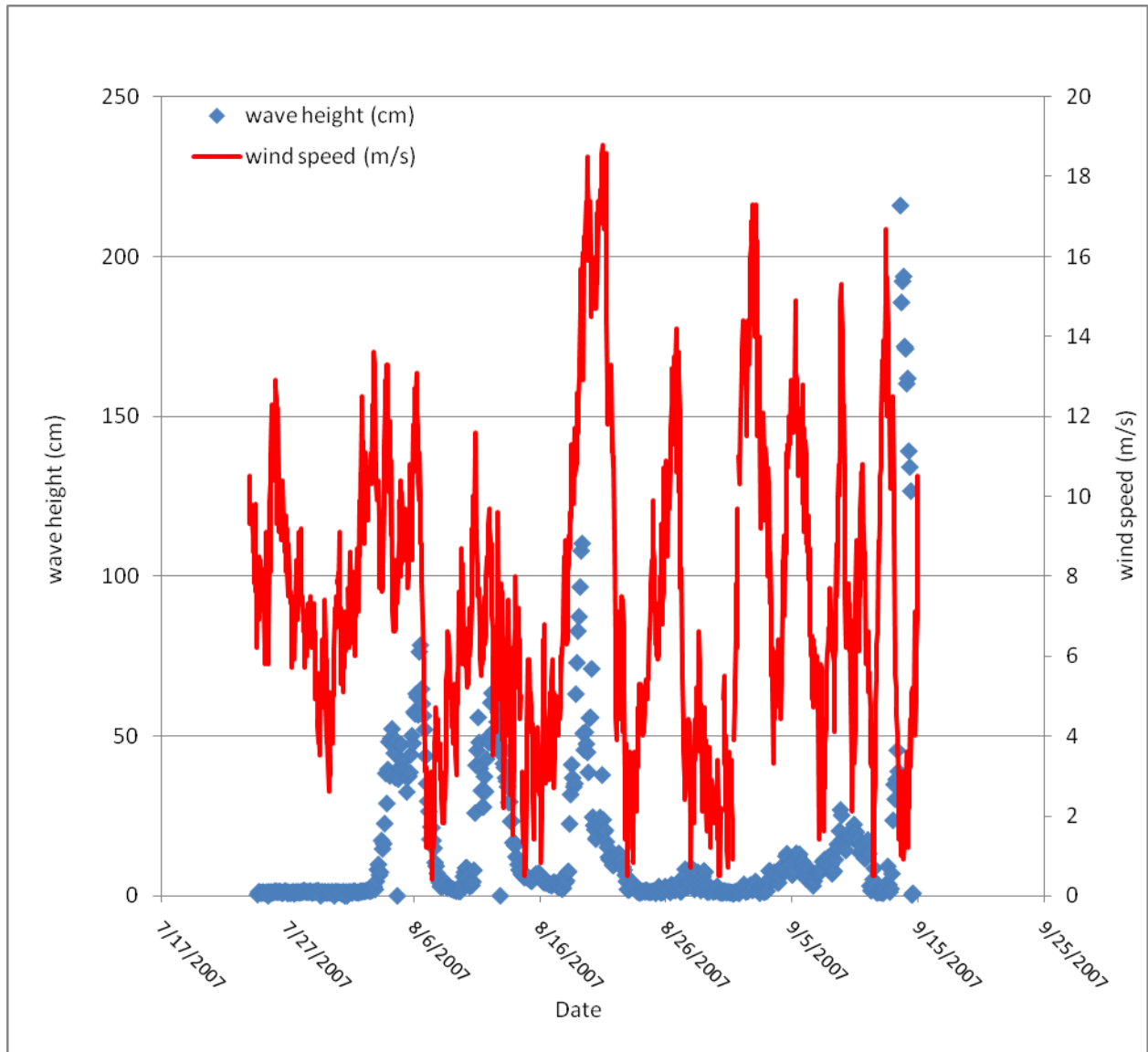


Figure 8. Results of the topographic surveys conducted in 2006 and 2007 showing short-term changes in the morphology of Narwhal Island with reference to the 1955 baseline.

### ***Time-series changes on the wave climate and wind statistics***

Figure 9 summarizes the record of the time-series on the wave heights (cm), as documented by the ADCP deployed from 24 July, 2007 to morning of 14 September, 2007 at the 10 m depth site off Narwhal Island. The wave record depicts measurements for each two-hour period for 53 days of deployment. On September 15, 2007 the unit was retrieved and recording ceased. In Figure 9 are shown also the wind speeds (m/s) at Deadhorse (Prudhoe Bay region, the closest meteorological center for the study site) for the period coinciding with the period of the ADCP deployment. It is clear that during the recording period there were four relatively elevated wave episodes and several heightened wind events (Fig. 9). However, only four of the many stormy episodes coincided with higher wave occurrences. The records of the ADCP including the time-series on the wave direction, period, height and length were downloaded and this information together with the wind data were used, as appropriate, for the computation of the potential alongshore volume transport rate of sand along the Narwhal Island beach (for details refer to the DISCUSSION section).



**Figure 9. Time-series of wave heights (cm) and wind speeds (m/s) in July-September, 2007, as recorded by the ADCP off Narwhal Island and at Deadhorse, respectively.**

## ***Time-interval surveys of alongshore movements of fluorescent-dyed sands and PIT-tagged gravel particles on Narwhal Island***

The beach survey made on 26 July, 2006 intercepted 21 (or 42%) of the tagged gravel around site 1A, and 11 (or 22%) around site 2A of the original 50 PIT tagged gravel particles that were injected at each of these sites on 30 June, 2006. Of the 21 particles identified in the vicinity of site 1A three were from the subtidal zone (~1 m depth). The onshore samples were located either on the beach surface or ~5 cm below the surface. Further, some of the PIT tagged particles had drifted east and others west of the marked stake up to 3 m away from the stake. A survey in mid-August showed that the drift of the PIT tagged gravel from site 1A had extended further up to 8m (total 11m) from the initial point of injection. Additional surveys of the beach on 13 October, 2006 and 25 July, 2007 adjacent to the four beach sites resulted in no recovery/detection of the PIT-tagged particles. Only one tagged particle out of the 200 that were originally injected on the beach (i.e., 30 June, 2006 at sites 1A and 2A, and on 26 July, 2006 at sites 3A and 4A) was intercepted on 25 July, 2007. The sole tagged particle was located at 29 m west of the site 1A. During the July 2007 survey we reworked randomly using a shovel the gravel mounds located east and west adjacent to the four beach sites, in an effort to find any buried tagged-gravel, but this search proved futile.

The October 2006 and July 2007 surveys also indicated that there were notable displacements of the tagged gravel particles since their injection in 2006 at the base of each of the berms. The numbers of tags (out of the original 15 injected) that were intercepted at site 1B, 2B, 3B and 4B were 8, 9, 13, and 19, respectively. The maximum distances that the tagged particles had moved away from berm sites 1B, 2B, 3B and 4B during one year (from the original dates of injection in July 2006 to July 2007) were 6.6 m, 2.46 m, 2.15 m and 1.85 m, respectively.

The July 26, 2006 survey in the vicinity of site 1B indicated a small clump of the red dyed-sands accompanied by three tagged gravel particles in ~0.5 m subtidal zone off the site. That survey indicated also that a larger portion of the rest of the red dyed sands was drawn into a band of streak at high-tide mark (16cm AMSL) parallel to the shore, concentrated generally toward the west and extending up the beach to ~2-3 m from the 1A site. However, the subsequent beach surveys 2006 and 2007 showed no evidence of the presence of the red dyed sands, either aligned in a specific orientation or in any of the several random beach sand samples that were collected east and west of the site. We also did not observe any dyed sand (red or green) concentrations about the other three beach sites in July 2007. None of the surface beach sand samples that were collected subsequent to July 25, 2006 showed the red or green fluorescence-dyed grains in the hand-picked sand samples that were examined microscopically using ultraviolet radiation in dark.

## ***Results of the storm-surge model***

A simple sediment transport semi-empirical model was applied as the first order approach to study the peculiarities of sediment motion around McClure Islands. Model results show that during the clockwise circulation regime the sediments tend to move from the north-west to south-east relative to the island chain and are accumulated at the south-eastern side of the chain. The region of Narwhal Island is devoid of sediments. During the counterclockwise circulation regime the opposite situation occurs. The sediments move from the south-east toward the north-west and are accumulated in proximity to the Narwhal Island.

## **DISCUSSION**

### ***Dynamics of the Narwhal Island relief and morphology***

Comparison of the 2006 and 2007 profiles across eight crests to shoreline transects shows that the island is generally increasing in elevation toward the crest in the westward direction. This trend is more pronounced in the 2007 profiles than in the 2006 profiles. The profiles also show a slight increase in elevation toward the crest from 2006 to 2007. The increase in elevation appears to cease at a point approximately 30 m seaward of the baseline. The 2007 profiles exhibit a remarkably stable elevation at 30 m distance along the transect. The base line stations remained constant in elevation as well. Beyond 30 m seaward the beach profile appears to be moving to lower elevation. This is particularly evident in the 2007 profiles.

The island profiles as recorded in 2006 are marked by some changes in the relief in the lower backshore to foreshore zone. This is explained to the undulations resulting from pervasive reworking and redistribution of the beach deposits on the Narwhal Island by shorefast ice during the 8-9 months of winter. The action of ice in the form of gouging, plowing and pushing of the beach substrate invariably occurs, manifested at spring in an haphazard relief marked by sand-gravel mounds of various dimensions (up to 2 m high), furrows, ice 'wallows' and scour depressions that are especially pronounced adjacent to the margin of the shorefast ice-waterline. Some of these features typical of arctic beaches were described in Greene (1970), and illustrated in Plates 2, 3, 4, 5, and 6 for the seaward beach of Narwhal Island. The presence of relatively smooth profiles in 2007 would seem to suggest that during the relatively short summer (mid June to August) the major undulations on the above zone were smoothed out by the action of melt water, wind and/or wave swash and backwash. The pattern of beach profiles recorded for Narwhal Island is consistent with an island that is experiencing wave driven longshore sediment transport from east to west, (Komar 1976; Nummedal 1979; Komar 1983).

The island has experienced substantial temporal changes in its dimensions and morphology since 1955. Figures 7 and 8 indicate that there have been significant long-term (1955-2007) and short-term (June 2006-September 2007) time-interval changes in the configurations of the Narwhal Island. The USGS map (United States Army Map Service, 1955) indicates that Narwhal Island was a single geomorphic entity in 1955. (Morack and Rogers (1981) reported that the island was breached and fragmented to five islets at the time of their

work. The NOAA chart, (National Oceanographic Service, 1990) of the area also depicts the island in five fragments. Later aerial photographs taken in the 1990's show the island existing in two major islets.

From comparison of the temporal morphology of the Narwhal Island and estimation of the changes in the island's aerial extent (Figs. 7 and 8) it is revealed that there is a net westward drift of the island with variable annual rates. From 1955 to 2007 the western end of the island has moved ~590 m. From 1955 to 1990 the same portion of the island moved 214 m. During the period of 1990 to 2007 there were 384 m of movement. The distances moved and their annual rates corresponding from various time-intervals are indicated in Table 2.

**Table 2. The time-interval distances (m) and annual rate (m/yr) of migration of the western tip of Narwhal Island.**

Period	Distance (m)	Annual Rate (m/yr)
1955 – 1990	214	6
1990 - 2007	384	23
1955 - 2007	590	11

From 1990 to 2007 the eastern tip of the west segment of Narwhal Island moved ~70 m east and 100 m south. This relatively modest change could be due to accumulation of sediment that was transported to the west from the eastern segments of the island. It is to be noted that Morack and Rogers (1981) based on seismic work identified the presence of permafrost 2m below the surface on the eastern portion of the island. They found no subsurface frozen soils on the western end of the island that close to the surface. These authors stated that the presence of subsurface frozen sediments serve to stabilize the island. The lack of these frozen sediments at the western end of the island contributed to its increased susceptibility to long shore transport.

Comparison of the 1955 and 1990 coast of Narwhal Island reveals that the island was occasionally separated by breaches into five segments. Each of these pieces was transported to the west and slightly to the south. The greatest movement of the western end of the island was 590 m and the smallest was 160 m. The southern tip of the island did not appear to move to the south. This was possibly due to accumulation of sediment transported around the tip of the island that served to replenish the southern tip from the western side (back side). The average amount of western movement of the southeast portions of the island was 350m with an average annual rate of 10m.

Barnes *et. al.* (1977) have investigated the long-term migration of Cross Island, a barrier island located approximately 10 km northwest of Narwhal Island (Fig. 1). They analyzed nautical charts and aerial photographs that covered the period of 1949 to 1974, and concluded that the Cross Island had migrated ~150 m westward during the above period at a mean rate of ~ 6m/yr, and also that the migration was landward. The southern and northern tips exhibited

greater movement. The northern tip moved about 200 m west. The southern tip moved 50m southwest.

The time-interval changes in the morphology of Narwhal Island as gathered, indicates that the island has undergone major changes during the past 55 years, reflecting its instability and dynamic nature. In 1955, Narwhal Island was a 4 km long and 30 to 200 m wide barrier, located at 145° 30' W and 70° 24' N, about 20km offshore of the North Slope coast by Foggy Island Bay and near Prudhoe Bay. According to available aerial photographs, by 1979, the island had breached in 4 locations creating a five island chain. By 1984, the chain consisted of three pieces indicating a reformation process. In subsequent years, the chain appears to have gone through a couple of more cycles of breakup and reformation. The island is subject to wind, waves, sea-ice impacts, and storm surges. Preliminary GIS analysis and recent GPS surveys indicate that, in the past 50 years, the western end of the island had migrated about 200m to the west consistent with the direction of sea-ice movement and consistent with the frequent east winds during the summer (open water) period. The direction of migration was, however, not consistent with the available storm surge data which indicates that surge is mainly driven by winds from the northwest. In addition to the island's westward migration, the northern (seaward) side of the island has retreated landward by about 5m/year during the past decade. The net direction and rate of migration are consistent with the findings of earlier studies on barriers in the North Slope region.

The GIS analysis demonstrates that the Narwhal Island is a dynamic environment as reflected in significant changes in the island's morphology over the past 50 years recorded history. Narwhal Island has a crescent shape that is seaward convex (Figs. 2 and 7). This shape is consistent with barrier morphology that is dominated by wave induced longshore transport (Komar, 1983).

### ***Empirical and theoretical investigations on alongshore sand and gravel transport on Narwhal Island: challenges, scope and assessment***

The two-year (2006-2007) beach experiment using fluorescent-dyed sands and PIT-tagged gravel particles, has demonstrated some of the practical problems beset in working on the ice-stressed Narwhal Island, in attempting to assess empirically the annual net direction and rate of alongshore transport of sand and gravel. In the case of sands, the experiment failed to achieve the goal set as none of the dyed sand particles were detected on the beach two months following their injection on 30 June, 2006 around sites 1A and 2A. Likewise, no red or green dyed sands were detected on the beach in mid-August and 13 October, 2006 around sites 3A and 4A subsequent to their injection on 26 July, 2006. Additionally, none of the beach samples that were collected at the time of the field examinations and subsequently examined microscopically in the laboratory showed dyed sand. The exception to the above is the beach survey conducted around site 1A on 26 July, 2006, twenty-six days after the initial injection there of the dyed sand. As mentioned earlier, a minor portion of the dyed sand was distributed in a clump in less than one

meter water depth and about one meter away from the stake 1A. The rest of the dyed sand was drawn into a concentrated, narrow linear streak on the beach surface ~2.7 m from the stake (Plate 5). The extent of the sand concentrate in the west of the stake was 6.9 m, but the maximum dispersal identified was up to 10 m. In east of the stake the concentrate extended to 2.6 m and the maximum dispersal identified was up to 3.6 m. Obviously the above emplacement pattern on the beach of the dyed sand is affected by high tide moving onshore from NE (the dominant wind direction). Apparently, the clump of dyed sand under water was due to an initial entrainment of the sand in shorefast ice that subsequently, at spring, backwashed to the subtidal zone. The limited extent onshore of the dyed sand is consistent with the low tidal range (~16 cm) in the study area.

We suggest some of the possible reasons to explain the failure to detect dyed-sand particles in the field as well as in the grab samples that were collected from the beach and examined microscopically after July 2006. One reason could be a consequence of dilution by mixing of overwhelming proportion of untagged beach sand with tracer sand. Presumably, such a thorough mixing occurs by ice reworking and mass shoving of beach deposits in winter and occasional storm surges in summer. The action of ice is clearly visible from the association of sand and gravel mounds at the shoreward edge of shorefast ice-waterline (Plate 4). An additional possibility is that most of the dyed-sands were lost to the subtidal zone by backwash of storm waves, or ice fragments and/or ice melt water at spring.

We are not sure of the fate of the 199 gravel particles remaining unaccounted for in the 2007 survey. It is quite possible that some tagged gravel particles remain undetected on the beach below the maximum depth of scanning by the PIT reader. It is also possible (Naidu et al., 2006) that some of the tagged gravels could have been dragged into the subtidal zone by melting shorefast ice or by the backwash following a storm surge. The other reason could be that the reader failed to intercept tagged gravel particles that lie very close to each other. The October 2006 and July-August 2007 surveys at the base of each of the berms also indicated that there were some displacements of the tagged gravel particles since their injection in 2006. In contrast the September 2007 field study indicated that the maximum dispersal of the tagged gravel at 1B berm site was 6.62m. All these findings, particularly that of September 2007, were a surprise, because during the latter month storms are generally common and therefore it is to be expected that there would be large-scale displacement of the berm gravel by the storm surges and the following backwash along the beach slope.

It would, thus, seem obvious that prolonged and haphazard reworking of beach sediment by shorefast ice and/or storm backwash complicate the assessment, using PIT tags and dyed sand, of the annual rate of littoral sediment transport along Northern Alaskan Arctic beach.

### ***Storm surge model and potential sediment mass transport***

A set of storm surge models developed by Kowalik (1984) and Proshutinsky (1993) for simulation of sea level, currents, ice movement and ice concentration, forced by wind and tides is used in this study to investigate the sediment transport on a site-specific basis. In order to investigate circulation

and sediment transport in the vicinity of Narwhal Island (located in the McClure Islands chain) we have developed two numerical models, namely: a relatively coarse resolution (13.89km) model of the Canada Basin and a very high resolution model (0.1389km) of the region surrounding McClure Islands. The models were calibrated and validated based on the data from coastal stations and have demonstrated a good agreement between the observed and simulated sea levels for the storm surges of August 2000 and August and September 2007. During the storm of August 2000 the sea level changes along the entire coastal region of the Beaufort Sea reached 1m. This was an important storm for comparison of the observed and simulated ice distribution and concentration.

Two major factors, potentially important for sediment transport were considered for analysis: permanent barotropic currents due to sea level gradient between the Pacific and Atlantic Ocean, and wind-driven circulation due to storm surges.

The roles of the permanent currents and wind-driven circulations (counterclockwise and clockwise island-trapped patterns characterizing different regimes of sea level change around the McClure Islands) were investigated in details through the high resolution model. A simple sediment transport semi-empirical model was applied as the first order approach to study the peculiarities of sediment motion around McClure Islands. The high-resolution model has demonstrated that the currents around McClure Island chain and around every individual island in the chain have tendency to the circulatory clockwise or counterclockwise motion. This trapped motion results in the specific pattern of the sediment transport.

Model results have shown that during the clockwise circulation regime the sediments tend to move from the north-west to south-east along the island chain and are accumulated at the south-eastern side of the chain. At this pattern of circulation the region of Narwhal Island is denuded of sediments. During the counterclockwise circulation regime the opposite situation occurs. The sediments move from the south-east toward the north-west and are accumulated in the proximity to the Narwhal Island.

## ***Computation of the alongshore transport rate of sand on Narwhal Island***

### **Selection of the Longshore Transport Model**

Most longshore transport prediction relationships have been developed and tested using sand sized sediments – e.g., grain sizes in the range of 0.0625mm to 2mm. The lower grain-size limit for the material composing most beaches is in the 0.1 to 0.15 mm range (King, 2005) because finer material is winnowed out of the beach by the wave turbulence. Finer grain sizes are mobilized by the turbulence generated in the bottom boundary layer and kept in suspension during each successive half-wave cycle. Absent the time to settle out, the fine material remains in suspension and is transported to more quiescent waters either off shore or into back bays and estuaries while the coarser grains are retained in the longshore system (de Meijer, et al., 2002; King 2005). The sand particles are moved predominantly by saltation and suspension, by both currents and waves. Though sand beaches are permeable, the interstices in the swash zone are rapidly saturated leaving a nearly impermeable surface. The resulting beach slope may vary from 1:100 to 1:10 depending on grain size, wave regime and currents. Several studies have

shown a direct relationship between the foreshore slope and particle size (Bascom, 1951; Komar, 1998, Chapter 3).

Gravel beaches have grain sizes greater than 2mm and may sometimes be dominated by cobbles with grain sizes 64mm to 256mm. The gravel is very permeable. Beaches tend to be sorted by size in the cross-shore direction, with large material forming steep storm crests. Slopes range from 1:10 to 1:2 depending on grain size and sorting. Larger grain sizes and better sorting lead to steeper beach slopes. On some cobble beaches, slopes may be close to the maximum angle of repose ( $\sim 32^\circ$ ) of unconsolidated material (Komar, 1998). The gravel is moved mainly by sliding and rolling and has a propensity for onshore movement due to its high threshold of motion and asymmetry of shoaling wave and swash zone action. The waves will produce asymmetric bottom orbital velocities in shallow water, stronger and in the direction of wave propagation under the crests and weaker (but of longer duration) and against the direction of wave propagation under the troughs.

Mixed beaches make up the intervening beach between sand and gravel, comprising a mixture of grain sizes including sand and gravel and sometimes cobbles. The distribution of mixed beach material may vary across shore, along shore, vertically through the beach and over time.

Over the last fifty years a considerable amount of research has been conducted on longshore transport of sandy beaches but the scientific and engineering communities still do not have the means to accurately predict the rate of longshore transport of material based on physical “first principles.” Practical prediction of longshore transport depends on empirically based engineering oriented formulae. These, in turn, are critically dependent upon field data for their calibration and verification. Most of the verification data come from observations on sand beaches in temperate climates, and most observations are made during relatively benign conditions rather than during storms when the majority of transport is presumed to occur.

A review on the research conducted on transport along gravel beaches appears in Van Wellen et al. (2000). Comparatively, little published data exists on mixed gravel-sand beaches (Pontee et al., 2004; Osborne, 2005). Though research results are not yet widely available, the importance of predicting sediment processes on mixed beaches has been recognized in recent years (Blanco, 2003). A number of recent papers have described mixed beach behavior and have evaluated the importance of grain size influence on sediment transport (Pontee et. Al., 2004; Pye and Blott, 2004; King, 2005; Soulsby and Dangaard, 2005). Van Wellen et al., (2000) concluded that, in spite of the limitations of having to tune the models to the site, the U. S. Army Corps of Engineers, Coastal Engineering Research Center (CERC, a and c, 2002) based equations that relate total longshore transport to the energetics of the waves and currents, provide reasonable predictions of mean annual transport when compared to data. The CERC equations (CERC, a and c, 2002) have the added advantage of being relatively simple to use, with a minimum of input variables.

The following explanation of the derivation of the CERC equations has been taken primarily from Komar (1998) and from Rosati et al. (2002). A history of the development of the “CERC formula” can be found in the latter reference. The CERC formula (CERC, a and c, 2002) is the most commonly used relationship for calculating the total potential longshore transport rate. In spite of its limitations, which will be described below, it continues to be useful primarily because of its simplicity and because of the failure of more sophisticated models to clearly demonstrate substantially superior accuracy relative to the effort required to employ them. The term “potential” sediment transport rate is used because calculations of the quantity imply that sediment is available in sufficient quantity for transport and that natural or man-made obstructions do not slow or stop transport in the alongshore direction. With adequate calibration, the CERC formula can estimate the potential longshore transport rate within  $\pm 50$  percent. Without calibration its accuracy may degrade to one or two-orders-of-magnitude (King, 2005).

The symbols for the variables in the following and subsequent equations, relating to derivation of CERC equations and calculation of sand transport rates, are defined below.

$\alpha$  Wave crest angle relative to bottom contours [deg]

$\alpha_b$  Wave breaker angle relative to the shoreline [deg]

$\beta$  Angle of the beach slope [deg]

$\kappa$  Breaker index,  $H_b/d_b$  or as determined by Weggel (1972) formula [dimensionless]

$\rho$  Mass density of water (salt water = 1,025 kg/m<sup>3</sup> or 2.0 slugs/ft<sup>3</sup>; fresh water = 1,000kg/m<sup>3</sup> or 1.94 slugs/ft<sup>3</sup>) [force time<sup>2</sup>/length<sup>4</sup>]

$\rho_s$  Mass density of sediment grains (2,650 kg/m<sup>3</sup> or 5.14 slugs/ft<sup>3</sup> for quartz-density material) [force time<sup>2</sup>/length<sup>4</sup>]

$a$  Dimensionless parameter

$a'$  Solid fraction of sediment (fractional void space =  $1 - a'$ )

$b$  Dimensionless parameter

$C_{gb}$  Wave group speed at breaking [length/time]

$C_n$  Wave group velocity [length/time]

$D_{50}$  Sediment median grain diameter [length]

$d_b$  Water depth at the breaker line [length]

- $E$  Total wave energy in one wavelength per unit crest width [length-force/length<sup>2</sup>]
- $E_b$  Combined potential and kinetic wave energy at the breaker line per unit crest width [length-force/length]
- $g$  Gravitational acceleration (32.17 ft/sec<sup>2</sup>, 9.807m/sec<sup>2</sup>) [length/time<sup>2</sup>]
- $H$  Wave height in the surf zone [length]
- $H_b$  Wave height at breaking [length]
- $H_{br}$  Breaker height based on root-mean-square height [length]
- $H_{bs}$  Breaker height based on significant wave height [length]
- $H_{mo}$  Zeroth moment wave height [length]
- $H_{rms}$  Root mean square wave height [length]
- $I_l$  Immersed weight longshore transport rate [force/sec]
- $K$  Empirical proportionality coefficient [dimensionless]
- $K'$  Dimensionless coefficient
- $m$  Beach slope ( $m = \tan\beta$ ) [dimensionless]
- $P_l$  Longshore component of wave energy flux or lonshore power
- $Q_l$  Potential volumetric longshore transport rate [length<sup>3</sup>/time]
- $T$  Wave period [time]
- $u_m$  Maximum horizontal orbital velocity of the wave evaluated at the breaker zone [length/time]
- $v_l$  Longshore current velocity (mean) measured at the mid-surf position [length/time]

*Derivation of the CERC Equations:* The CERC formula equates the total immersed-weight longshore transport rate ( $I_l$ , N/s) with the longshore component of wave energy flux or power ( $P_l$ ). The relationship is:

$$I_l = KP_l \quad 1.$$

where K is a dimensionless coefficient.

The wave energy flux ( $P_l$ ) is:

$$P_l = (ECn)_b \sin \alpha_b \cos \alpha_b \quad 2.$$

The sub-script indicates that all values are evaluated at the point of wave breaking.

$E_b$  is the combined potential and kinetic wave energy at breaking:

$$E_b = \frac{\rho g H_b^2}{8} \quad 3.$$

and  $C_n$  is the wave group velocity ( $C_g$ ) at breaking:

$$C_{gb} = \sqrt{gd_b} = \left( g \frac{H_b}{\kappa} \right)^{1/2} \quad 4.$$

where  $\kappa$  is the breaker index ( $\kappa=H_b/d_b$ ). The value of  $\kappa$  is often taken as 0.78 for beaches of very shallow slopes but apparently depends on wave characteristics and beach slope, and values from 0.73 to as high as 2.8 have been observed in laboratory experiments.

Weggel (1972) reinterpreted laboratory results and showed an empirical dependence on beach slope ( $m=\tan\beta$  where  $\beta$  is the angle of the beach). Weggel's results were:

$$\kappa = b - a \frac{H_b}{gT^2} \quad 5.$$

where T is wave period and :

$$a = 43.8(1.0 - e^{-19m}), \text{ and} \quad 6a.$$

$$b = 1.56(1.0 + e^{-19.5m})^{-1} \quad 6b.$$

Other methods of estimating wave height through the surf zone for both regular and irregular waves can be found in Smith (2003).

In Equation 2, the sine and cosine functions are to calculate the longshore component of wave power ( $\sin\alpha$ ) and the wave energy flux per unit wave-crest length ( $\cos\alpha$ ), respectively. Using the identity,  $\sin\alpha\cos\alpha = \frac{1}{2} \sin 2\alpha$ , Equation 2 can be written:

$$I_l = K \left( \frac{\rho g^{3/2}}{16\kappa^{1/2}} \right) H_b^{5/2} \sin(2\alpha) \quad 7.$$

The immersed rate transport rate can be converted to volume transport rate (*e.g.*, cu.yds/yr) by using the relationship:

$$Q_l = \frac{I_l}{(\rho_s - \rho)ga'} \quad 8.$$

Where  $\rho_s$  and  $\rho$  are the density of sediment and water respectively and  $a'$  is the solid fraction of the sediment (fractional void space =  $1-a'$ ), frequently taken as 0.6 for sand. The potential volume transport rate can then be expressed as:

$$Q_l = K \left( \frac{\rho\sqrt{g}}{16\kappa^{1/2}(\rho_s - \rho)a'} \right) H^{5/2} \sin(2\alpha_b) \quad 9.$$

One advantage of using  $I_l$  instead of  $Q_l$  is that the immersed weight transport rate accounts for the density of sediment grains. Except for coral sand and areas where unusual minerals are significant, specific gravity of the sediment is assumed to be 2.65.

The equations for longshore transport rate (Equations 7 and 9) do not show a dependency on grain size, as would be expected from an intuitive assessment. One would expect the value of  $K$  to decrease as grain size increases for grains of constant density. The  $K$  coefficient in the equations has been shown to depend on several factors including grain size, beach slope, breaker type, and whether wave height is specified as significant wave height ( $H_{sig}$ ) or root-mean-square wave height ( $H_{rms}$ ) (Komar, 1998). If  $H_{rms}$  is used, the often-recommended value of  $K$  is 0.78, which is similar to the value of 0.77 initially determined by Komar and Inman (1970) (King, 2005). The selection of the appropriate  $K$  value is further confused by recommendations in Rosati et al. (2002, p.12), which indicate that  $K$  based on  $H_{rms}$  should be 0.92.

The longshore transport rate can also be related to the wave conditions and the total longshore current. In this scheme, the waves are considered to suspend the sediment and the current, generated by both waves and wind, move the sediment in the longshore direction. The relationship for immersed potential transport rate can be expressed as:

$$I_l = K'(ECn)_b \frac{\bar{v}_l}{u_m} \quad 10.$$

Where  $v_l$  is the longshore current velocity measured at the mid-surf position, and  $u_m$  is the maximum horizontal orbital velocity of the wave evaluated at the breaker zone. Using relationships from linear wave theory for  $E_b$ ,  $Cn$  and  $u_m$  and selecting  $K'$  as 0.25 (Kraus et al, 1982), one can show that:

$$I_l = 0.088 \rho g H_{br}^2 \bar{v}_l \quad 11a.$$

and

$$I_l = 0.044 \rho g H_{bs}^2 \bar{v}_l \quad 11b.$$

depending on whether root-mean-square wave height or significant wave height respectively is used.

As pointed out by Komar (1998), it is often easier to use Equation 9 rather than Equation 7 to determine longshore transport since it is often easier and more accurate to measure  $v_l$  than it is to determine breaker angle. In addition, origin of the longshore current can be due to oblique-wave approach, tidal currents, part of the cell circulation with rip currents or driven by local winds.

The relationships for sediment transport have been tested primarily for sand beaches and do not explicitly include grain size as one of the parameters. It is reasonable, however, that transport rate will depend on other environmental factors such as grain size, beach slope and wave steepness.

*Mixed Sand and Gravel Beaches:* The most comprehensive descriptions of beach deposits and processes along the Beaufort Sea coast have been made at Pingok Island, near Oliktok Point and on the sea side of Simpson Lagoon by Wiseman, et al (1973) and Naidu and Mowatt (1975). Though not as comprehensively reported, other North Slope beaches were also observed (Point Lay, Leavitt, Tapkaluk, Long and Egg Islands). Beaches on the North Slope have been observed to be primarily mixed beaches composed of a significant coarse fraction, typically 33 percent pebbles (4 to 64 mm) and granules (2 to 4 mm) (Wiseman, et al., 1973). Three distinctive sediment-size zones were noted across the beach face. Proceeding shoreward, the shallow inner bar consisted of medium sized (0.5 to 0.25 mm), poorly sorted sand; the swash bar consisted of gravel (2 to 4 mm); and the shoreward beach face was medium, well-sorted sand. Wiseman, et al (1973, p. 108) conclude that Pingok Island sediments:

1. “are typical of Alaskan Arctic beach sediments;

2. possess size-sorting and size-skewness relationships similar to those exhibited by non-arctic beaches; and
3. are zoned by size across the surf zone.”

Short-term beach response was related to wave conditions, which in turn depended on location of the pack ice (fetch), wind conditions (storms, wind direction) and duration of the wind/wave event. However, it is to be noted that the above sediment granulometry though may be typical of beaches adjacent to tundra mainland coast and non-barrier islands (Pingkok Island) of the Alaskan Arctic, the granulometry of Narwhal Island (a barrier island) beach is quite different, as indicated earlier, inasmuch as the deposits there are poorly sorted and have no consistent pattern of size skewness. Further, on Narwhal Island no definite pattern of sediment gradation (coarse to fine) is observed across the beach surface.

### **Estimates of Sediment Transport at Narwhal Island, Summer 2007**

During the summer of 2007, from 24 July, until 14 September, experiments were conducted near Narwhal Island in the Alaskan Beaufort Sea to estimate the sediment transport rate along the island shoreline. As mentioned a SonTek<sup>®</sup> (ADCP) was placed at a position 1.3 Km due north (°T) of the Narwhal Island beach study site in ten meters water depth. The position of the profiler was latitude 70° 24.561'N and longitude 147° 31.531'W; the position of the center of the study area is latitude 70° 23.833'N and longitude 147° 31.531'W based on measurements from NOAA Chart 16046, *McClure and Stockton Islands and Vicinity*. Confirmation of the locations of the beach study site and wave measurement site was also made using MapTech<sup>®</sup> navigation software.

**Measurement protocol:** Data collection was begun by the ADCP at 14:53:41 local time on 24 July, 2007 and was continued at two-hour intervals for the deployment period. The current was recorded for the first two minutes of the period followed by measurement of the pressure and U, V components of current for an additional 1024 seconds. The U, V components of current and the pressure were analyzed by SonTek<sup>®</sup> to provide the directional wave spectrum for the measurement interval. From that record the significant wave height ( $H_{m0}$ ), dominant period ( $T_p$ ) and mean direction were extracted in order to estimate the breaking wave conditions at the shoreline. All directions were converted to degrees true (°T) based on the reported variation and secular trend (NOAA Chart 16046).

**Identification of storms:** Waves were measured by the ADCP for each two-hour period for 53 days from 24 July, 2007 until close to afternoon of 14 September, 2007 when the unit stopped recording. During the observation time, three complete “storms” were observed and one was in progress when the unit stopped recording (Figure 10). A storm was considered to start when the measured wave height ( $H_{m0}$ ) exceeded 10cm at the beginning of an event in which wave height eventually exceeded 25cm. The duration of the storm continued until the measured wave height again fell below the 10cm threshold. A fourth storm was partially recorded and was in progress when the unit ceased recording at 1053 on 14 September. Two minor events also

occurred (around interval 406, 27 August and around interval 500-595, 12 September), but they did not reach the criterion set to qualify as “storms”. The relative intensity and timing of the events during the measurement period are shown in the wave plots of Figure 10. Wind data, measured at Deadhorse, Prudhoe Bay were also obtained from the NOAA web site (<http://tidesandcurrents.noaa.gov>) for the measurement period and are shown in Figure 11 for the same period. Winds were primarily from the easterly direction during the period and were often measured at speeds greater than 30kts. The high wave events can be easily correlated by eye with the high wind events. The arrows along the top of Figure 11 indicate the approximate time of the center of each measured high-wave event. It is obvious that there were several high wind events measured at Prudhoe Bay (e.g., 1-4 September) during which high waves were not observed (Figs. 9 and 11). A likely explanation for this is the limited fetch at such low wave height events, resulting from incursion inshore of sea ice. The waves are dampened by the increased ice cover which correspondingly decreases fetch.

**Wave refraction and shoaling:** Wave direction estimates were obtained from the U, V components of the current and were confirmed to be from an easterly direction by comparison to the NOAA wind directions measured during the storm periods observed. All measurements were transformed from magnetic north, measured by the ADCP, to true north prior to calculating the refraction and shoaling. There is little bathymetric data for the study area so straight and parallel contours were assumed from the shoreline of Narwhal Island to the wave measurement site. The study reach trends in nearly an east-west direction ( $105^{\circ}\text{T} - 285^{\circ}\text{T}$ ) allowing for the simple calculation of offshore wave angle. Shoaling and refraction coefficients were calculated using linear wave theory and the wave angle at breaking was determined from Snell's law (CEM, 2002a). Wave breaking was assumed to occur at a breaker index ( $\gamma_{br} = H_{br}/d_{br}$ ) of 0.8 and the breaker height, breaker angle ( $\theta_{br}$ ) and water depth were determined.

The breaking wave height and offshore wave heights for each storm have been compared to the NOAA-measured winds at Prudhoe Bay (refer to Figs. 12 to 21). The dark vertical lines in Figure 13 show the approximate timing of the first of the three storms. Similar comparisons are shown in Figures 14, 15, 16 and 17. The scale of the wave height axis is the same in each figure for ease in visual comparison, though the wind speed axis (m/s) is different in each figure.

During these three storms, the winds were generally from the east for the beginning of each storm period and became variable near the end. Figures 18 and 19 show waves and winds, respectively, for storm 4. Winds prior to storm event were significantly higher than during the period when the large waves were measured suggesting that winds measured at Prudhoe Bay are not particularly good indicators of wave conditions at Narwhal Island. Measurements of waves and winds nearer to the study site should be used to predict conditions where possible.

**Estimate of relative longshore sediment transport rate:** Winds from the east generate waves at the ADCP location that have their crest very nearly perpendicular to the study site shoreline trend. The angle of wave breaking is therefore large and leads to a large relative longshore volume transport rate. This can be seen from Equation 12 restated below.

$$Q_l = K \left( \frac{\rho \sqrt{g}}{16\kappa^{1/2}(\rho_s - \rho)a'} \right) H^{5/2} \sin(2\alpha_b) \quad 12.$$

Where:

K is a proportionality coefficient described below,

$\rho$  is water density taken as 1024kg/m<sup>3</sup>,

$\rho_s$  is density of quartz density material, 2650kg/m<sup>3</sup>,

g is gravity, g = 9.81m/s<sup>2</sup>,

$\kappa$  is the breaking wave index ( $\kappa = H_{br}/d_{br}$ ), assumed to be 0.8,

a' is the sediment void ratio, a'=0.6,

H is breaking wave height, and

$\alpha_b$  is the breaker angle.

The K coefficient was taken to vary with grain size following the empirical relationship of del Valle, Medina and Losada (1993) for coarse sediment. The relationship used was:

$$K = 1.4e^{(-2.5D_{50})} \quad 13.$$

The volume transport rate relationship was based on  $H_{rms}$ , so breaker height was converted from significant height ( $H_{mo}$ ) to  $H_{rms}$  using factors in CEM (2002c, Eq. II-1-132).

**Table 3. Total relative volume longshore transport during each of the storms for which waves were measured.**

Storm Number	Total relative longshore volume transported, m <sup>3</sup>	Storm duration, hr	Transport rate, m <sup>3</sup> /hr
1	55.4	106	0.52
2	81.2	82	0.99
3	121.6	98	1.24
4	1191.6	36	33.1

In each case the transport was from east to west along the shoreline. The volume transport rates for each 2-hour measurement interval are shown for storms 1-3 and storm 4 in Figures 20 and 21 respectively and Table 3.

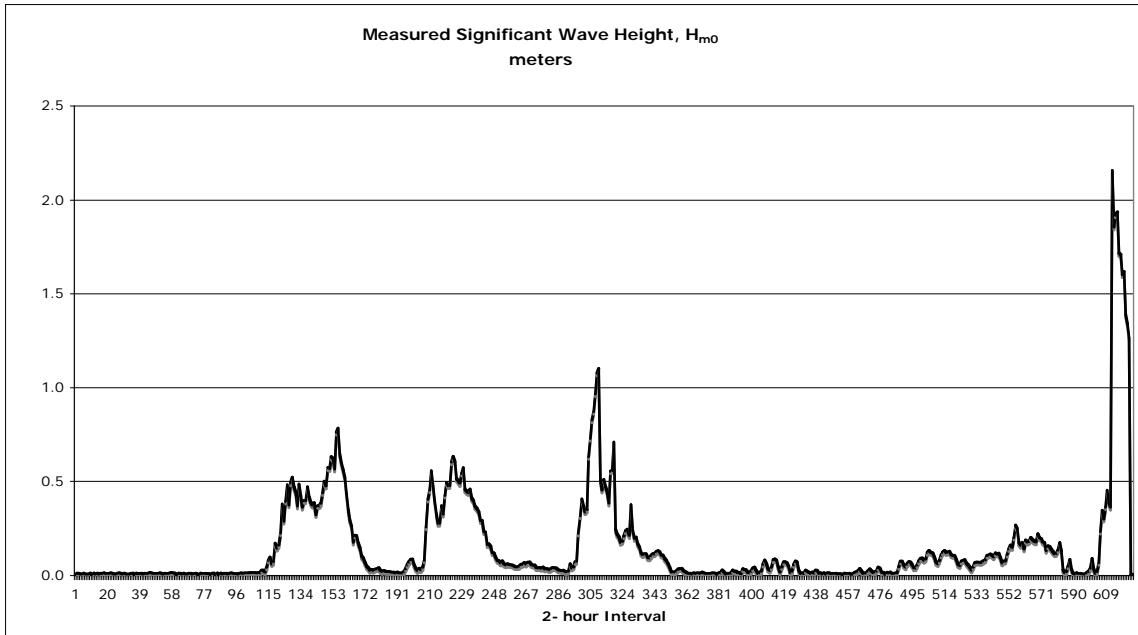


Figure 10. Significant wave heights determined each 2-hour interval during the ADCP deployment period from 24 July until 14 September, 2007.

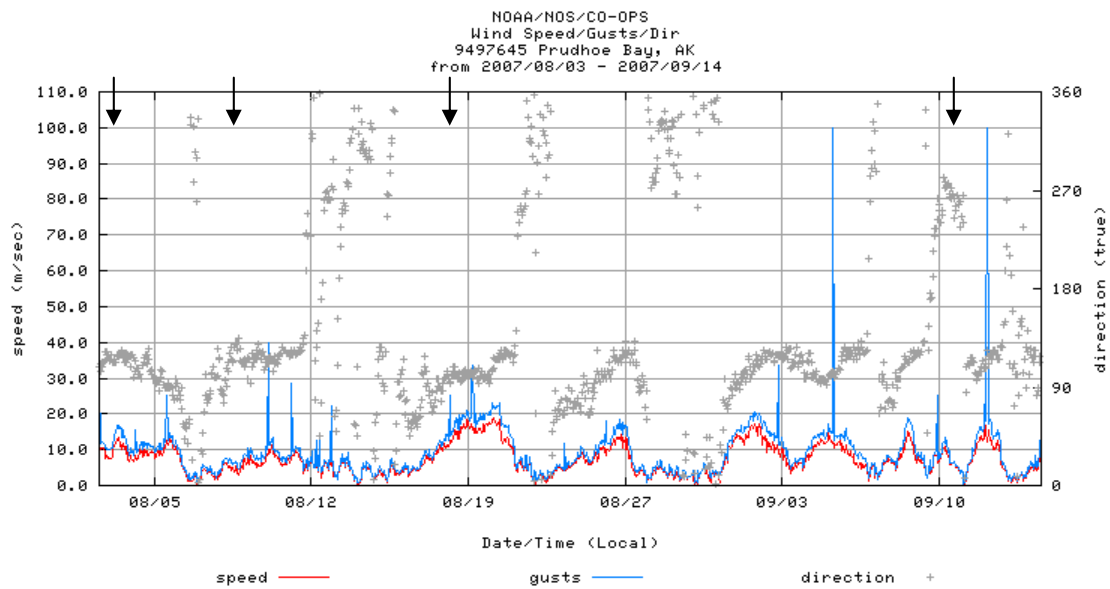


Figure 11. NOAA wind data recorded at Prudhoe Bay during the wave measurement interval of 24 July to 14 September, 2007.

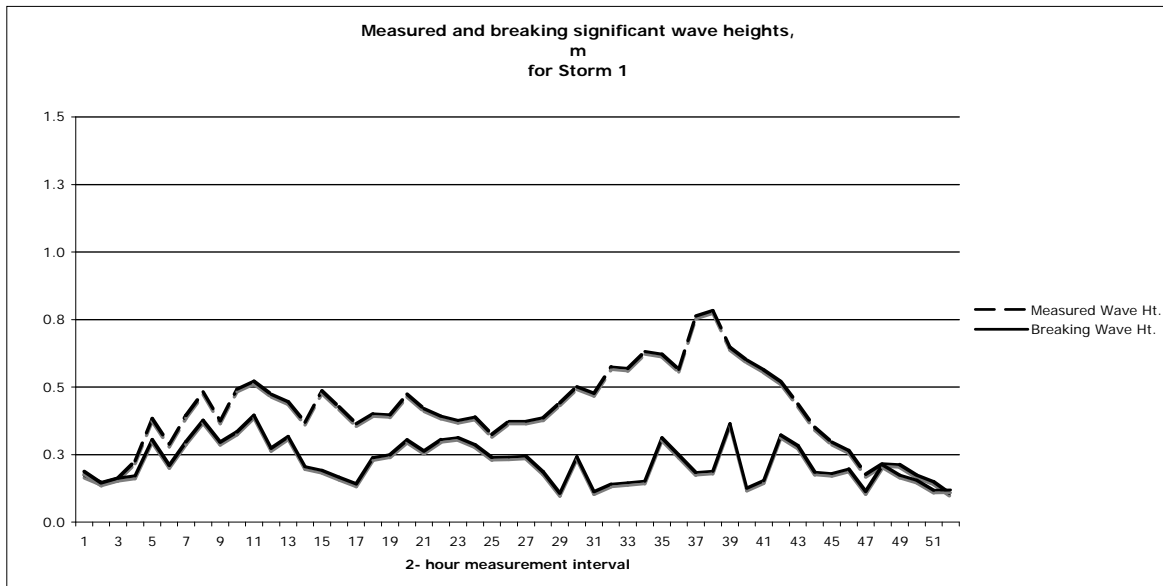


Figure 12. Comparison of measured wave height and breaking wave height during storm 1.

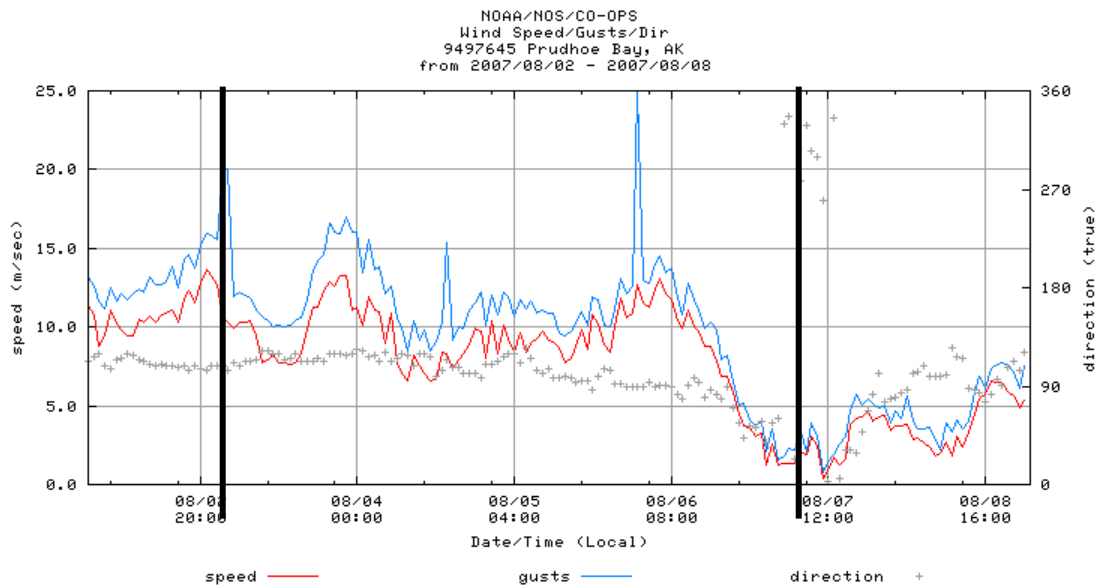


Figure 13. NOAA-measured winds at Prudhoe Bay during the period of storm 1 (between dark vertical lines) from about 0900, 3 August to 1700, 7 August, 2007 local time.

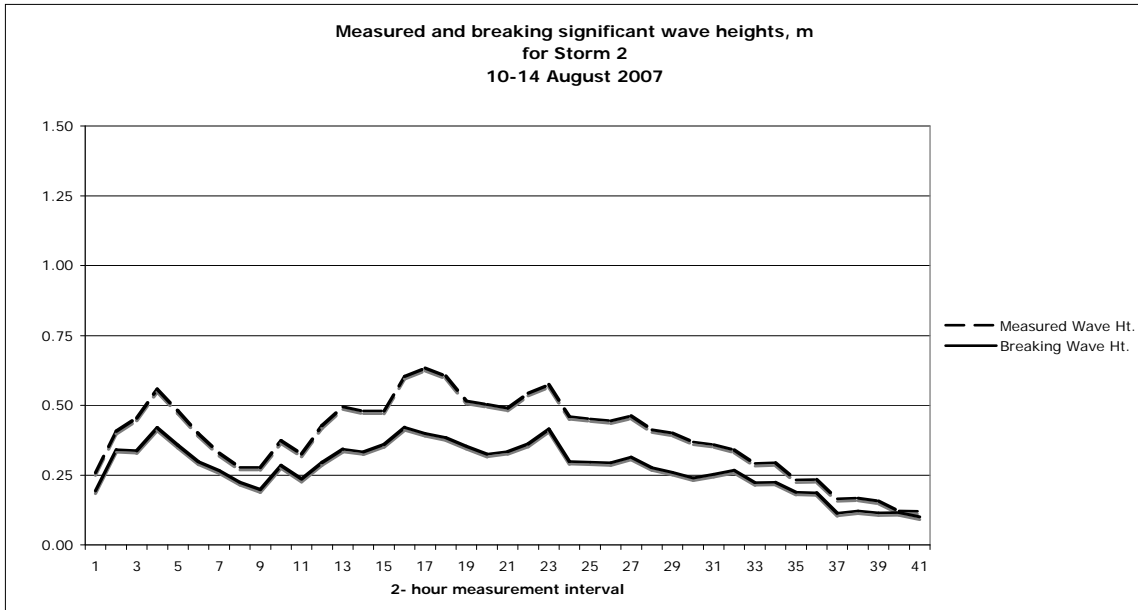


Figure 14. Comparison of measured wave height and breaking wave height during storm 2.

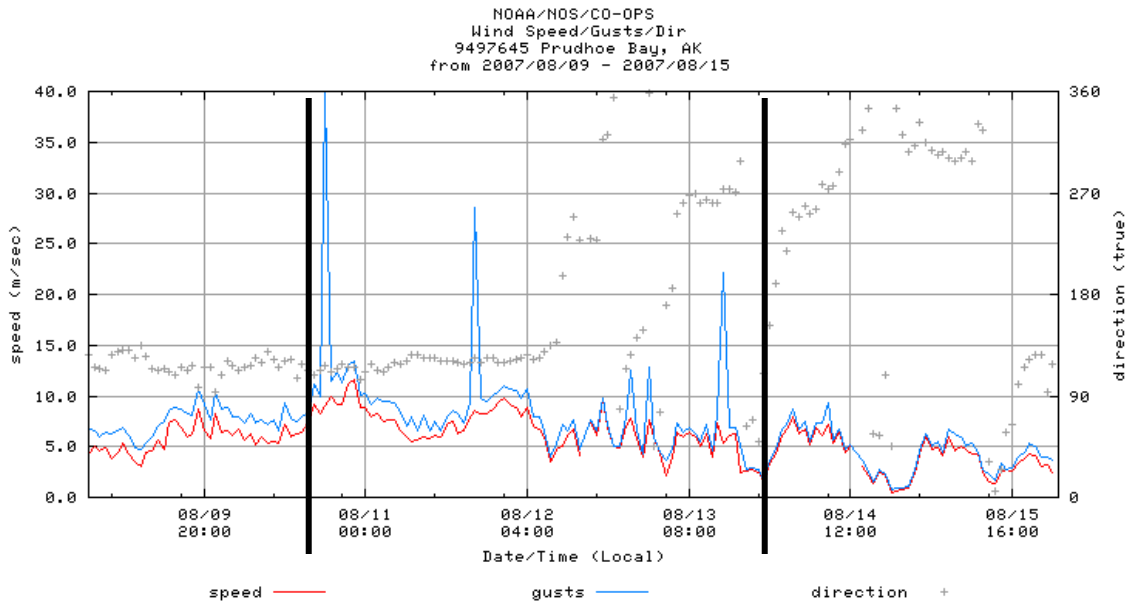


Figure 15. NOAA-measured winds at Prudhoe Bay during the period of storm 2 (between dark vertical lines) from about 2000, 10 August to 0400, 14 August, 2007 local time.

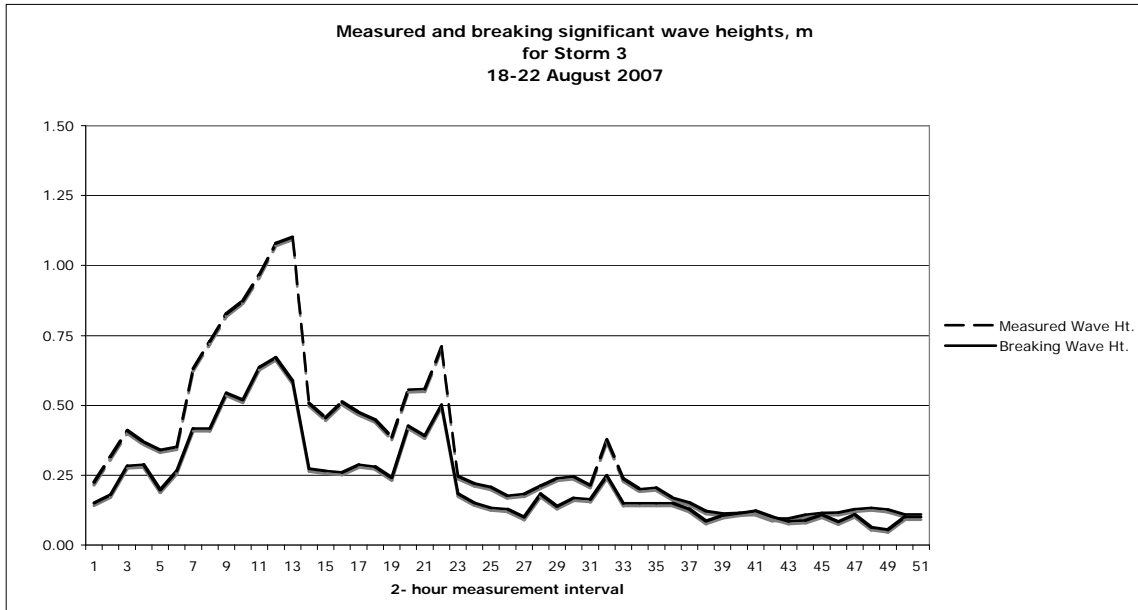


Figure 16. Comparison of measured wave height and breaking wave height during storm 3.

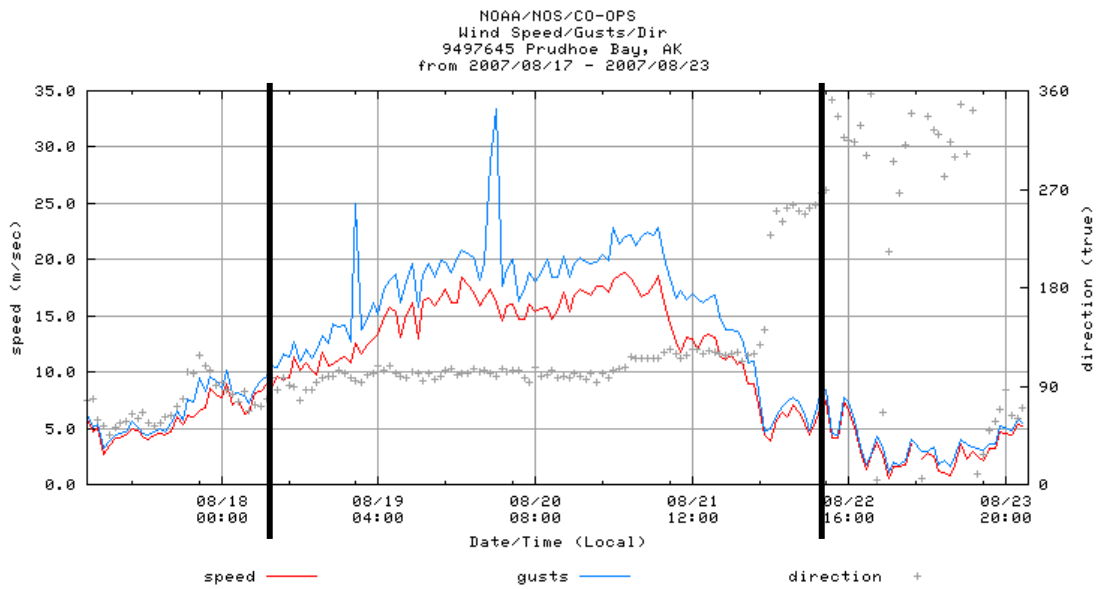


Figure 17. NOAA-measured winds at Prudhoe Bay during the period of storm 3 (between dark vertical lines) from about 0900, 18 August to 1300, 22 August 2007 local time.

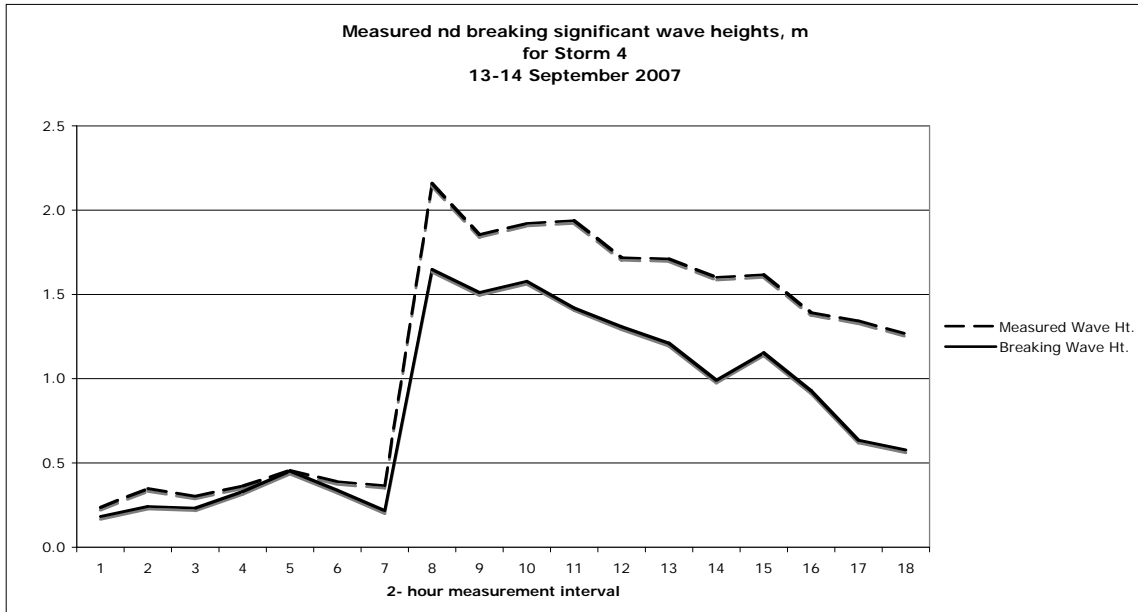


Figure 18. Comparison of measured wave height and breaking wave height during storm 4. The ADCP ceased recording on 14 September 2007.

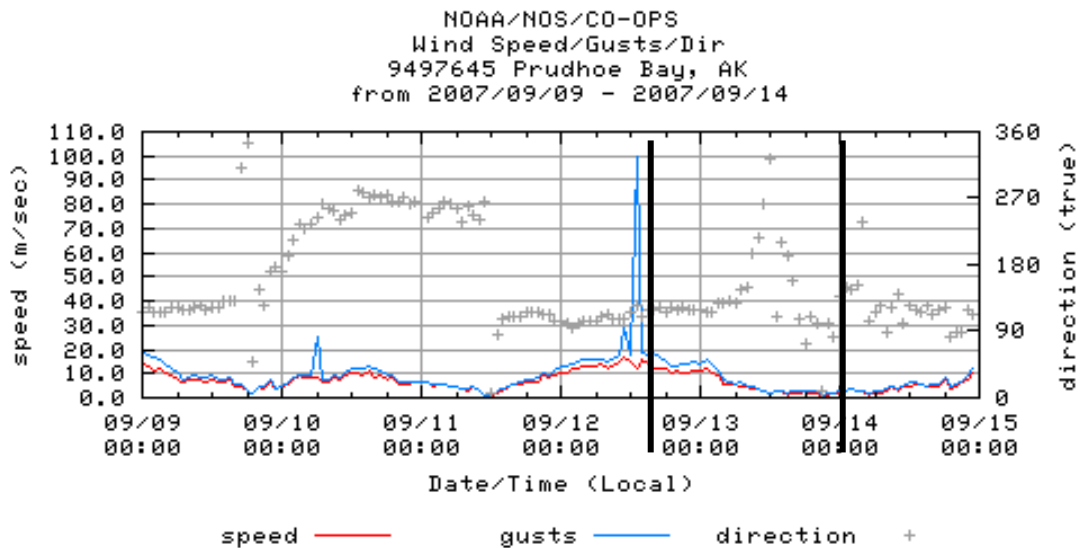
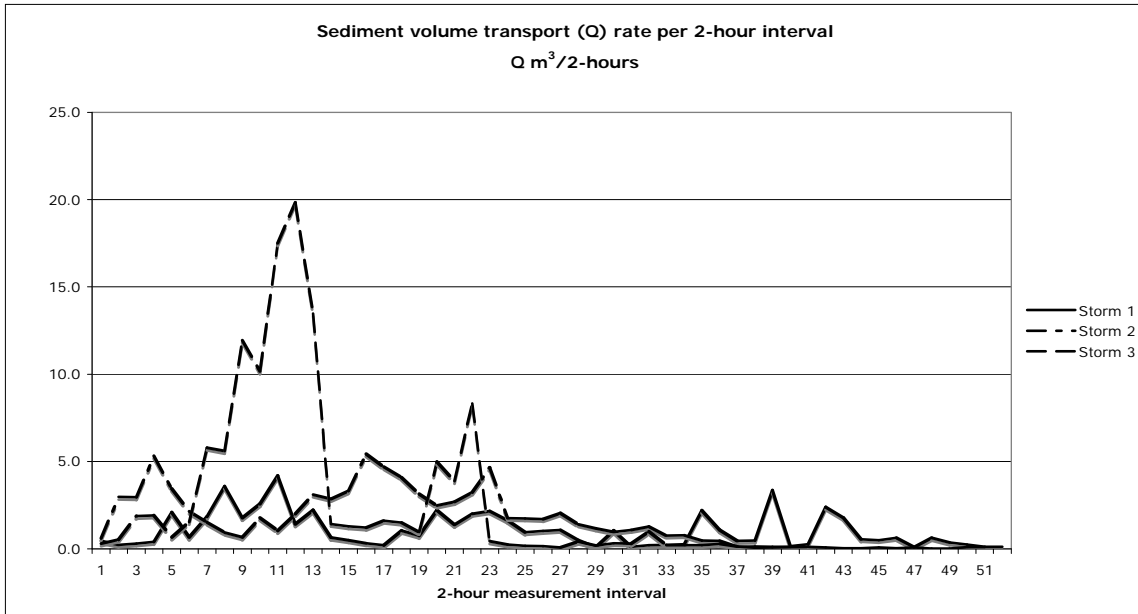
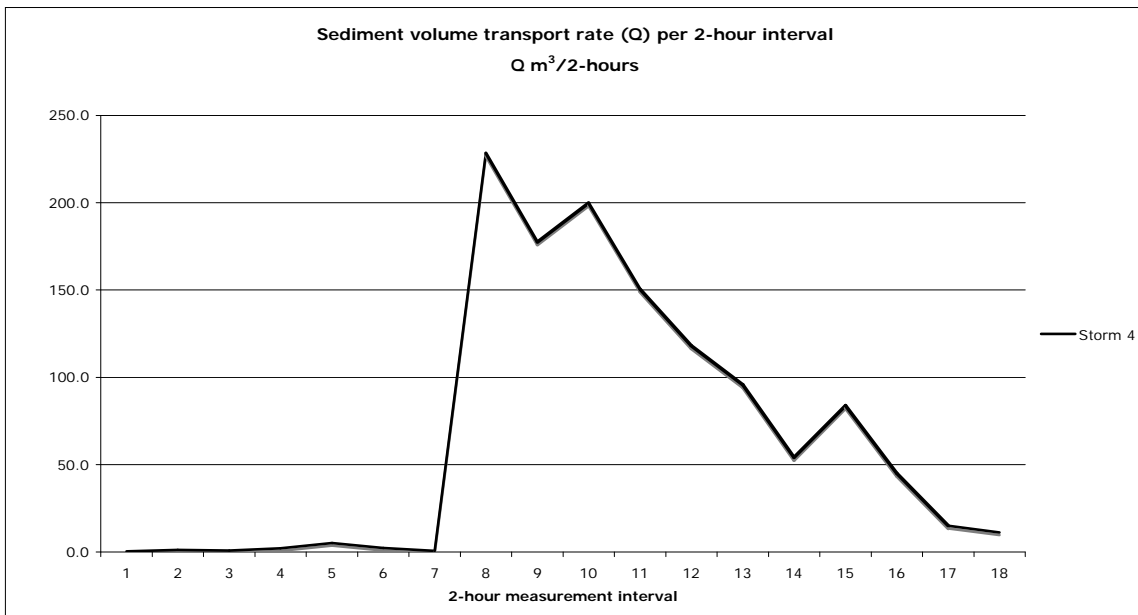


Figure 19. NOAA-measured winds at Prudhoe Bay during the period of storm 4 (between dark vertical lines) from about 0000, 13 September to 1000, 14 September 2007 local time.



**Figure 20. Estimated relative longshore transport rate for storms 1 – 3 plotted for each 2-hour interval of the storm. Note that each storm is of different duration.**



**Figure 21. Estimated relative longshore transport rate for storms 4 plotted for each 2-hour interval of the storm.**

## CONCLUSIONS

Our experiments indicate that assessing the annual rate (by integration of the seasonal observations) of alongshore sediment transport along the north Alaskan arctic beach of Narwhal Island, using PIT-tagged gravel and fluorescent dyed-sand, has been only marginally successful. However, the technique offers scope for assessing the short-term direction and rate of transport of gravel and sand by alongshore currents providing the assessing is confined to one ice-free summer. The tracking of the tagged gravel particles on the beach has been frustrating in post-summer as the tagged gravel particles are presumably emplaced under large sediment mounds (at depths beyond the limit of the PIT reader, about 0.3 m), resulting from piling of the beach deposits by shorefast ice. Such beach reworking also greatly dilutes the dyed sand by mixing with ambient sand (not dyed) to the extent that hardly any tagged sand particles are identified in post-summer beach samples. However, in ice-free summer one month after injection the dyed sand had moved up to ~6.9 m west on the seaward beach. The 2006 and 2007 investigations, encompassing one summer to spring cycle, indicate that the gravel movement can be up to 3 m, 8 m and 29 m westward subsequent to lapse of 1, 2 and 12 months respectively following their time of injection on 30 June, 2006. The October 2006 and July 2007 surveys showed that at berm sites 1, 2, 3 and 4 the maximum displacements seaward on the beach of the tagged gravels were 6.6m, 2.46m, 2.15m and 1.85m respectively. These relatively short displacements were surprising considering that there were a few summer storm surges that extended up to the berm and which were followed by backwash along the beach slope.

The potential volume rate ( $\text{m}^3/2\text{-hr}$ ) and direction of longshore sand transport for the Narwhal Island were computed using the SWAN wave propagation model and the CERC sand transport equations (Rosati et al, 2002). The rates corresponding for each two-hour measurement interval for four storm periods are 55.4, 81.2, 121.6 and 1191.6, all of which were from east to west.

A study of the time-intervals aerial photos, satellite images and historical maps of Narwhal Island indicates occurrence since 1955 of fragmentation of the island into several segments and regrouping of the disjointed units. In the past 50 years, the western end of the island had migrated about 200m to the west which is consistent with the direction of sea-ice movement and coinciding with the frequent east winds during the open water summer period. The net direction of migration was, however, inconsistent with the direction of storm surges which are mainly driven by winds from the northwest. In addition to the island's westward migration, the island has retreated landward by ~5m/year during the past decade, which is close to the findings of others on several North Slope barriers. This database will provide basic information potentially useful for estimating sediment budget changes on the island consequent to alterations in wave-current regime, ice action, and storm frequency, especially resulting from global climate change.

## **Presentations**

During the project period five Quarterly Reports were submitted to the CMI, and a PowerPoint talk on the progress of research was presented by Dr. Kelley and Dr. Naidu at the 2007 and 2008, respectively, CMI/MMS Annual Research Review on February 6, 2007 and 2008. Additionally, the following three oral presentations were made.

Naidu, A.S., J.J. Kelley, Z. Kowalik, W. Lee, M.C. Miller, T.M. Ravens, O.P. Smith and W. Streever. 2007. Assessment of longshore transport rates of gravel and sand on Narwhal Island, north Arctic Alaska: approaches, challenges and progress. Oral presentation at the 58<sup>th</sup> Annual AAAS meeting, September, 2007, Anchorage, AK.

Ravens, T.M., A.S. Naidu, and W. Lee. 2007. Morphodynamics of a North Slope barrier island (Narwhal Island, North Arctic Alaska) 1955-2007. Oral presentation at the 58<sup>th</sup> Annual AAAS meeting, September, 2007, Anchorage, AK.

Naidu, A.S., J. J. Kelley, Z. Kowalik, W. Lee, M.C. Miller, T. M. Ravens, O. P. Smith and R. Gens. 2008. Use of Passive Integrated Transponder tag for assessing transport rate of gravel, north Arctic Alaska. Proc. (Poster) Ocean Sciences Annual Mtg., March 2008, Orlando, FL.

## **Acknowledgements**

This study was funded by the Minerals Management Service, U. S. Department of the Interior through Cooperative Agreement 1435-01-98-CA-33090 (Task Order 0105T039380) between the MMS Alaska Region and the Coastal Marine Institute, University of Alaska Fairbanks. Matching funds were provided by the Institute of Marine Science, University of Alaska Fairbanks; the School of Engineering, University of Alaska Anchorage; the British Petroleum Exploration, Inc (Alaska), Anchorage; the Battelle/PNL/Sequim, and the Coastal and Ocean Concepts, Sequim, Washington State.

Thanks are due to Tony D'Aoust, Thomas Oomen, Mindy Krazykowsky, C. Alstrom and Richard David for assistance in the field and laboratory. Bill Streever, Environmental Studies Leader, British Petroleum Exploration, Inc (Anchorage) has been of immense help by actively participating in the field measurements and beach surveys and in coordinating the partnership between the BP and this study. The encouragements by Vera Alexander and M. Castellini (the respective past and present Directors of the CMI), R. Prentki, Heather Crowley (Project ROTCs) and C. Cowles of the MMS (Anchorage) are appreciated. Thanks are also due to Wilson Cullor, Dianne Sanzone and Dayne Haskell of BP (Anchorage) for arranging the field logistics, and to Ruth Post, Kathy Carter, Maggie Billington, and Marilyn Herkstroeter in the management of the project. The assistance of Sharice Walker in the report preparation is appreciated.

## REFERENCES

- Allen, J.C., R. Hart and V. Tranquili. 2006. The use of Passive Integrated Transponder (PIT) tags to trace cobble transport in a mixed sand-and-gravel beach on the high-energy Oregon coast, USA. *Marine Geology*, 232: 63-86.
- Barnes, P.W. and E. Reimnitz. 1974. Sedimentary processes on arctic shelves off the northern coast of Alaska. In J. C. Reed and J. E. Sater (Eds.), *The Coast and Shelf of the Beaufort Sea*. Arctic Inst. North America, Arlington, VA, 439-475.
- Barnes, P.W., E. Reimnitz, G. Smith and D. McDowell. 1977. Bathymetric and shoreline changes in northwestern Prudhoe Bay, Alaska. *Northern Engineer*, 9:7-13.
- Barnes, P.W. and E. Reimnitz. 1977. Miscellaneous hydrological and geological observations on the inner Beaufort Sea Shelf, Alaska. United States Geological Survey, Washington, D. C., 99 p.
- Barnes, P.W. and P.W. Minkler. 1982. Sedimentation in the vicinity of a causeway groin, Beaufort Sea, Alaska. USGS Open File Rept. 82-615.
- Barnes, P.W. and E. Reimnitz. 1982. Net flow of near-bottom waters on the inner Beaufort Sea shelf as determined from seabed drifters. USGS Open-File Rept. 82-717 pp.
- Barnes, P.W., D.M. Schell and E. Reimnitz (Eds.). 1984. *The Alaskan Beaufort Sea: Ecosystems and Environments*. Academic Press, NY, 466 p.
- Bascom, W.N. 1951. The relationship between sand-size and beach-face slope. *Trans. Am. Geophys. Union*, 32: 866-74.
- CEM (Coastal Engineering Manual), Part I and III. 2002. *Coastal Sediment Processes*. Engineering Manual 1110-2-1100. U. S. Army Corps of Engineers, US Government Printing Office, Washington, D.C.
- da Silva, P.A., A. Temperville and F.S. Santos. 2006. Sand transport under combined current and wave conditions: A semi-unsteady, practical model. *Coastal Engineering*, 53:987-913.
- de Meijer, R.J., J. Bosboom, B. Cloin, I. Katopodi, N. Kitou, R.L. Koomans and F. Manso. 2002. Gradation effects in sediment transport. *Coastal Engineering*, 47:179-210.
- Dygas, J.D. and D.C. Burrell. 1976a. Dynamic sedimentological processes along the Beaufort Sea coast of Alaska. In: D. W. Hood and D. C. Burrell (Eds.), *Assessment of the Arctic marine environment: selected topics*. Ocl. Pbl. 4, Inst. Marine Sc., Univ. Alaska, Fairbanks, AK, 189-203.
- Dygas, J.A. and D.C. Burrell. 1976b. Response of waves and currents to wind patterns in an Alaskan lagoon. In: D. W. Hood and D. C. Burrell (Eds.), *Assessment of the Arctic marine environment: selected topics*. Ocl. Pbl. 4, Inst. Marine Sc., Univ. Alaska, Fairbanks, AK, 263-285.
- Envirosphere Company. 1987. *Endicott Environmental Monitoring Program*. Final Rept. to U.S. Army Corps of Engineers, Alaska District, Anchorage, AK.
- Environmental Systems Research, Inc. 2007.
- Greene, H.G., 1970. Microrelief of an Arctic beach. *Jour. Sedimentary Petrology*, 40:419-427.
- Hale, D.A., M.J. Hameedi, L.E. Hachmeister, and W.J. Stringer. 1989. Effects of the West Dock causeway on nearshore oceanographic processes in the vicinity of Prudhoe Bay, Alaska. Rept. for the USEPA, Region 10, NOAA/OAD, U. S. Dept. Commerce, Anchorage, AK. 50 pp.

- Hume, J.D. and M. Schalk. 1967. Shoreline processes near Barrow, Alaska: a comparison of the normal and the catastrophic. *Arctic*, 20:86-103.
- IPCC (Intergovernmental Panel on Climate Change). 2001. IPCC Third Assessment Report- Climate Change 2001: The Scientific Basis. Cambridge University Press, Cambridge, UK. 639-693.
- Jorgenson, T. and J. Brown. 2004. Classification of the Alaskan Beaufort Sea coast and estimates of sediment and carbon inputs from coastal erosion. In: V. Rachold and G. Cherkashov (eds.), Report 4<sup>th</sup> International Workshop on Arctic Coastal Dynamics, St Petersburg (Russia), Ber. Polarforsch. Meeresforsch, 482:32.
- King, D.B. 2005. Influence of Grain Size on Sediment Transport Rates with Emphasis on the Total Longshore Rate. U.S. Army Engineer Research and Development Center, Vicksburg, MS, ERDC/CHL CHETN-II-48. 24pp.
- Kobayashi, N., A. Agrawal and B.D. Johnson. 2007. Longshore current and sediment transport on beaches. *Jour. Waterway, Port, Coastal and Ocean Engineering*, ASCE July/August, pp. 296-404.
- Komar, P.D. 1976. Beach Processes and Sedimentation. Englewood Cliffs, Prentice-Hall, NJ.
- Komar, P.D. 1983. Handbook of Coastal Processes and Erosion. Chemical Rubber Co., Austin, TX.
- Komar, P.D. 1998. Beach Processes and Sedimentation. Upper Saddle River, Prentice Hall, New Jersey, 544p.
- Komar, P.D. and D.L. Inman. 1970. Longshore sand transport on beaches. *Jour. Geophys. Res.*, 75:5914-5927.
- Kowalik, Z. 1984. Storm surges in the Beaufort and Chukchi Seas. *Jour. Geophys. Res.*, 89: 10,570-10,578.
- Kozo, T.L. 1984. Mesoscale wind phenomena along the Alaskan Beaufort Sea coast. In: Barnes, P. W., D. M. Schell and E. Reimnitz (Eds.). *The Alaskan Beaufort Sea: Ecosystems and Environments*. Academic Press, NY, 23-45.
- Lamarre, H., B. Mac Vicar, A.G. Roy. 2005. Using Passive Integrated Transponder (PIT) tags to investigate sediment transport in gravel bed rivers. *Jour. Sediment. Res.*:75(4).
- Matthews, J.B. 1970. Tides at Point Barrow. *The Northern Engineer*. 2:12-13.
- Li, D., V. Panchang, and J. Jin. 2005. Development of an online coastal wave prediction system. *Solutions to Coastal Disasters 2005. Proceedings of the Conference, May 8-11, 2005, Charleston, SC; pp 24-32.*
- Middleton, G.V. and J.B. Southard. 1978. *Mechanics of Sediment Movement*. Lecture notes for short course #3, Soc. Economic Paleontologists and Mineralogists, Binghamton, New York.
- Miller, M.C. and P. Gadd. 1983. Shoreline processes near Flaxman Island, U. S. Beaufort Sea, Alaska. *Proc. Workshop on Regional Coastal Erosion and Sedimentation Calgary, Alberta*, pp. 69-91.
- Morack, J.L. and R.C. Rogers. 1981. Seismic evidence of shallow permafrost beneath is lands in the Beaufort Sea. *Arctic*, 34:168-174.
- Naidu, A.S. and T.C. Mowatt. 1994. Origin of gravels from the southern coast and continental shelf of Beaufort Sea, Arctic Alaska. *Proc. International Conference on Arctic Margins.*

- D. K. Thurston and K. Fujita (Editors), Minerals Management Service (Anchorage), 351–356.
- Naidu, A.S. and T.C. Mowatt. 1975. Depositional environments and sediment characteristics of the Colville and adjacent deltas, Northern Arctic Alaska. In: M. L. Broussard (Ed.), *Deltas: Models for Subsurface Exploration*. Houston Geol. Soc., Houston, 283-309.
- Naidu, A.S., T.C. Mowatt, S.E. Rawlinson and H.V. Weiss. 1984. Sediment characteristics of the lagoons of the Alaskan Beaufort Sea coast, and evolution of Simpson Lagoon. In: Barnes, P. W., D. M. Schell and E. Reimnitz (eds.), *The Alaskan Beaufort Sea: Ecosystems and Environments*. Academic Press, NY, 275-292.
- Naidu, A.S., J. Kelley, Z. Kowalik, W. Lee, M. Miller, and O. Smith. 2006. Assessment of the direction and rate of alongshore transport of sand and gravel in the Prudhoe Bay region, North Arctic Alaska. Annual Report No.13, Coastal Marine Institute, Univ. Alaska Fairbanks, Fairbanks, AK, 1-10.
- National Geodetic Survey, 2007. National Geodetic Survey-CORS. Silver Springs, National Geodetic Survey.
- National Oceanographic Survey. 1990. McClure and Stockton Islands and vicinity. U. S. Dept. Commerce, Washington, D. C.
- Nummedal, D. 1979. Coarse-grained sediment dynamics- Beaufort Sea, Alaska. Proc. 5<sup>th</sup> Conference on Port and Ocean Engineering under Ice Arctic Conditions, Trondheim, Norway, V.II:845-858.
- Owens, E.H., J.R. Harper and D. Nummedhal. 1980. Proc. 17<sup>th</sup> Intn'l. Coastal Engr. Conf., ASCE/Sydney, 1344.
- Osborne, P.D. 2005. Transport of gravel and cobble on a mixed-sediment inner bank shoreline of a large inlet, Grays Harbor, Washington. *Marine Geology*, 224:145-156.
- Pontee, N.I., K. Pye and S.J. Blott. 2004. Morphodynamic behavior and sedimentary variation of mixed sand and gravel beaches, Suffolk, UK. *Jour. Coastal Research*, 20:256-276.
- Proshutinsky, A. Yu. 1993. Arctic Ocean Level Oscillations. Gidrometeoizdat, St. Petersburg, 216 pp. (in Russian).
- Ravens, T.M., A.S. Naidu, and W. Lee. 2007. Morphodynamics of a North Slope barrier island (Narwhal Island, North Arctic Alaska) 1955-2007. Proc. 58<sup>th</sup> Annual AAAS Meeting, September 2007, Anchorage.
- Reimnitz, E. and E.W. Kempema. 1987. Thirty-four-year shoreface evolution at a rapidly retreating Arctic coastal site. In: T. D. Hamilton and J. P. Galloway (eds.), *Geological Studies in Alaska by the U. S. Geological Survey During 1986.*, U. S. Geol. Survey Cir. 99:161-164.
- Ris, R.C., L.H. Holthuijsen and N. Booij, 1999. A third-generation wave model for coastal regions 2. Verification. *Jour. Geophys. Research*. 104(C4):7667-7682.
- Rosati, J., T. Walton and K. Bodge. 2002. Longshore Sediment Transport. In: *Coastal Engineering Manual, Part III, Chapter 2*. US Army Corps of Engineer, Engineering Research and Engineering Development Center (ERDC), Vicksburg, MS. EM 1110-2-1100 (Part III), 30 April 2002. 113pp.
- Roussel, J.M., A. Haro, R.A. Cunjak. 2000. Field test of a new method for tracking small fishes in shallow rivers using Passive Integrated Transponder (PIT) technology. *Can. J. Fish Aquat. Sci.*, 57:1326-1329.

- Schwartz, M.L. 1972. Spits and Bars. Dowden Hutchinson and Ross, Stroudsburg, Pa. 452 pp.
- Shepard, F.P. 1973. Submarine Geology. Harper and Row, New York, NY. 517pp.
- Short, A.D., J.M. Coleman, and L.D. Wright. 1974. Beach dynamics and nearshore morphology of the Beaufort Sea coast. Alaska. In J. C. Reed and J. E. Sater (Eds.), The Coast and Shelf of the Beaufort Sea. Arctic Inst. North America, Arlington, VA, 477-488.
- Soulsby, R.L. and J.S. Damgaard. 2005. Bedload sediment transport in coastal waters. Coastal Engineering, 52:673-689.
- Trimble Navigation Ltd. 2001. Trimble Geomatics Office., Trimble Navigation Ltd., Sunnyvale.
- Trimble Navigation Ltd. 2005. Trimble Pathfinder Office. Trimble Navigation Ltd., Sunnyvale.
- United States Army Map Service. 1955. Beechey Point (B-1) Quadrangle. 1:63,360 Series (Topographic). U. S. Geological Survey, Reston, VA.
- Voropayev, S.I., A.W. Cense, G.B. McEachern, D.L., Boyer and H.J.S. Fernando. 2001. Dynamics of cobbles in the shoaling region of a surf zone. Ocean Engineering, 28:763-788.
- Voropayev, S.I., F.Y. Testik, H.J.S. Fernando and D.L. Boyer. 2003. Morphodynamics and cobbles behavior in and near the surf zone. Ocean Engineering, 30:1741-1764.
- Van Wellen, E.V., A.J. Chadwick, and T. Mason. 2000. A review and assessment of longshore sediment transport equations for coarse-grained beaches. Coastal Engineering, 40:243-275.
- Weggel, J.R. 1972. "Maximum Breaker Height", Journal of the Waterways, Harbors, and Coastal Engineering Division, 98(No. WW4):529-548.
- Wiseman, Wm. J., J.M. Coleman, A. Gregory, S.A. Hsu, A.D. Short, J.N. Suhayda, C.D. Walters, Jr., and L.D. Wright. 1973. Alaskan Arctic Coastal Processes and Morphology. Louisiana State Univ., Coastal Studies Inst., Tech. Rept. 149, 171p.
- Work, P., F. Fehrenbacher and G. Voulgaris. 2004. Nearshore impacts of dredging for beach nourishment. Jour. of Waterway, Port, Coastal and Ocean Engineering. 130(6): 303-311.

**Appendix 1. Storm Surges and Sediment Transport Models in the Beaufort Sea by Zygmunt Kowalik.**

# Storm Surges and Sediment Transport Models in the Beaufort Sea

By Zygmunt Kowalik, Institute of Marine Science, University of Alaska, Fairbanks

## 1. Introduction

In the shallow water of the Arctic Ocean the sediment transport is forced by a large number of interacting mechanisms. Dynamics of sediments changes on the temporal and spatial scales under influence of storm surges, wind waves, tides, river runoff, and ice.

The main components of natural forcing which can influence sediment motion in the vicinity of the Beaufort Sea shelf are: (i) permanent circulation due to sea level gradient between the Pacific and Atlantic Oceans, (ii) wind and surface waves, (iii) tides, (iv) thermohaline currents, and (v) ice gauging. The latter factor caused by the sea ice with its ridges, stamukhas, and deep keels can move sediments and disturb bottom surface quite significantly. In summer and especially in fall, when the coastal regions are free of ice the water motion impart sediment transport mainly through two mechanisms (in addition to permanent currents): wind generated waves and wind-driven currents. Throughout the winter/spring season, the shore-fast ice (in the shallow coastal water) and the pack ice (over shelf) reduce the energy of wind and wave generated currents substantially, but under sea ice, the permanent and tidal currents still may cause suspended sediment motion.

We investigate mainly the summer/fall dynamical processes in the vicinity of the Narwhal Island (located at the north-western end of the McClure islands chain) employing models capable to resolve two basic motions of sediments: under influence of wind-driven currents and caused by wind-waves. Although the both mechanisms of sediment transport and erosion work in interaction, our first order approach is to investigate them separately employing, respectively storm surge (wind-driven) and wind-wave models designed for coastal regions.

A set of storm surge models developed by Kowalik (1984) and Proshutinsky (1993) for simulation of sea level, currents, ice movement and ice concentration, forced by wind and tides is aided by the sediment transport equations.

This report is organized as following: first we describe storm surge and sediment transport models employed in this study (section 2). Section 3 is dedicated to the investigation of the specifics of sediment transport in the region under research and includes studies of the basic circulation features and their influence on the sediment transport. Section 4 summarizes project results and provides major conclusions and recommendations.

## 2. Basic equations

The vertically averaged equations of motion and continuity in the spherical system are (Kowalik, 1984):

$$\begin{aligned} \frac{\partial u}{\partial t} + \frac{u}{R_o \cos \phi} \frac{\partial u}{\partial \lambda} + \frac{v}{R_o} \frac{\partial u}{\partial \phi} - \left(2\Omega + \frac{u}{R_o \cos \phi}\right) v \sin \phi = \\ - \frac{g}{R_o \cos \phi} \frac{\partial \zeta}{\partial \lambda} - \frac{g}{R_o \cos \phi} \frac{\partial P_a}{\partial \lambda} + \frac{(1-c)\tau_\lambda^a}{\rho_o D} + \frac{c\tau_{\lambda,i}^w}{\rho_o D} - \frac{\tau_\lambda^b}{\rho_o D} + A\Delta u \end{aligned} \quad (1)$$

$$\frac{\partial v}{\partial t} + \frac{u}{R_0 \cos \phi} \frac{\partial v}{\partial \lambda} + \frac{v}{R_0} \frac{\partial v}{\partial \phi} + \left(2\Omega + \frac{u}{R_0 \cos \phi}\right) u \sin \phi =$$

$$-\frac{g}{R_0} \frac{\partial \zeta}{\partial \phi} - \frac{g}{R_0} \frac{\partial P_a}{\partial \phi} + \frac{(1-c)\tau_\phi^a}{\rho_o D} + \frac{c\tau_{\phi,i}^w}{\rho_o D} - \frac{\tau_\phi^b}{\rho_o D} + A\Delta v$$
(2)

$$\frac{\partial \zeta}{\partial t} + \frac{1}{R_0 \cos \phi} \frac{\partial u D}{\partial \lambda} + \frac{1}{R_0 \cos \phi} \frac{\partial}{\partial \phi} (Dv \cos \phi) = 0$$
(3)

In the above equations,  $R_0$  is the radius of Earth and is equal to 6370 km,  $u$  is the velocity in the  $\lambda$  (E-W) direction,  $v$  denotes the velocity in the  $\phi$  (N-S) direction, and  $\zeta$  is the sea level,  $t$  is the time,  $g$  is Earth's gravity acceleration ( $g=981 \text{ cm s}^{-2}$ ),  $\rho$  is sea water density,  $H$  is the average (undisturbed) water depth, and  $D$  is the total depth  $D = H + \zeta$ . The Coriolis parameter will be taken as  $f = 2\Omega \sin \phi$ . It is a function of the Earth's angular velocity  $\Omega = 7.29 \times 10^{-5} \text{ s}^{-1}$  and the latitude  $\phi$ .

The water motion is imparted by the air stresses  $\tau_{\lambda}^a, \tau_{\phi}^a$  and/or by the stress between ice and water  $\tau_{\lambda,i}^w, \tau_{\phi,i}^w$  but the strength of the air stress over the sea depends on the ice concentration  $1 - c$  and the strength of the ice stress is proportional to  $c$ . When the water surface is free of ice ( $c = 0$ ), the water motion is imparted by the air stress only, on the other hand when the water surface is completely covered by the ice ( $c = 1$ ) the water motion is caused by the ice motion only.

The components of the bottom friction force are nonlinear functions of water velocity:

$$\tau_{\lambda}^b = ru\sqrt{(u^2 + v^2)} \quad \text{and} \quad \tau_{\phi}^b = rv\sqrt{(u^2 + v^2)},$$

or:

$$\frac{\tau_{\lambda}^b}{\rho_o D} = \frac{ru\sqrt{(u^2 + v^2)}}{\rho_o D} = R_x u$$
(4a)

$$\frac{\tau_{\phi}^b}{\rho_o D} = \frac{rv\sqrt{(u^2 + v^2)}}{\rho_o D} = R_y v$$
(4b)

The dimensionless bottom friction coefficient  $r$  is taken as  $3.3 \times 10^{-3}$ .

The ice motion induced by wind is investigated through the equations of ice drift (Rothrock, 1975)

$$m \frac{\partial u_i}{\partial t} + m \frac{u_i}{R_0 \cos \phi} \frac{\partial u_i}{\partial \lambda} + m \frac{v_i}{R_0} \frac{\partial u_i}{\partial \phi} - m \left(2\Omega + \frac{u_i}{R_0 \cos \phi}\right) v_i \sin \phi =$$

$$-m \frac{g}{R_0 \cos \phi} \frac{\partial \zeta}{\partial \lambda} - hc \frac{g}{R_0 \cos \phi} \frac{\partial P_a}{\partial \lambda} + c(\tau_{\lambda,i}^a - \tau_{\lambda,i}^w) + F_{\lambda,i}$$
(5)

$$\begin{aligned}
m \frac{\partial v_i}{\partial t} + m \frac{u_i}{R_o \cos \phi} \frac{\partial v_i}{\partial \lambda} + m \frac{v_i}{R_o} \frac{\partial v_i}{\partial \phi} + m(2\Omega + \frac{u_i}{R_o \cos \phi}) u_i \sin \phi = \\
-m \frac{g}{R_o} \frac{\partial \zeta}{\partial \phi} - hc \frac{g}{R_o} \frac{\partial P_a}{\partial \phi} + + c(\tau_{\phi,i}^a - \tau_{\phi,i}^w) + F_{\phi,i}
\end{aligned} \tag{6}$$

The rate of change of the ice mass ( $m$ ) over a specific area is equal to the net influx of mass to that area plus sources and sinks ( $S$ ). The above considerations lead to the following equation for the ice mass conservation:

$$\frac{\partial m}{\partial t} + \frac{1}{R_o \cos \phi} \frac{\partial um}{\partial \lambda} + \frac{1}{R_o \cos \phi} \frac{\partial}{\partial \phi} (mv \cos \phi) = S \tag{7}$$

In the above equations,  $h$  is the ice thickness,  $u_i$  and  $v_i$  denote the ice velocity along the E-W and N-S, respectively,  $\tau_{\lambda,i}^a$  and  $\tau_{\phi,i}^a$  are the components of the wind stress vector over the ice.  $F_{\lambda,i}$  And  $F_{\phi,i}$  are components of the internal ice stresses.

Other parameters which influence sea level variability during storm events are wind waves which characteristics depend on sea ice conditions, wind strength, duration and direction. In the near-shore domain the breaking waves induce a sea level setup which results in the sea level gradient responsible for the along and offshore-currents. This motion is important for the coastline and bottom erosion and sediment transport.

To include current-waves interaction during storms expressed by the wave-driven radiation stresses the storm-surge model is refined following Zhou and Li (2005). An additional stresses  $\tau_{\lambda,s}$  and  $\tau_{\phi,s}$  is introduced in equations (1) and (2) to reproduce this effect. The wave-driven radiation stresses  $S_{\lambda\lambda}$ ,  $S_{\phi\phi}$  and  $S_{\lambda\phi}$  are calculated as:

$$\tau_{\lambda,s} = -\frac{1}{\rho DR_o \cos \phi} \frac{\partial}{\partial \lambda} (S_{\lambda\lambda} + S_{\lambda\phi}); \quad \tau_{\phi,s} = -\frac{1}{\rho DR_o} \frac{\partial}{\partial \phi} (S_{\phi\phi} + S_{\lambda\phi}) \tag{8}$$

The simplified components of wave-driven radiation stress are given as:

$$S_{\lambda\lambda} = E \frac{c_g}{c_{ph}} (1 + \cos^2 \alpha) - 0.5 \quad S_{\phi\phi} = E \frac{c_g}{c_{ph}} (1 + \sin^2 \alpha) - 0.5$$

$$S_{\lambda\phi} = \frac{E}{2} \frac{c_g}{c_{ph}} \sin 2\alpha \tag{9}$$

Where:  $E$  is the wave energy,  $c_g$  group velocity,  $c_{ph} = \sqrt{gD}$  is the phase velocity and  $\alpha$  is the wave angle.

### Storm-Induced Sediment Transport

The depth-averaged sediment concentration ( $c_s$ ) is calculated from equation of transport:

$$\begin{aligned}
\frac{\partial c_s D}{\partial t} + \frac{1}{R \cos \phi} \frac{\partial uc_s D}{\partial \lambda} + \frac{1}{R \cos \phi} \frac{\partial}{\partial \phi} (c_s v D \cos \phi) = \\
+ \frac{1}{R^2 \cos^2 \phi} \frac{\partial}{\partial \lambda} (D_\lambda D \frac{\partial c_s}{\partial \lambda}) + \frac{1}{R^2 \cos \phi} \frac{\partial}{\partial \phi} (D_\phi D \cos \phi \frac{\partial c_s}{\partial \phi}) + S
\end{aligned} \tag{10}$$

In the above equation  $D_\lambda$  and  $D_\phi$  denote sediment diffusivity coefficients and  $S$  denotes sources and sinks of sediments due to exchange of sediments between suspended and bed loads. This term can be defined in terms of the upward and downward sediment flux (Zhou and Li, 2005)

$$S = E_n \rho_s - w c_b \quad (11)$$

Here  $\rho_s$  is the density of sediment particles,  $E_n$  is the entrainment function,  $w$  is the settling velocity and  $c_b$  is the sediment concentration at the bottom.

Upward flux ( $E_n \rho_s$ ) at the bed is due to entrainment of individual sediment particles into the flow. Such entrainment occurs when the bottom stress caused by a near-bed shear is strong enough to set particle into motion. The possibility of entrainment is commonly defined by the *Shields* parameter

$$\Theta = \frac{u_*^2}{(s-1)gd} \quad (12)$$

Here,  $s = \rho_s / \rho$ ,  $d$  is the sediment diameter and  $u_*$  is the friction velocity defined by the bottom stress.

A simplified approach for calculations of sediment transport could be based on the following equation for the sediment mass conservation which is similar to equation of concentration (10),

$$\frac{\partial m}{\partial t} + \frac{1}{R_o \cos \phi} \frac{\partial um}{\partial \lambda} + \frac{1}{R_o \cos \phi} \frac{\partial}{\partial \phi} (mv \cos \phi) = S \quad (13)$$

In the above equations,  $m$  is the sediment mass, and  $u$  and  $v$  denote the sediment velocity  $u_s$  along the E-W and  $v_s$  – along N-S, and  $S$  is a source of sediments. The sediment velocities are calculated based on water velocities according to empirical relations shown in Figure 1. This simplified relation describes the critical velocity which determines the sediment movement. It is based on the original Shields relation between critical shear stress and grain size (Open University Course Team, 1989).

Figure 1 depicts 3 phases of the sediment motion. The blue curve defines the threshold velocity for starting sediment motion (at the small grain size below 0.05mm the sediments ought to be unconsolidated). Initially the sediments are not distributed over the entire water column and sediment motions occur as a bed load transport, but slowly as water velocity increases the suspended sediments move from the near bottom area into the entire water column. For this motion, the water velocity needs to reach a second limit depicted by the red line. Above this line the sediments are transported as suspended load and are moved with the same velocity as water. In our calculation considering medium size sediments of 0.4 mm diameter (usually this is a non-cohesive/unconsolidated sand) we can define three basic regimes of sediments movement:

If water velocity  $u$  is less than  $u_b$  than there is no sediment transport and  $u_s = 0$ .

If  $u_e < u < u_b$ , the sediment moves as

$$U_s = \frac{u - u_b}{u_e - u_b} u \quad (14)$$

Notice that term  $\frac{u - u_b}{u_e - u_b}$  is 0 when  $u = u_b$  and  $\frac{u - u_b}{u_e - u_b}$  is 1 when  $u = u_e$  thus according to Eq. 14

the water motion is linearly transferred to sediments. Finally, when  $u \geq u_e$  the sediments will move with the same speed as water,  $U_s = u$ .

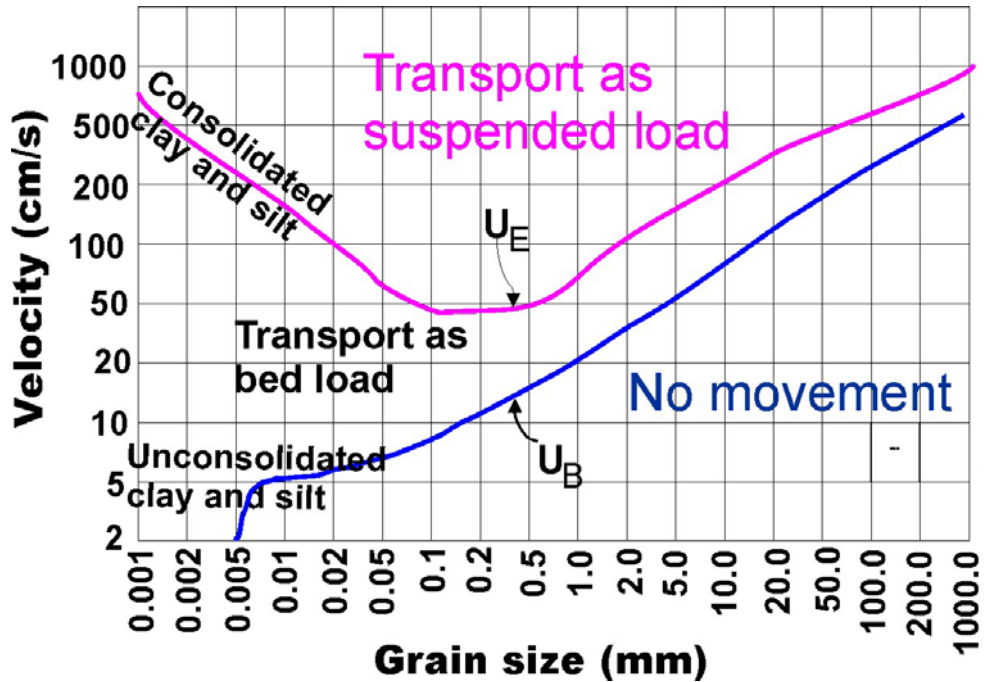
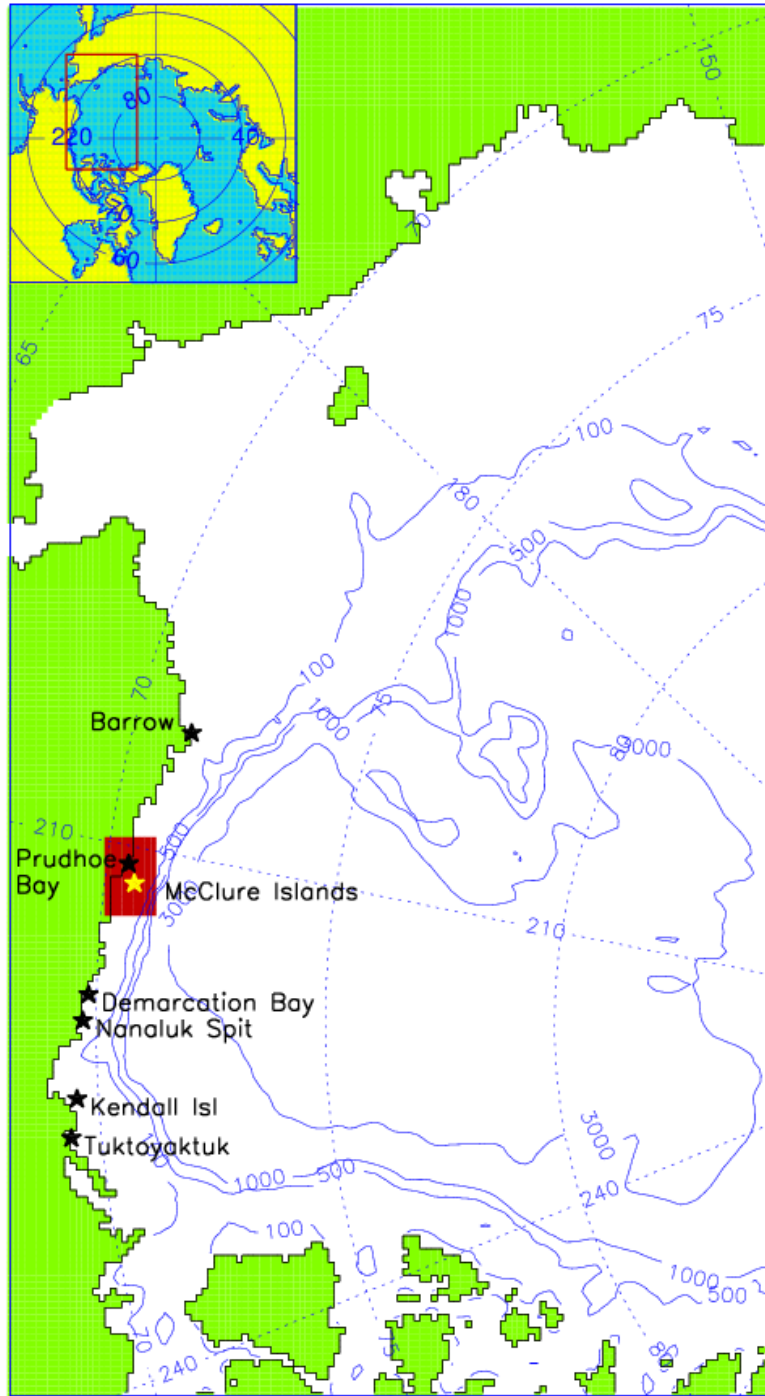


Figure 1 Empirical relations between critical water velocity and sediment transport. Blue line denotes the threshold velocity for the sediment motion (at the small grain size below 0.05mm the blue line is followed only by the unconsolidated sediments). Red line indicate critical velocity for the sediment transport as suspended load (at the small grain size below 0.05mm the red line denotes the threshold velocity for consolidated sediments).

### 3. Peculiarities of sediment transport in the vicinity of McClure Islands

#### 3.1 Models and model domains

In order to investigate circulation and sediment transport in the vicinity of Narwhal Island (70°23'45'' and 147°31'35''W, the first island on the north-western end of the McClure Island chain) we have developed two numerical models, namely: a relatively coarse resolution (13.89 km) model of the Canada Basin (see Figure 2 showing this model domain) and a very high resolution model (0.1389 km, see Figure 3) of the region surrounding McClure Islands.



**Figure 2. Coarse resolution (13.89 km) model domain and bathymetry (blue, m). Red rectangular shows location of the fine resolution model domain. Black stars denote locations of stations where sea level is verified against observations. Yellow star shows location of McClure Islands.**

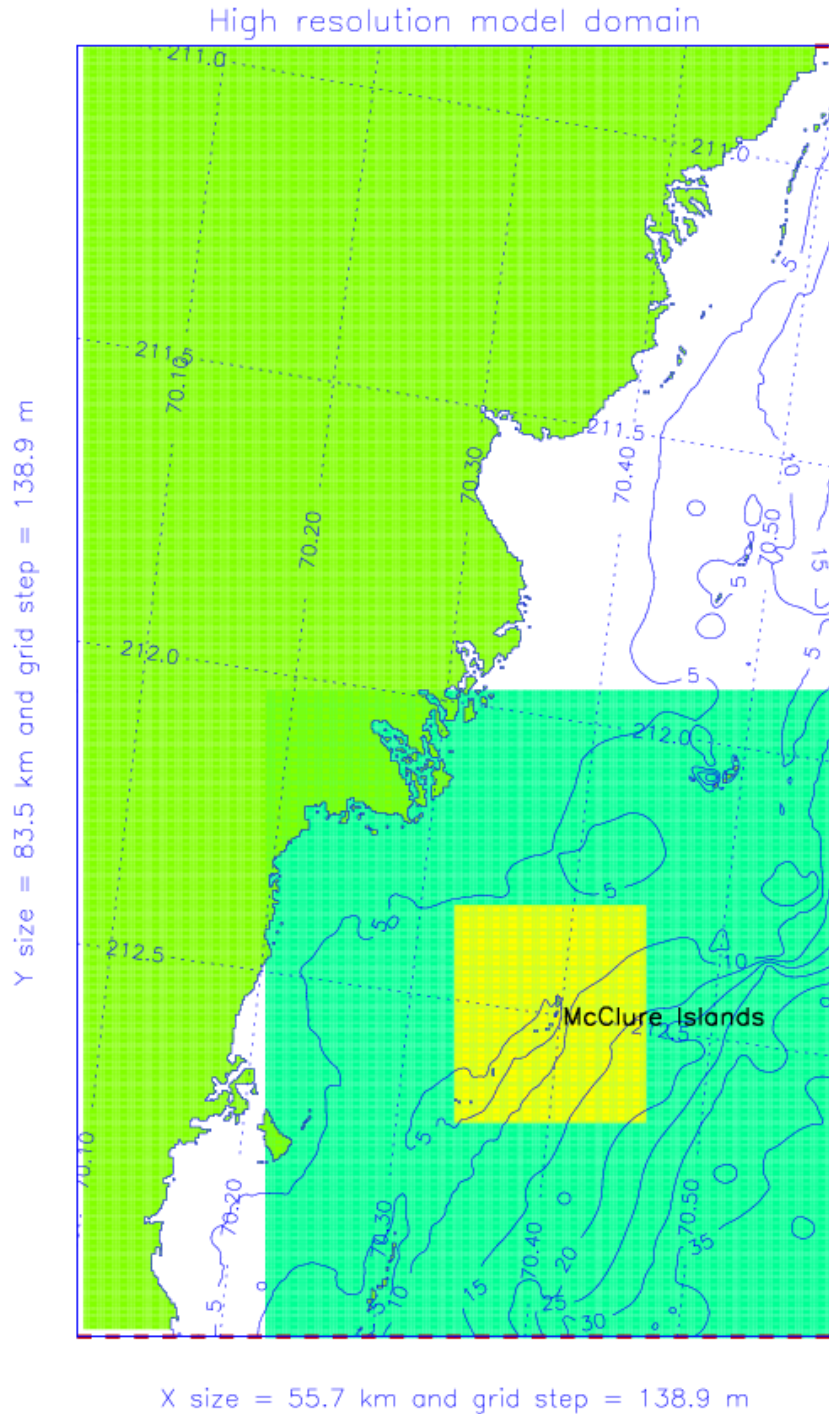


**Figure 3. Fine resolution (0.1389 km) model domain and bathymetry (blue, m). Yellow and green rectangular show location of subdomains where results will be illustrated in figures with more details.**

### 3.2. Major factors

There are four components of natural forcing which can influence sediment motion in the vicinity of McClure Islands: (i) permanent circulation due to sea level gradient between the Pacific and Atlantic Oceans, (ii) wind and surface waves, (iii) tides, and (iv) thermohaline currents. There is one more factor which can move sediments and disturb bottom surface significantly – this is the sea ice with its ridges, stamukhas, and deep keels but this factor is not investigated in this study.

Tidal velocities are relatively small in this region and are not taken into account here but in the future they have to be included in simulations because in combination with other factors the total forcing can exceed the threshold of  $u_b$  (see eq. 14) and participate in the sediment transport as well.

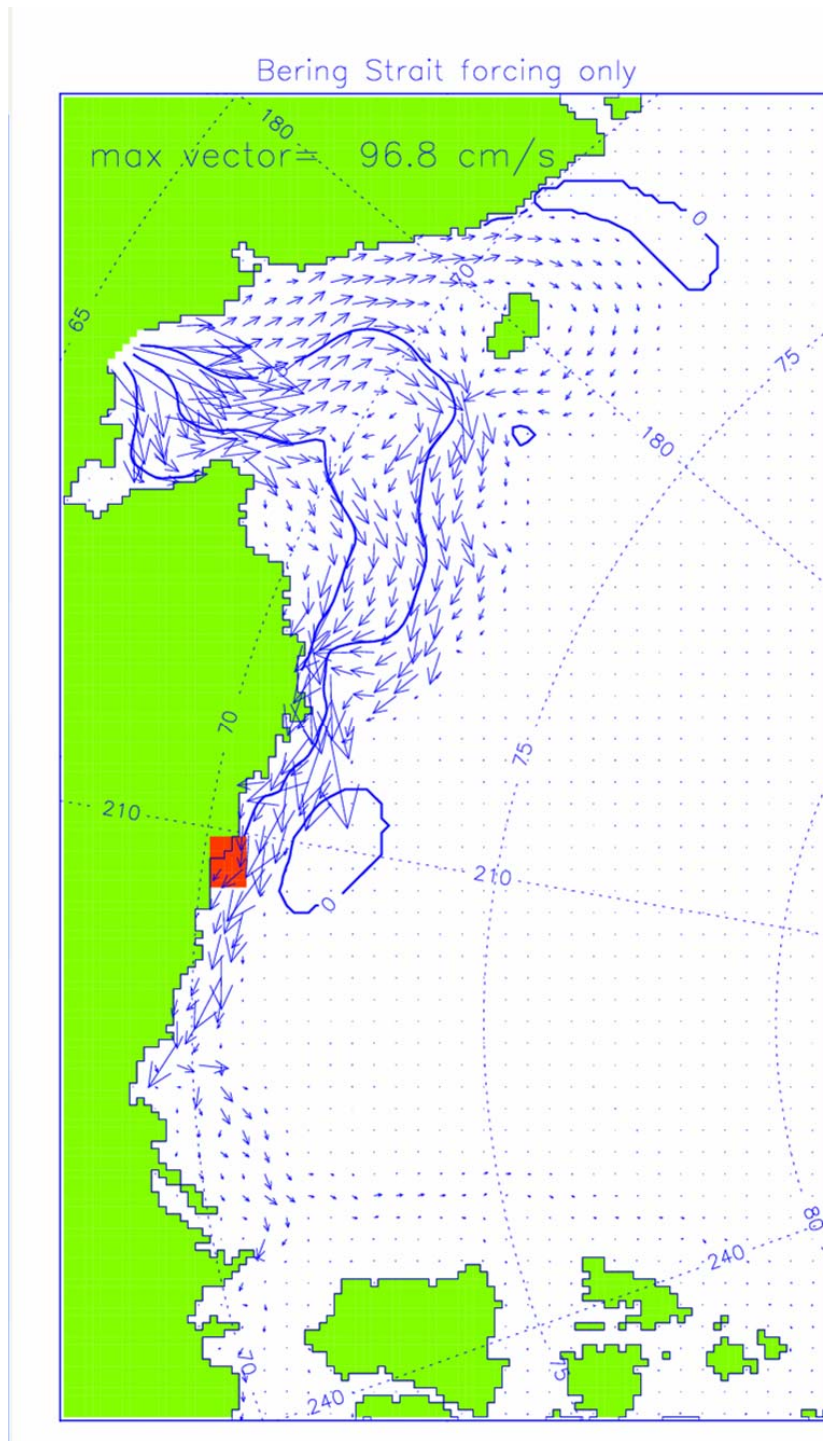


**Figure 4** Circulation and sea surface height contours (cm) in the coarse resolution model domain under Bering Strait inflow forcing only. Maximum vector velocity is 96.8 cm/s in the Bering Strait region. Red rectangular shows region of high resolution model domain (results are shown in Figure 5).

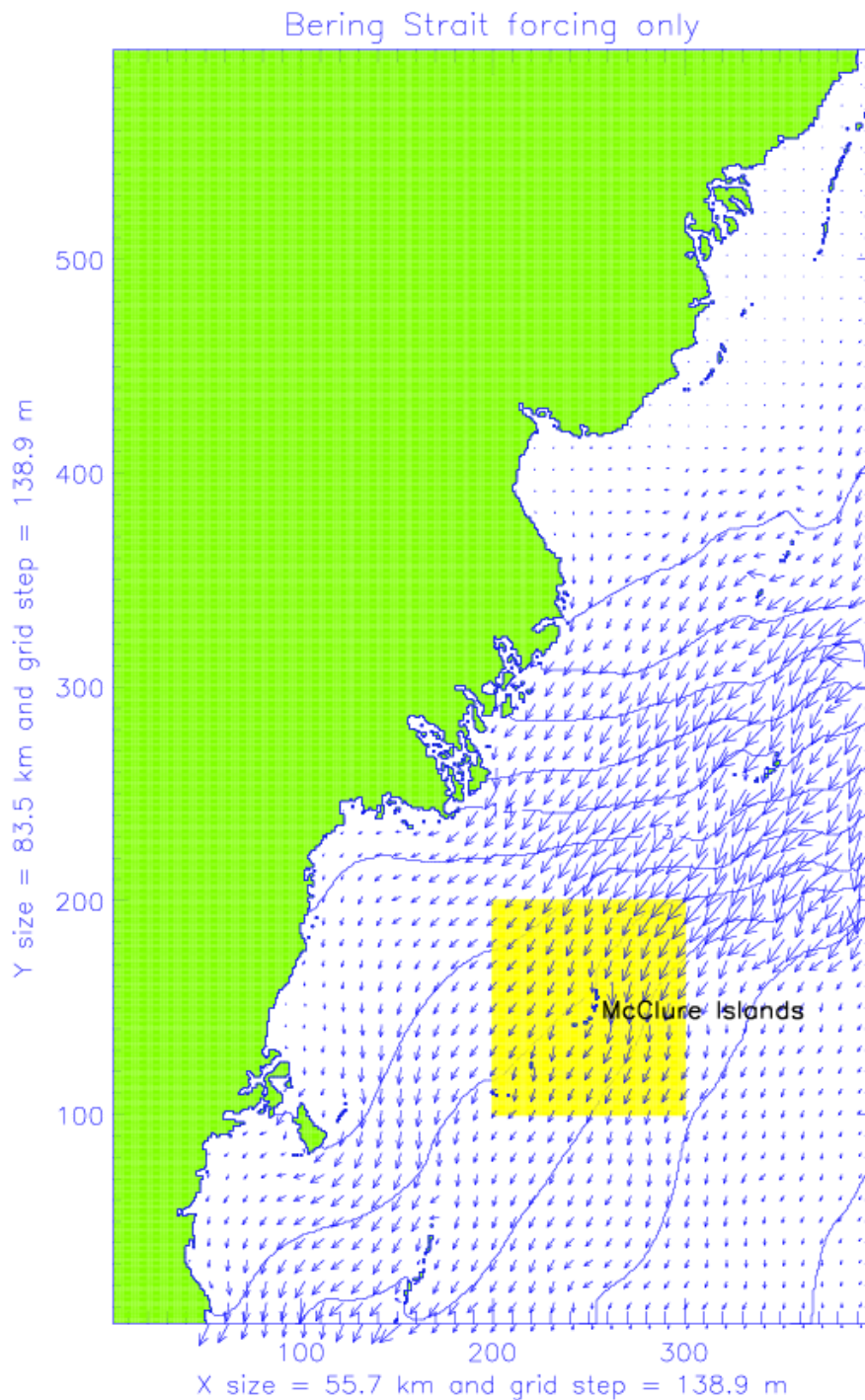


**Figure 5** Circulation and sea surface height contours (cm) in the high resolution model domain under Bering Strait inflow forcing only. Maximum vector velocity is 15 cm/s.

### 3.2.1. Permanent barotropic component

The pressure gradient between the Pacific and Atlantic Oceans is responsible for a system of permanent barotropic currents or a through-flow from the Pacific Ocean to the Atlantic Ocean which originates in the Bering Strait. The Bering Strait water transport is approximately 1 Sv ( $10^6 \text{ m}^3 \text{ s}^{-1}$ ). This transport changes seasonally. In winter it is approximately 0.7-0.8 Sv due to

strong eastern winds blocking the Bering Strait inflow. In summer when wind is weak this water flow is approximately 1.3-1.5 Sv [Coachman et al., 1976]. We have simulated this current system employing both the coarse and high resolution models. These patterns of barotropic currents are shown in Figures 4 and 5. From these figures one sees that the water velocities associated with the sea level gradient (hereafter Bering Strait Inflow, “BSI”) are relatively small but are close to the sediment threshold for initial motion (Figure 1). This means that there is no sediment transport associated with the mean BSI and additional forces are needed to start sand transport in this region.

### 3.2.2. *Wind-induced motions*

Among the mostly important factors is wave-generated sediment transport. This factor was identified as the strongest one for the Beaufort Sea region by Hill et al. [1989]. This forcing and its results are discussed in chapter [XXX] of this report.

The second important and prevailing factor which can generate strong currents is wind. Wind-driven circulation and storm surges in the Beaufort Sea have been a subject of numerous studies (Hunkins [1965], Harper et al. [1988], Henry [1975, 1984], Henry and Heaps [1976], Reimnitz and Maurer [1978, 1979], Marsh and Schmidt [1993], Kowalik [1984], Denard et al., [1984], Mason et al., 1995). Figure 6 (Brunner et al., 2004) shows several storm tracks for the Beaufort Sea region impacting significantly the Barrow community and the Beaufort Sea coastline.

### 3.2.3. *Storm climatology*

Maximum surge elevation with an approximate 100-year return period in the Tuktoyaktuk region is 2.4 m (Harper *et al.*, 1988). In the eastern Beaufort Sea the disaster storm was observed in 1963 (Brunner et al., 2004) causing significant erosion and flooding of the coastal environment. The storm “moved over 200,000 cubic yards of sediments, which is equivalent to 20 years’ normal transport” (Hume and Schalk, 1967:86). This conclusion was based on comparison of the estimated sediment transport during the storm surge and the accumulated transport over the years 1948 to 1962. The resulting coastline changes included shoreline retreat with a steepening and increase in the elevation of the beaches. The bluffs on the southern edge of Barrow retreated as much as 10 feet during this storm, exposing large ice masses that subsequently melted, causing some further shoreline collapse (Hume and Schalk, 1967). In the Arctic, warming of the climate leads to thaw of the permafrost, which destabilizes the coastline and makes it more vulnerable to both normal sediment transport and storm-induced transport.

Hudak and Young [2002] have investigated the storm climatology of the Southern Beaufort Sea for the 1970 to 1995 time period for the months of June to November inclusive. On the average, there were 14 storms per storm season, with a standard deviation of 5. The years 1976 to 1982 were the most stormy with an average of 19 storms per storm season. They concluded: “There was no discernable trend in the storm frequency over the 25-year period. By month, October had the highest storm frequency, July the lowest. There was an indication that Pacific storms have become less frequent in recent years.” Also, there was a decrease in the percentage of Arctic storms associated with strong cold air outbreaks.

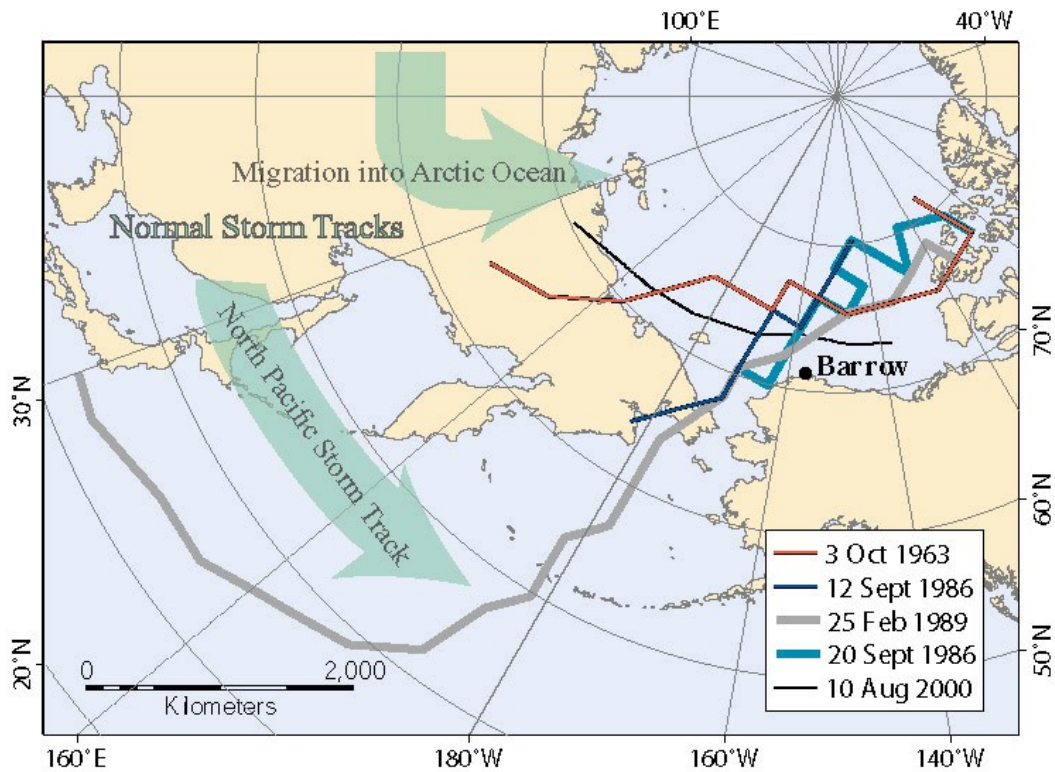


**Figure 6. Normal and Selected Storm Tracks Near Barrow (adapted from Brunner et al., 2004).**

Atkinson [2005] estimated storm event statistics for the open-water season (June–October) based on the data extracted from the terrestrial-based observational record throughout the circumpolar coastal regime (see Figure 7 for his region under research) over the period 1950–2000. In this study, the Chukchi sector exhibited large storm power values (defined as  $\text{speed}^2 \cdot \text{duration}$ ). Storm counts declined from 1950 to 1970, shifted rapidly from 1970 to 1974 to a level of greater mean activity and greater inter-annual variability, and declined after 1988. The Beaufort Sea region exhibited similar statistics but with less power values. Figures 8-9 adapted from Atkinson [2005] show statistics of storm winds in the Beaufort Gyre region (zone 6 in Figure 7) and characterize number of observed storms, their distribution in seasonal cycle and information about maximum winds and their duration.

Concluding with a description of the wind and storm surge climatology below (Figures 10 and 11) we show some results of numerical simulations characterizing theoretically possible extreme sea level heights along arctic coastlines under influence of direct wind forcing with a maximum possible wind fetch. A 2-D 13.89 km horizontal resolution vertically integrated coupled ice-ocean barotropic model developed by Proshutinsky (1993) was used to investigate the above formulated problem. This model is similar to the model described above (1-7) but is formulated for Cartesian coordinates on a stereographic map projection of the entire Arctic Ocean. This model does not have thermodynamics, sea ice thickness is fixed and corresponds to the mean climatic conditions (Proshutinsky and Johnson, 1997), and sea ice concentration is prescribed monthly from observations. The sea ice dynamics includes internal ice forces introduced by Rothrock (1975). The model was fully tested and calibrated against observed sea level time series along Siberian coast line and sea ice drift data from the International Arctic Buoy program (IABP, <http://iabp.apl.washington.edu/>) in Proshutinsky (1993) and Proshutinsky and Johnson (1997). This model in slightly different formulation (without atmospheric forcing) was used to simulate arctic tides (Kowalik and Proshutinsky, 1994). It also was used to investigate and predict storm surges in the Arctic Ocean

(Proshutinsky, 1993) and it has been employed as operational at the Arctic and Antarctic Research Institute (St. Petersburg, Russia) to predict sea ice conditions and sea level variability in the Arctic Ocean ([http://www.aari.nw.ru/clgmi/forecast/fc\\_2.html](http://www.aari.nw.ru/clgmi/forecast/fc_2.html)).

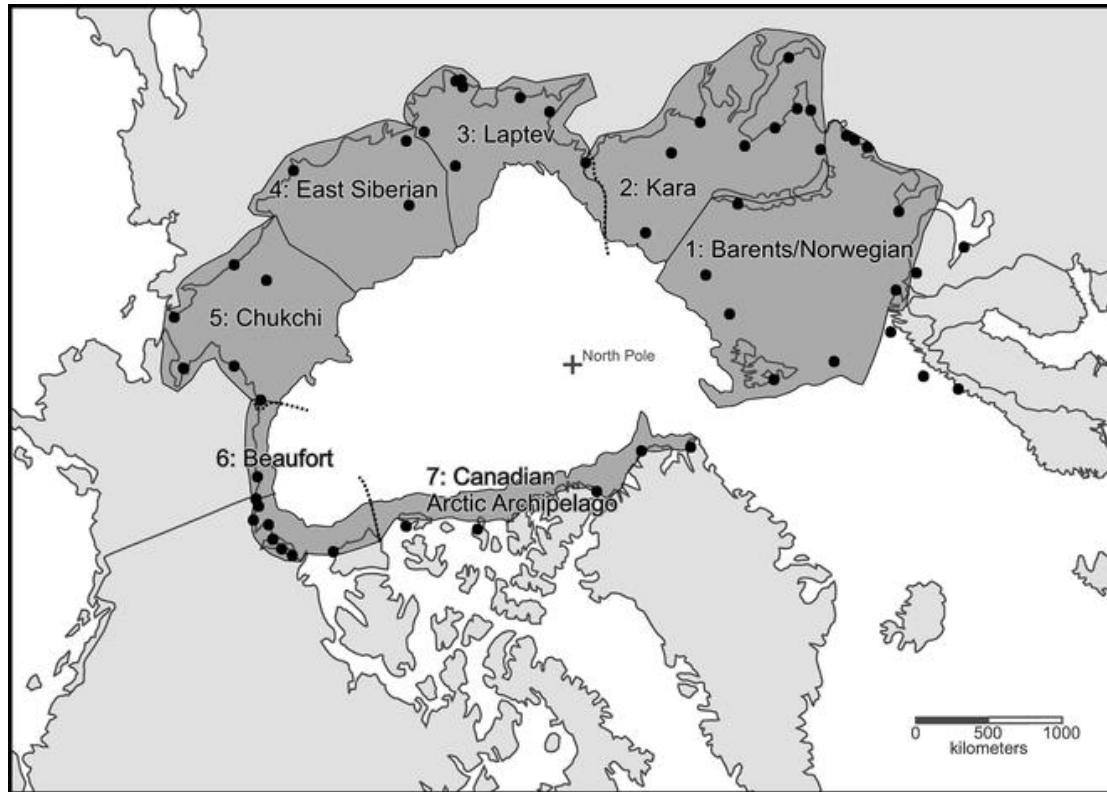


**Figure 7.** The circum-polar region. Sectors identified by the Arctic Coastal Dynamics project are identified as *grey zones*. Minor modifications adopted in this report are indicated with heavier *dashed lines*. Station locations are indicated by *black dots*. In some cases, two stations are located very close together and appear as *one dot* (courtesy of David Atkinson [2005]).

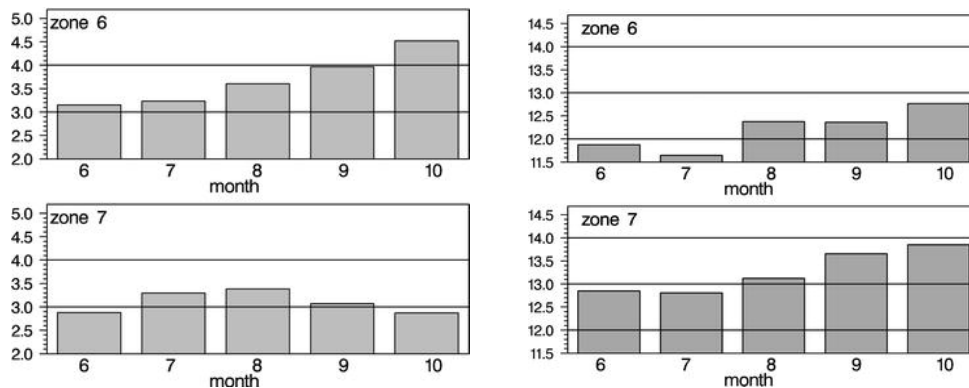


**Figure 8** Left: Mean annual storm event counts by month and right: Mean storm maximum wind speed (m/s) by month for the Beaufort Sea region (zone 6) and North of Greenland (zone 7). Adapted from Atkinson [2005].

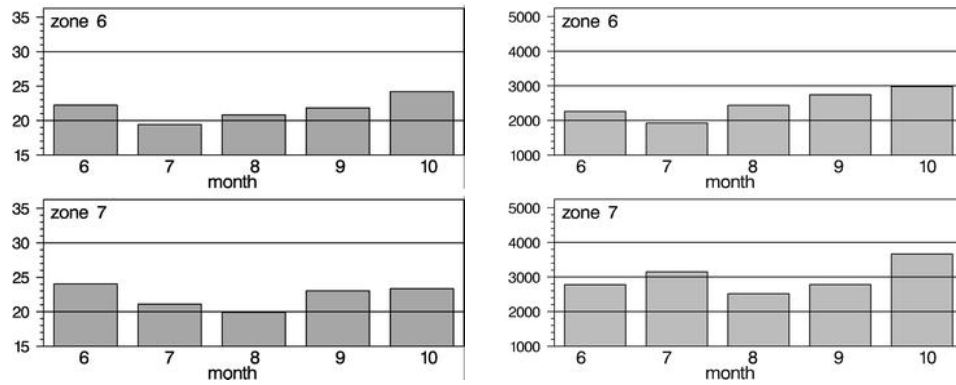


**Figure 9 Left: Mean duration of core winds (hours) and Right: Mean storm power (speed<sup>2</sup>\* duration) by month for the Beaufort Sea region (zone 6) and North of Greenland (zone 7). Adapted from Atkinson [2005].**

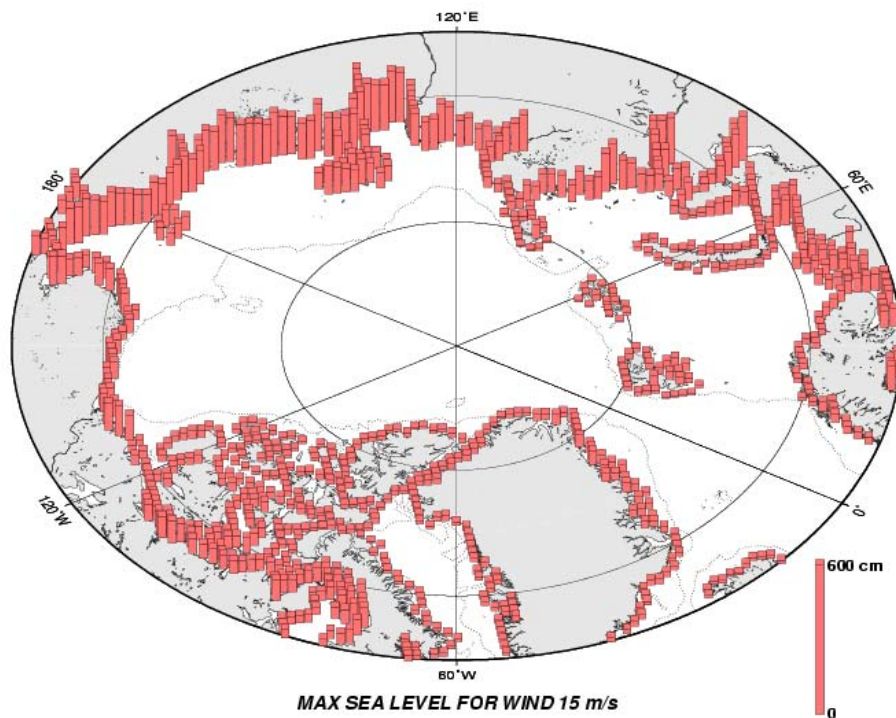


**Figure 10 Theoretically possible sea level elevations of sea level under forcing of winds of approximately 15 m/s.**

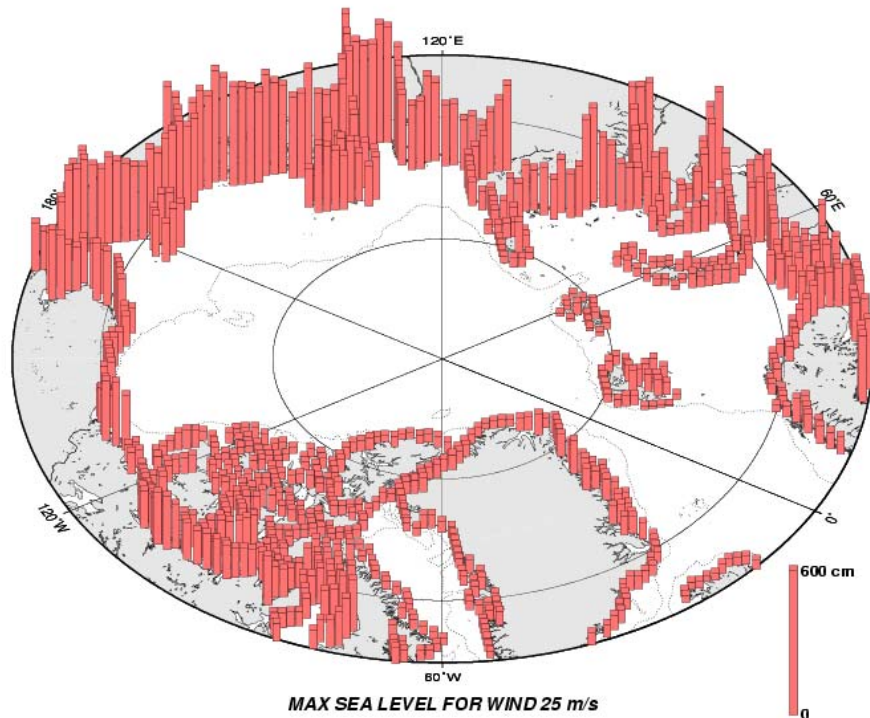


**Figure 11. Theoretically possible sea level elevations under forcing of wind of approximately 25 m/s.**

Initially, the dependent variables in the integration domain are taken as zero. Along the solid boundary we assume a no-slip condition for water transport and ice velocity. To solve equations with initial and boundaries conditions a semi-implicit finite-difference scheme with central differences on Arakawa C grid was employed.

The model was forced by winds from 5 to 30 m/s each with 24 directions (0, 15, 30, ..., 345, 360) and a duration providing the maximum sea level rise at every grid point along coastline. At the open model boundary in the North Atlantic we prescribed radiation conditions.

Figures 10 and 11 show expected maximum storm surge heights for winds of 15 m/s and 25 m/s respectively. One sees that the Beaufort Sea shelf is not “designed” for the extreme response on the extreme winds and its extreme storm surges are significantly weaker than storm surges expected along Siberian coastlines under the same winds. This is because the Beaufort Sea shelf is too narrow and relatively deeper than the Siberian shelf. On the other, the expected sea level rise along the Beaufort Sea coast can reach up to 2 meters under steady 15 m/s wind or up to 3.5 meters under winds of 25m/s. These numbers can be significantly higher in the real situations when sea level also changes due to changes in sea level atmospheric pressure (inverted barometer effect when the change in SLP of 1hPa results in the change of sea level of -1cm) and dynamically due to resonance conditions when the speed of atmospheric cyclone propagation coincides with the speed of ocean long-waves.

### *3.3. Model validation and calibration*

Among the recently observed storms in the Beaufort Sea region, the most powerful was a storm of August 2000. Some results of this storm simulation are shown in Figures 12-14. In order to simulate this storm we employed our 2-D coupled ice-ocean model with a resolution of 13.89 for the domain shown in Figure 2. The model was forced by BSI and NCAR/NCEP 6-hourly winds. At the right model’s boundary

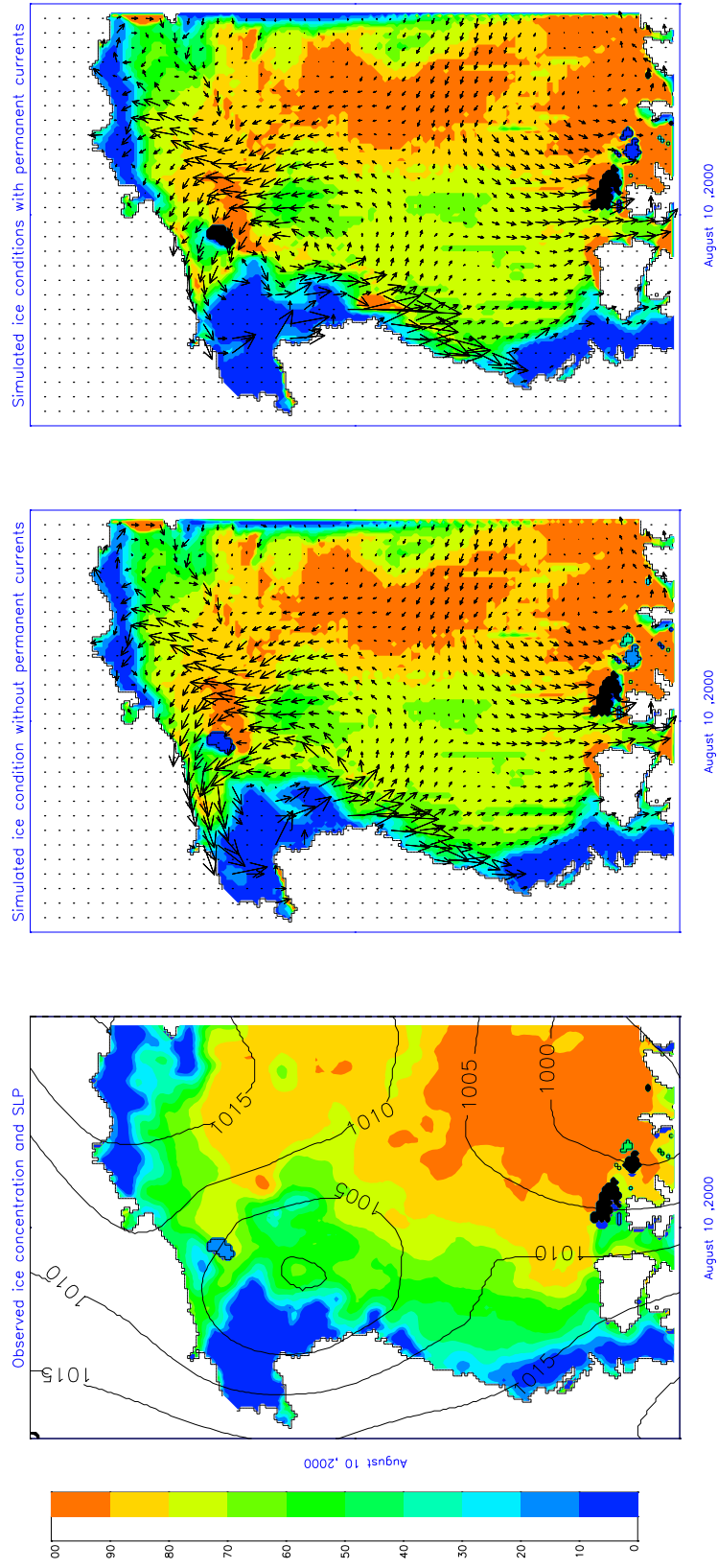


**Figure 12. Observed and simulated sea ice conditions on August 10, 2000.**

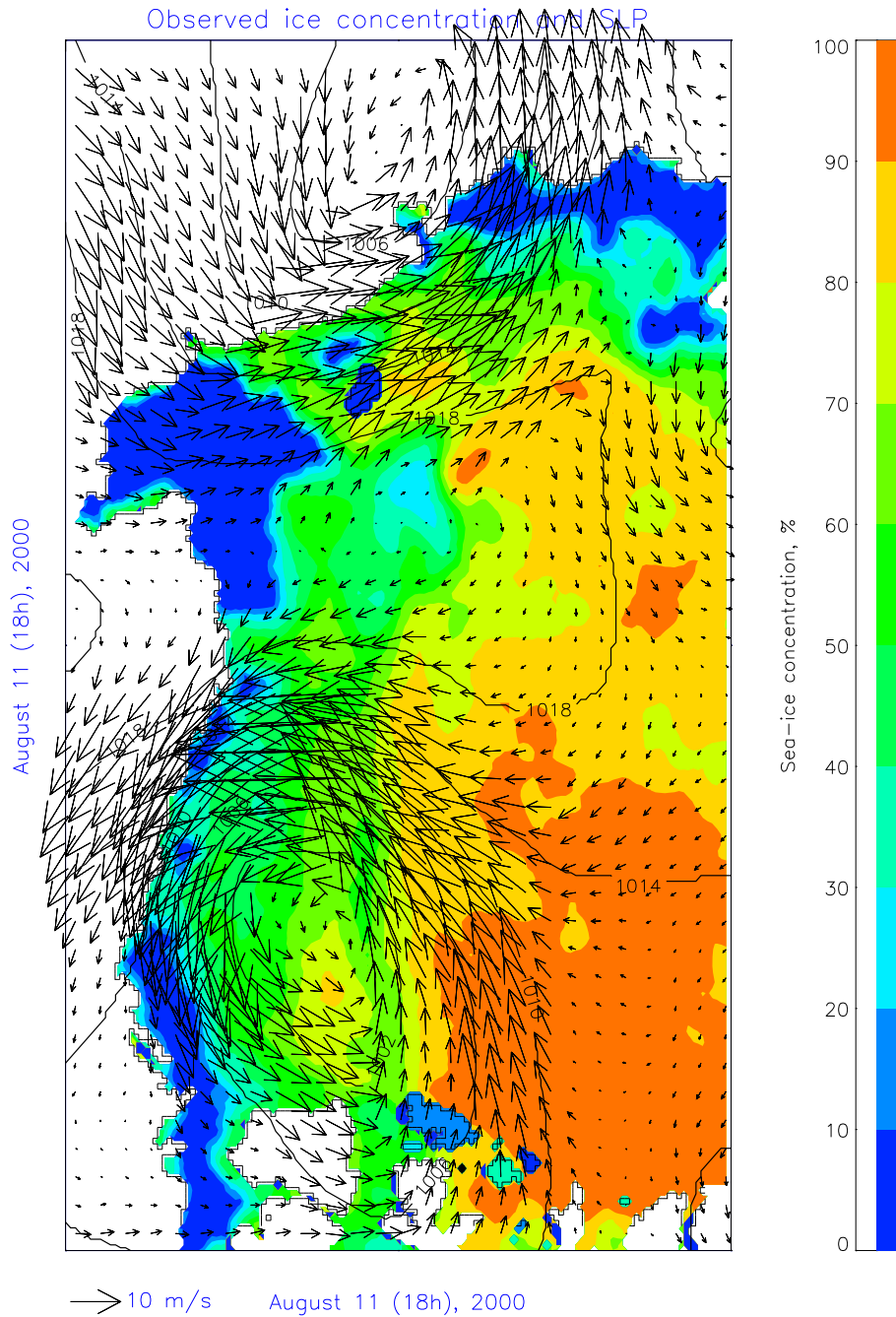


**Figure 13.** Sea ice drift, concentration and sea surface atmospheric pressure (SLP) distribution over the region on August 11 (18:00), 2000 when the maximum storm surge occurred in the region (see Figure 14).

we prescribed “radiation” conditions for ocean. The sea ice conditions were prescribed at all grid points of the model domain daily using NSIDC sea ice concentrations (Bootstrap Sea Ice Concentrations from Nimbus-7 SMMR and DMSP SSM/I, <http://nsidc.org/data/nsidc-0079.html>). Figure 12 shows some results of sea ice drift and concentration simulations for

August 10, 2000 and characterize storm conditions, changes in sea ice concentration and changes in sea level pressure (SLP) distribution. These conditions when maximum winds were observed are also shown in Figure 13.

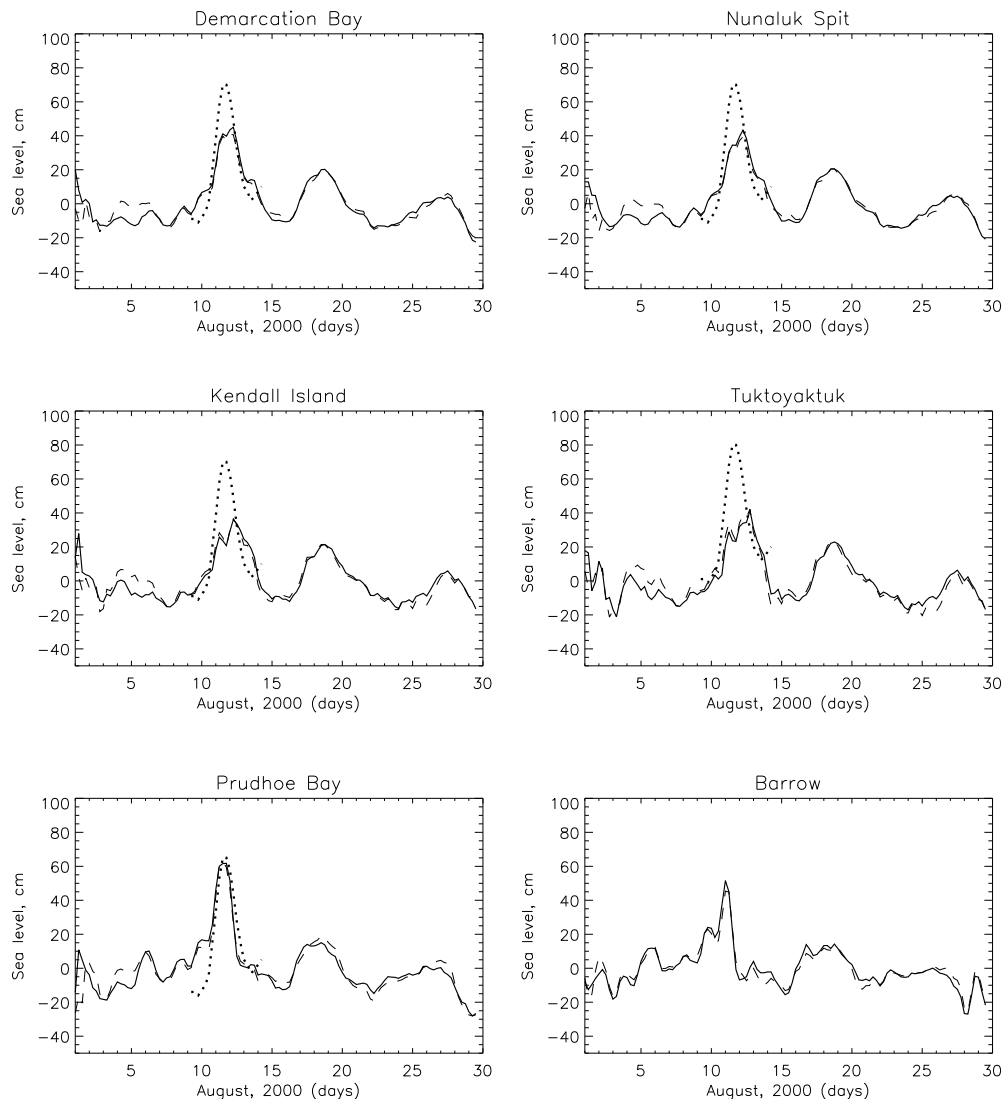


**Figure 14. Observed (dotted) and simulated (dotted/dashed: different experiments) sea level variability at coastal stations in August 2000.**

In order to validate and to calibrate our model we have used sea level observations collected by Steve Solomon from the *Natural Resources Canada, Bedford Institute of Oceanography, Dartmouth* (personal communications). The results of comparison of observed and simulated sea level heights at 8 coastal stations are shown in Figure 14. There is a very good correspondence between the observed and calculated sea level at Prudhoe Bay station but calculations at other stations underestimate sea level rise for this event. The major problem of this is the NCAR/NCEP winds which underestimated real winds observed in the region. Also 6-hourly winds and coarse resolution of the NCAR/NCEP product (2.5 degrees) are not able to reproduce peaks in forcing and exact trajectories of polar lows. But this exercise has allowed us to tune better our major model parameters regulating wind stress calculations, stresses between ice and ocean and parameters responsible for the ocean bottom and lateral friction.

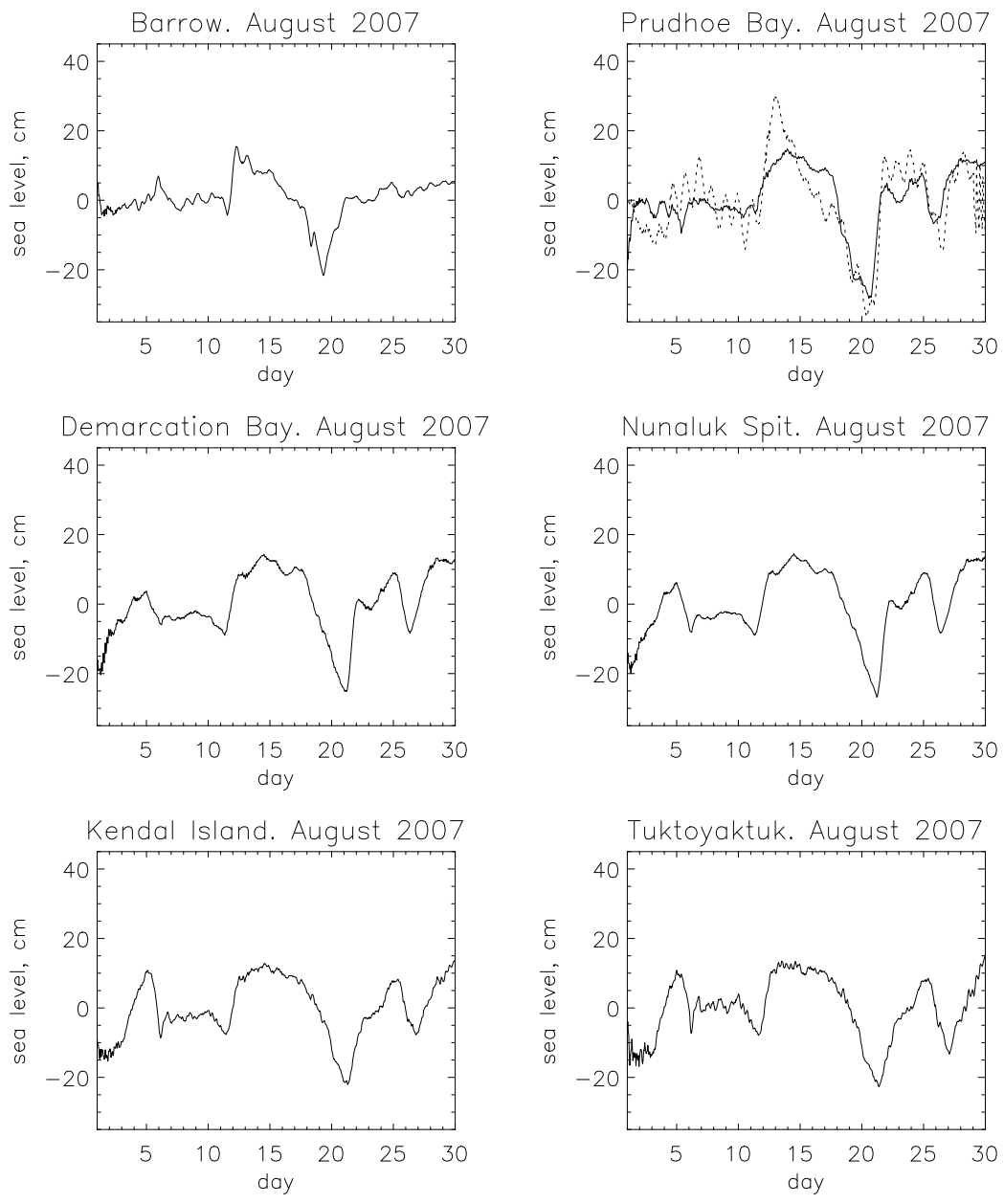


Figure 3. Simulated (solid line) and observed (dotted line) sea level variability in August, 2007

**Figure 15 Sea level variability at coastal stations in the Beaufort Sea (see Figure 2) in August, 2007. Solid lines depict simulated and dotted lines – observed sea level.**

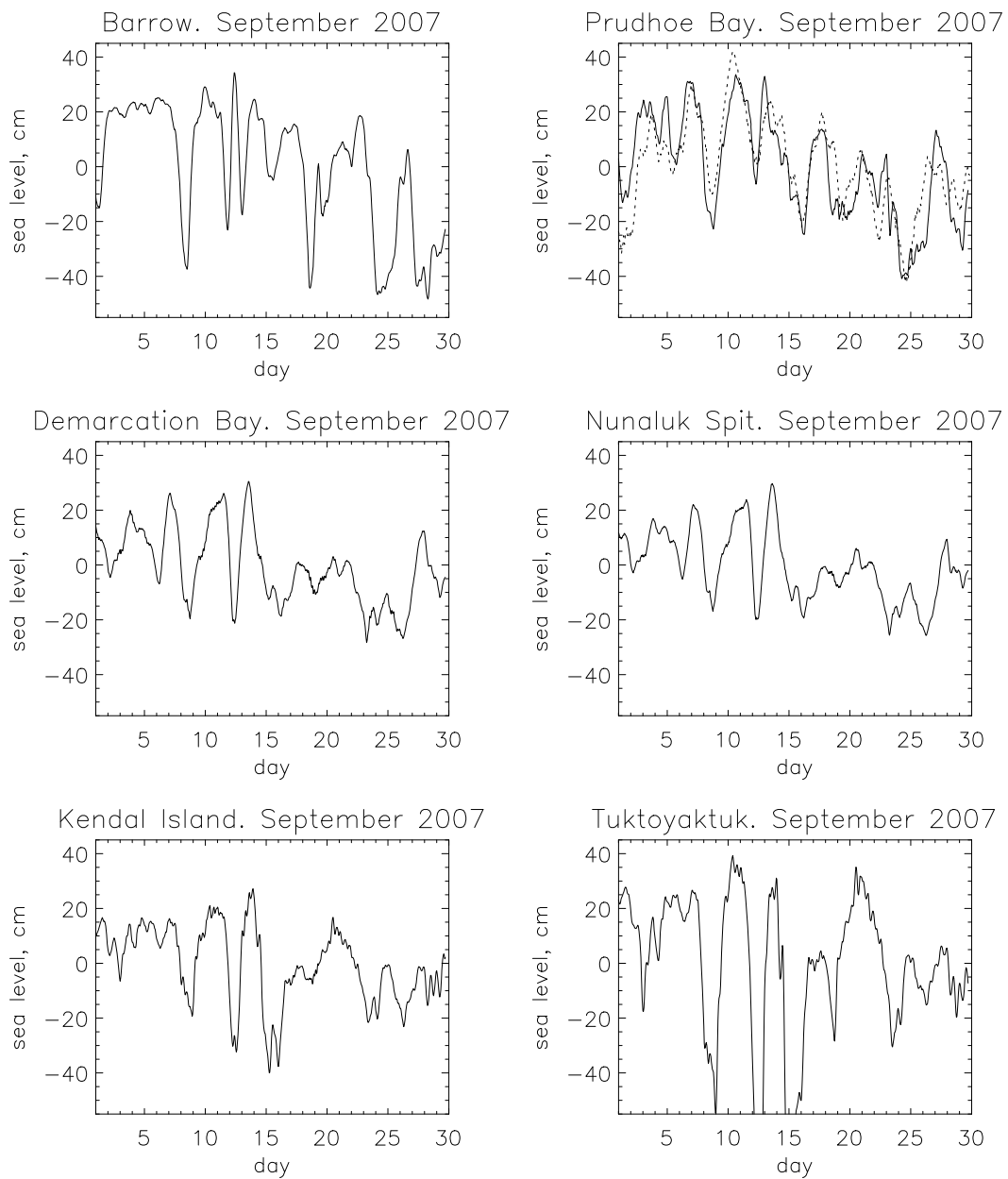
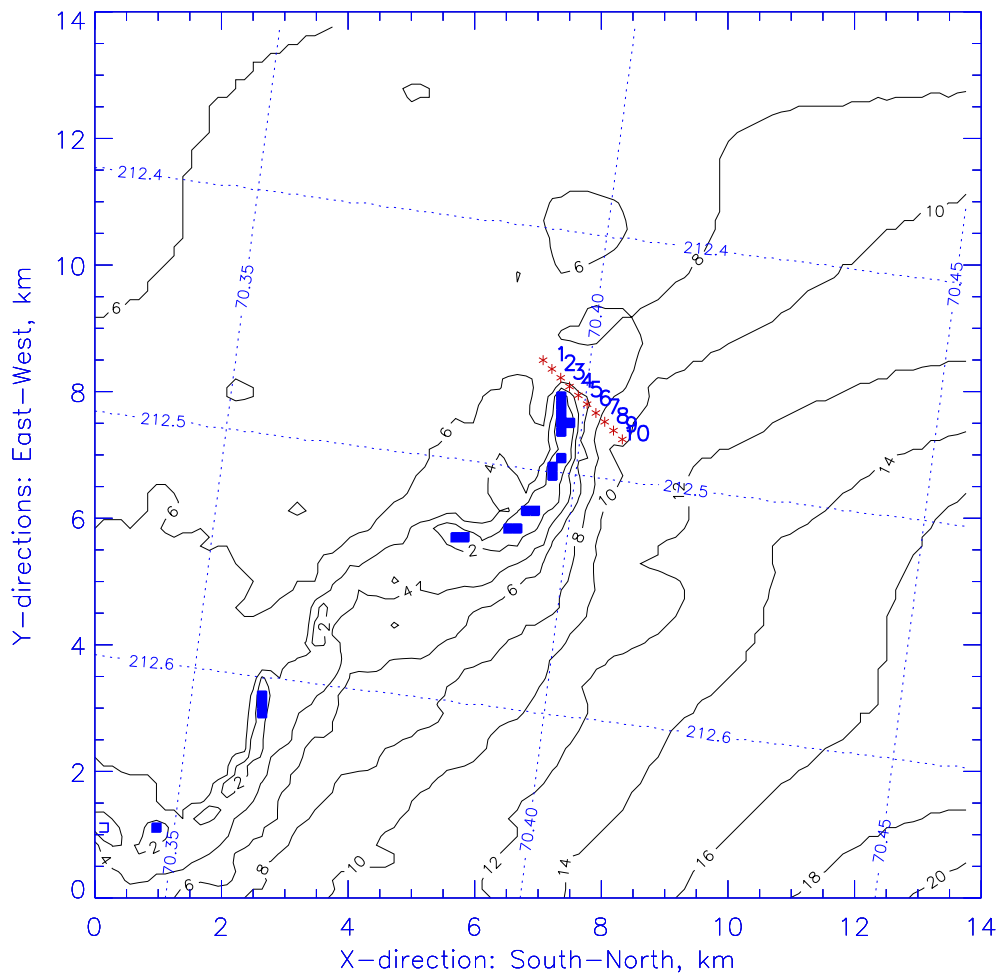


Figure 4. Simulated (solid line) and observed (dotted line) sea level variability in September, 2007

**Figure 16 Sea level variability at coastal stations in the Beaufort Sea (see Figure 2) in September, 2007. Solid lines depict simulated and dotted lines – observed sea level.**



**Figure 17. Bathymetry (black lines, m) surrounding McClure Island chain as a fragment of the high resolution model (see yellow rectangular in Figure 3). This region is used in investigations of sediment transport around McClure Islands. Red stars and blue numbers indicate locations of 10 particles released in the model in proximity to the Narwhal Island (located at the north-western end of the chain) for sediment transport studies.**

### 3.4 Sediment transport

We simulated wind-driven water motions and sediment transport in combination with BSI forcing for August and September 2007 conditions. We have carried out two-step simulations. First, we have run our coarse resolution model under influence of 6-hourly winds derived from NCEP/NCAR Reanalysis project. These calculations were validated against observations of sea level variability at Prudhoe Bay. Results of these simulations are shown in Figures 15 and 16 for August and September, 2007 respectively. There is a good agreement between observed (de-tided) and simulated sea levels in Prudhoe Bay. This experiment has allowed us to continue simulations with our high resolution model (138.9 m, Figure 3) which was forced by currents prescribed at open model boundaries at hourly intervals (derived from our coarse resolution model, Figure 2) and by local winds.

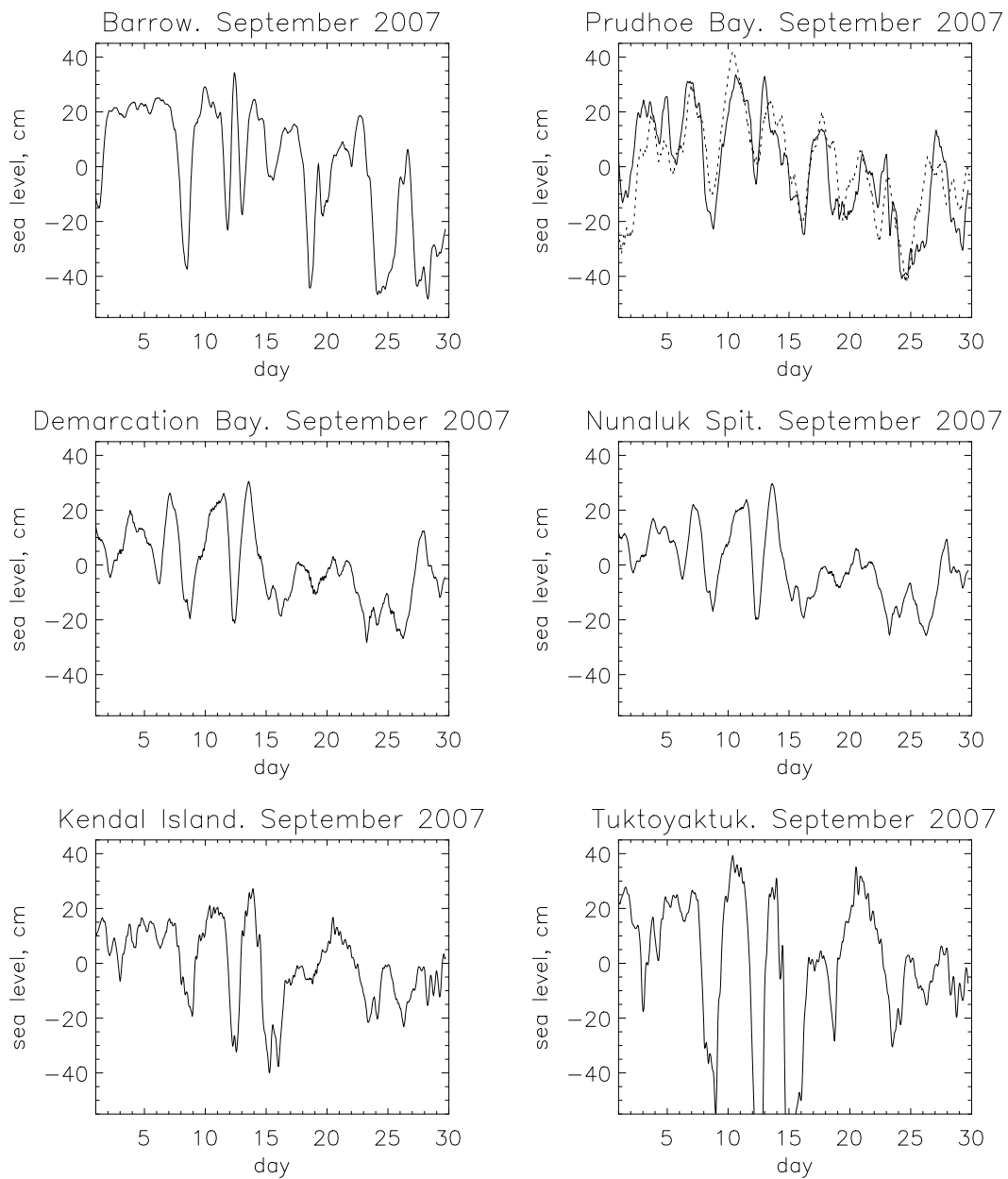
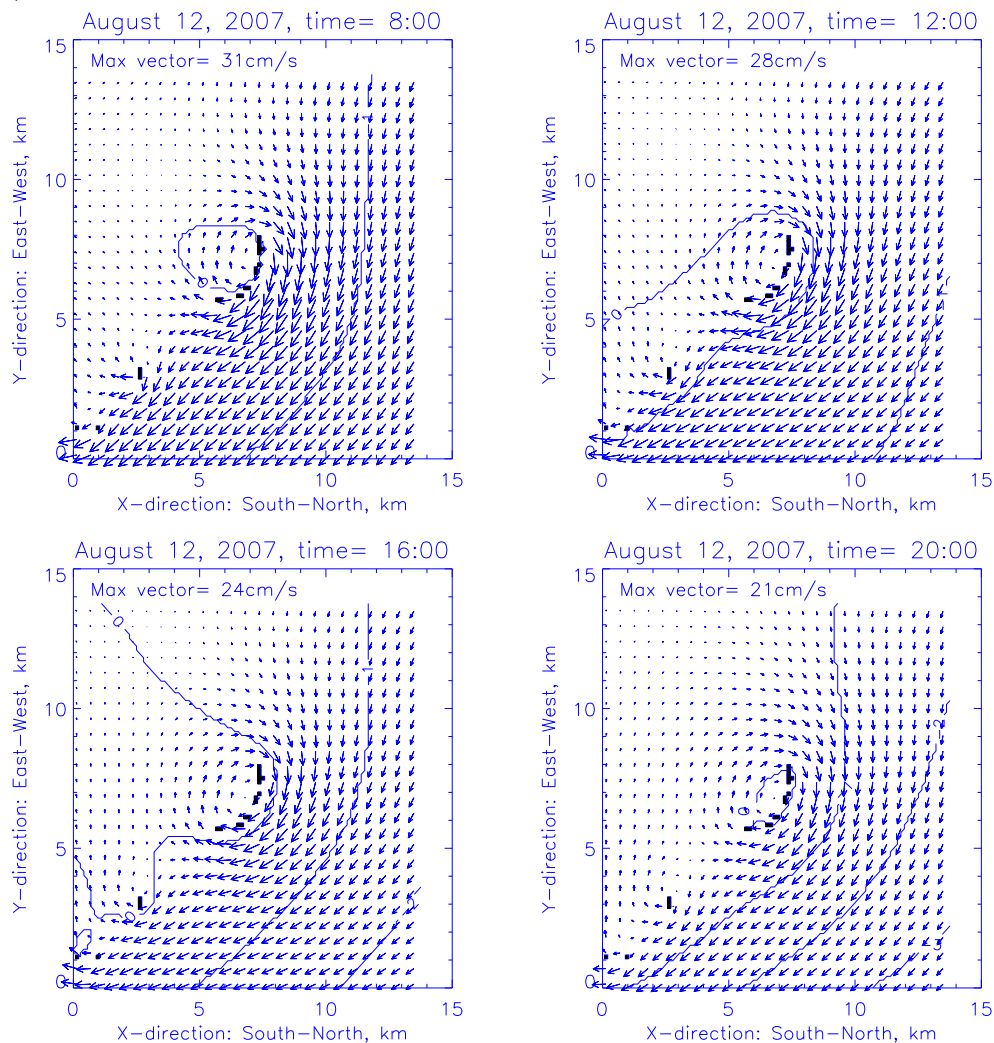


Figure 4. Simulated (solid line) and observed (dotted line) sea level variability in September, 2007

**Figure 16 Sea level variability at coastal stations in the Beaufort Sea (see Figure 2) in September, 2007. Solid lines depict simulated and dotted lines – observed sea level.**

We investigate sediment transport in the closed vicinity of McClure Islands limited by a region shown in Figure 17 (see also yellow rectangular in Figure 3). Figure 17 also shows initial locations of 10 particles used for sediment transport simulations.

Water circulation patterns and sediment transports for two cases corresponding to the periods of sea level rise (August 12, 2007) and sea level decrease (August 18, 2007) situations are shown in Figures 18 – 23 below. During sea level rise all water particle trajectories around McClure Islands are clockwise (Figure 19 and Figure 20). If currents are strong enough (see equation 14) this circulation will redistribute sediments as shown in Figure 20 and 21. We speculate that suspended sediments (very small size) are moved with a speed of ocean currents and their trajectories are shown in the upper panel in Figure 20. Some of these particles are trapped by the island but others can easily leave the region depending on the initial particle position (distance from island, see Figure 17). A different regime displays the motion of the grain particles of sand size. These particles can be transported both as the suspended material or/and the bed load. The motion of the bed load particles is limited by  $u_b$  (eq. 14).



**Figure 18 Water circulation around McClure Islands during sea level increase and clockwise circulation regime. Water currents converge (clockwise circulation), sea level goes up and sediments are redistributed as shown in Figures 19 and 20.**

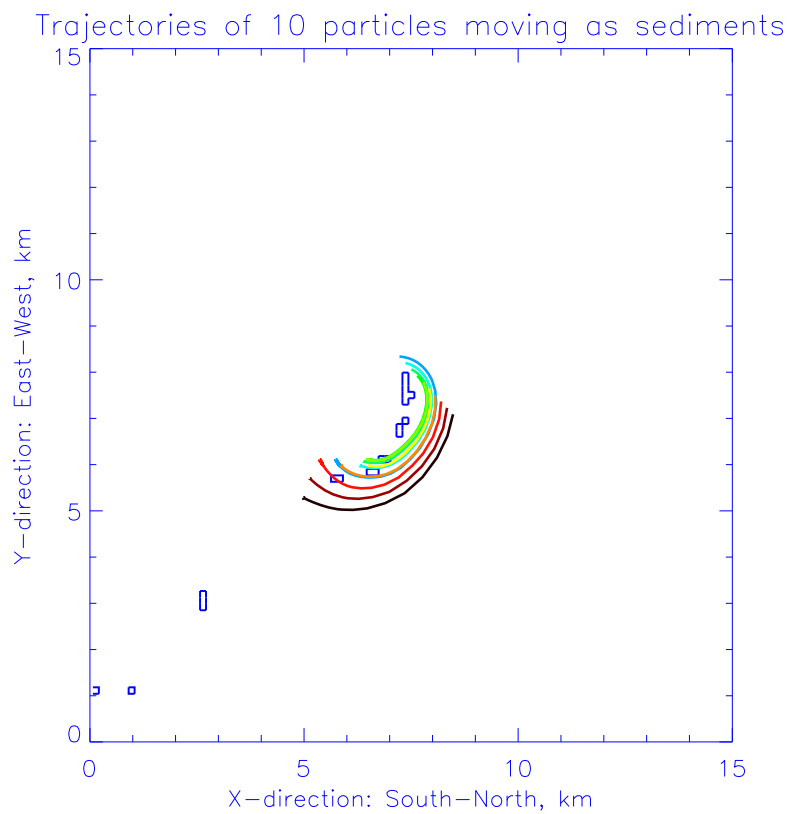
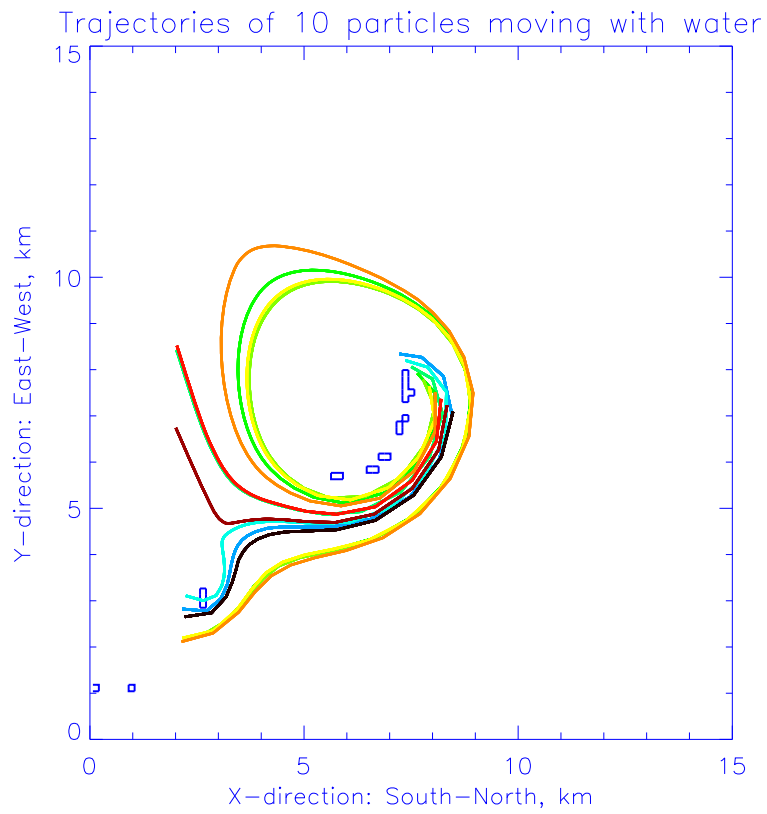


**Figure 19 Particle motion around McClure Islands during clockwise circulation regime. See also Figure 17 for initial locations of 10 particles shown here. Water currents converge; sea level rises and sediments move out from their initial location and are accumulated in the south-east end of the McClure Island chain (see also Figure 20). Top**

panel shows particles moving with water velocities and bottom panel shows trajectories of particles moving with the bed load sediment transport.

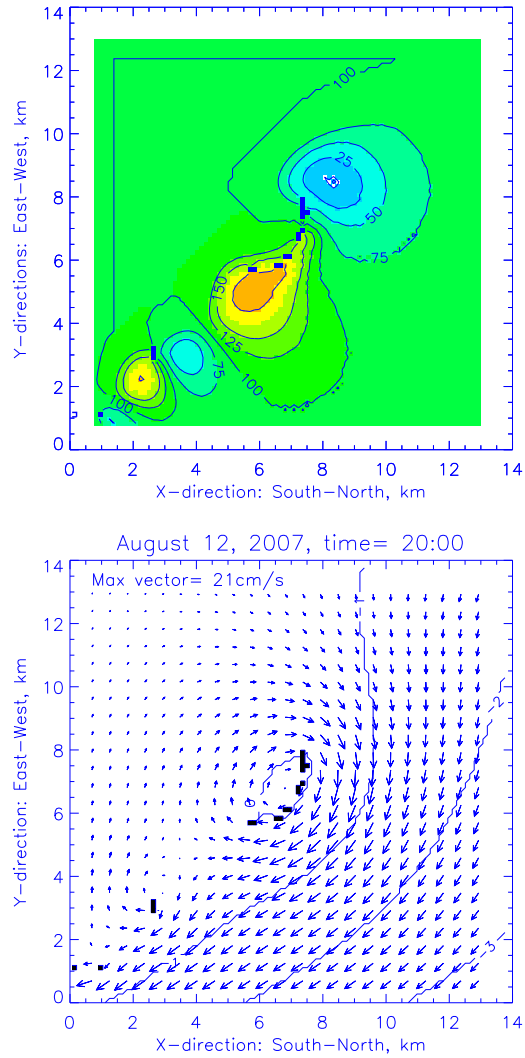


**Figure 20 Top panel: Conditional redistribution of sediments with bed load transport around McClure Islands during clockwise circulation (rising sea level). Higher numbers show region with accumulation of sediments. Bottom panel: clockwise circulation regime on August 12, 2007.**

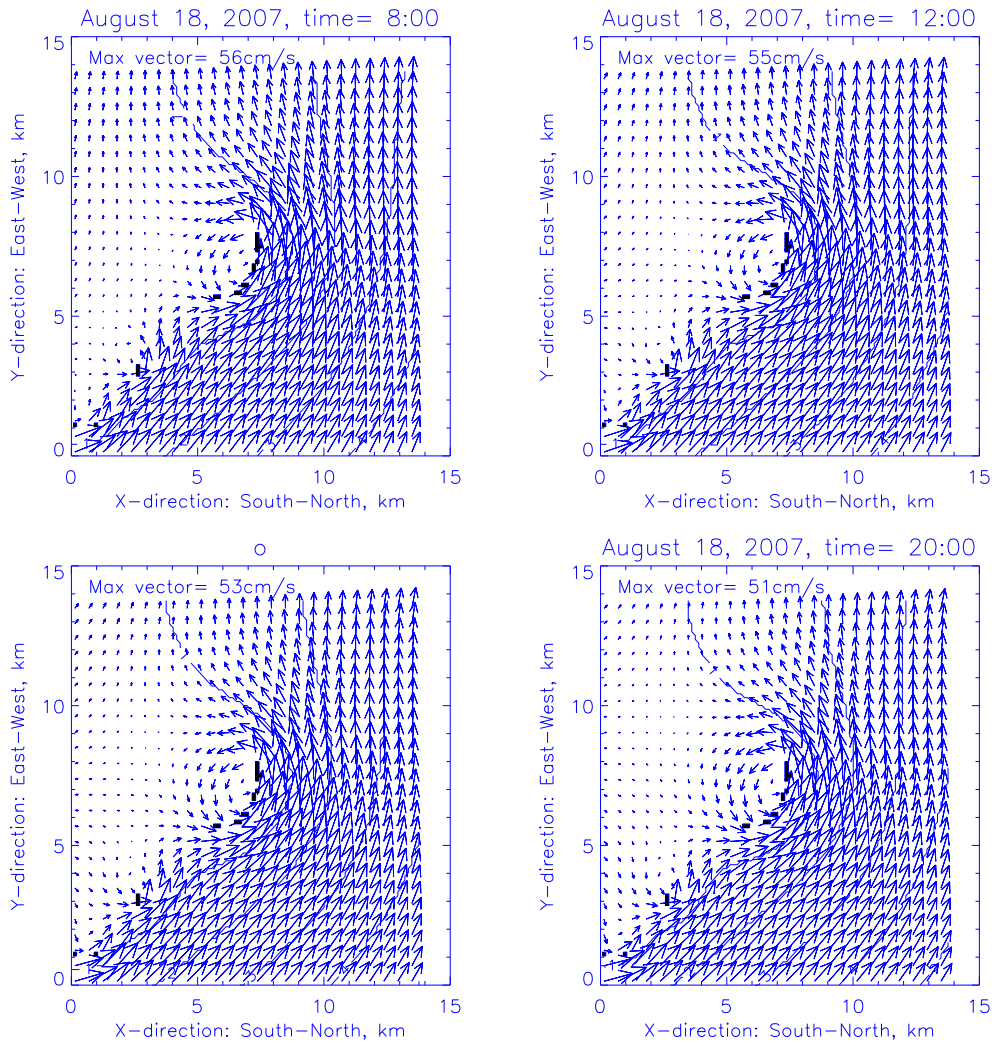


**Figure 21 Water circulation around McClure Islands during sea level decrease and counterclockwise circulation regime. Water currents diverge (counterclockwise circulation), sea level goes down and sediments are redistributed as shown in Figures 22 and 23.**

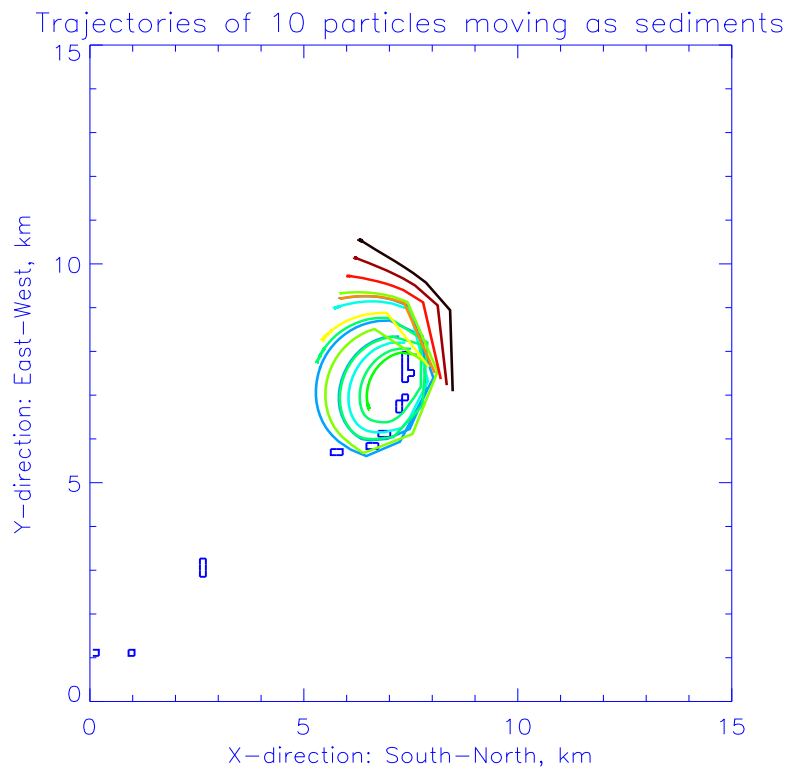
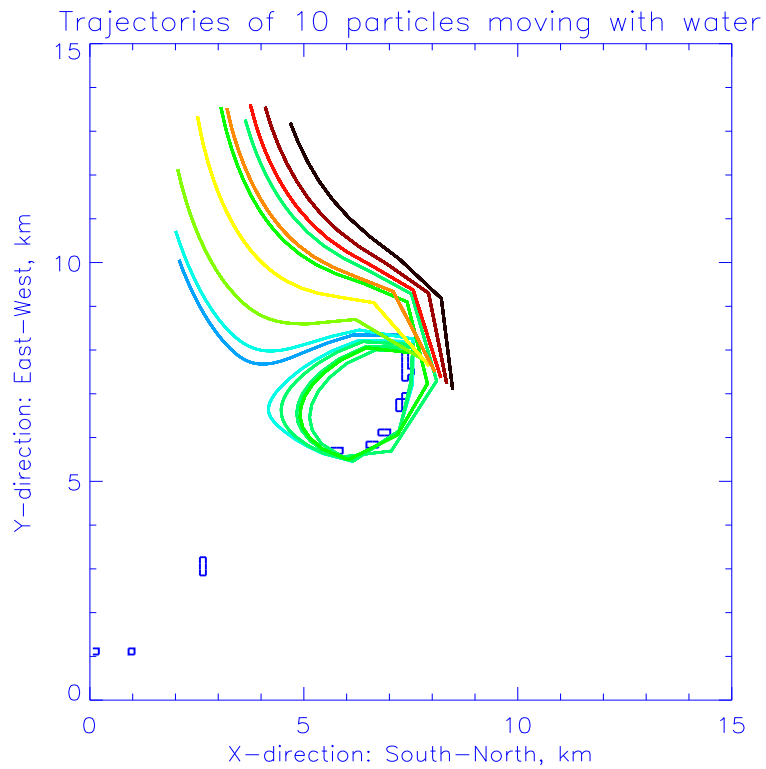


**Figure 22 Particle motion around McClure Islands during counterclockwise circulation regime. See also Figure 17 for initial locations of 10 particles shown here. Water currents diverge; sea level goes down and sediments move out from their initial location but then returned back and are accumulated in the north-west end of the McClure Island chain (see also Figure 20). Top panel shows particles moving with water velocities and bottom panel shows trajectories of particles moving with the bed load sediment transport.**

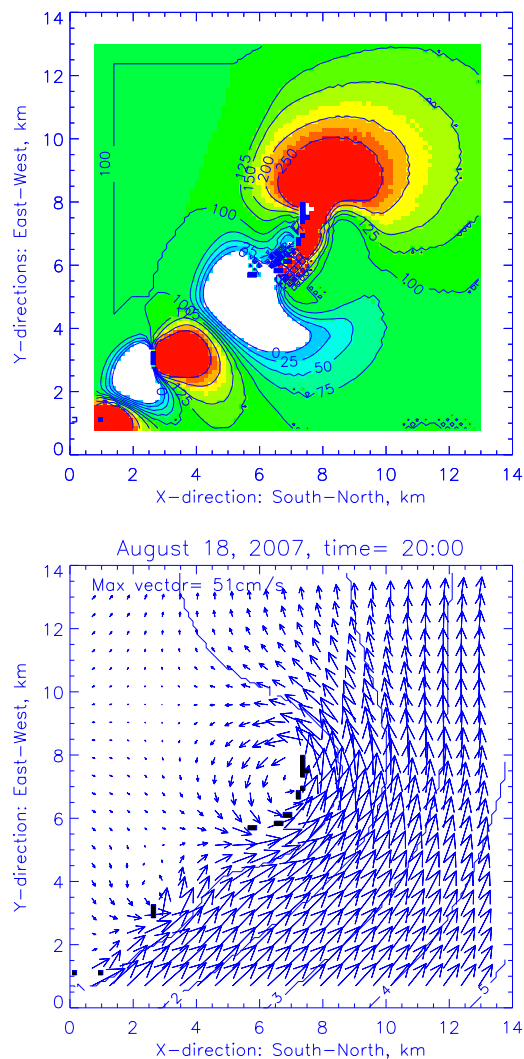


**Figure 23 Top panel: Conditional redistribution of sediments around McClure Islands during counterclockwise circulation (decreasing sea level). Higher numbers show region with accumulation of sediments. White region shows “negative” concentration of sediments indicating that there are no more sediment available for transport in this area.**

The opposite situation is shown in Figures 20, 21 and 23. These graphs show the prevailing counterclockwise motion of water and sediments around McClure Islands in the typical situation when sea level in the region is rapidly decreasing on August 18<sup>th</sup>, 2007. The simulated currents for this case are stronger than for case of clockwise motion and both the water and sediment particle trajectories are extended and particles travel longer distances than in the case of clockwise motion.

During the clockwise circulation regime the sediments tend to move from the north-west to south-east relative to the island chain and are accumulated there. During the counterclockwise circulation regime the opposite situation occurs.

In general, in the presence of the permanent currents associated with a pressure gradient between the Pacific and Atlantic Oceans the prevailing direction of sediment transport in the vicinity of McClure Islands would be from northwest to southeast assuming that the probability of occurrence of the counterclockwise circulation is balanced by the probability of

occurrence of clockwise motion. But in order to solve this problem a long-term integration is needed (at least during a typical seasonal cycle). Here we have studied only wind-driven and permanent barotropic circulation forcing but other factors have to be taken into account as well for the final conclusion about prevailing rate and direction of the sediment transport in the vicinity of McClure Islands.

#### 4. Conclusions and recommendations

- 1 We have developed a set of 2-D coupled ice-ocean models for the Arctic Ocean, Canada Basin and the McClure Islands area with a different spatial and temporal resolution. The models were calibrated and validated based on the data from coastal stations and have demonstrated a good agreement between the observed and simulated sea levels.
- 2 Two major factors, potentially important for sediment transport were considered for analysis: permanent barotropic currents due to sea level gradient between the Pacific and Atlantic Ocean, and wind-driven circulation due to storm surges.
- 3 The roles of the permanent currents and wind-driven circulations (counterclockwise and clockwise island-trapped patterns characterizing different regimes of sea level change around the McClure Islands) were investigated in details.
- 4 A simple sediment transport semi-empirical model was applied as the first order approach to study the peculiarities of sediment motion around McClure Islands. Model results have shown that during the clockwise circulation regime the sediments tend to move from the north-west to south-east relative to the island chain and are accumulated at the south-eastern side of the chain. The region of Narwhal Island is devoid of sediments. During the counterclockwise circulation regime the opposite situation occurs. The sediments move from the south-east toward the north-west and are accumulated in proximity to the Narwhal Island.
- 5 As a follow up to the model study it is recommended that sediment transport in the vicinity of McClure Islands be estimated by the long-term simulation and with a careful model calibration based on:
  - A. 3-4 tide bottom mounted tide gauges are needed to cover sea level variability and wave regime around McClure Islands to reproduce seasonal cycle and to validate the high resolution model results;
  - B. These gauges have to be accompanied by looking-up ADCPs to measure currents and their vertical structure. These data will be used to validate models and to better calibrate sediment transport models.
  - C. Ideally, the direct measurements of sediment transport are needed to verify simulation results.
  - D. Bottom studies are needed to assess the sediment transport associated with sea ice impact.

#### References:

- Atkinson, David E. (2005) Observed storminess patterns and trends in the circum Arctic coastal regime. *Geo-Marine Letters* 25(2-3)
- Brunner RD, Lynch AH, Pardikes J, Cassano EN, Lestak L, Vogel J (2004) An Arctic disaster and its policy implications. *Arctic* 57:336–346
- Coachmen, L. K., K. Aagaard, and R. B. Tripp. 1976. Bering Strait: The regional physical oceanography. Univ. Washington Press, Seattle and London. 172 p.

- Denard, M. B., M. C. Rasmussen, T. S. Murty, R. F. Henry, Z. Kowalik, and S. Venkatesh. 1984. Inclusion of ice cover in a storm surge model for the Beaufort Sea, *Natural hazards*, v.2, N.2, 153-171.
- Harper JR, Henry RF, Stewart GG (1988) Maximum storm surge elevations in the Tuktoyaktuk region of the Canadian Beaufort Sea. *Arctic* 41:48–52
- Henry, R.F. 1975. Storm surges. Beaufort Sea Project Technical Report No. 19. Sidney, B.C.: Institute of Ocean Sciences. 41 p.
- Henry, R. F. 1984. Flood hazard delineation at Tuktoyaktuk. Fisheries and Oceans , Canadian Contractor Report of Hydrography and Ocean Sciences No. 19. Sidney, B.C.: Institute of Ocean Sciences. 28 p.
- Henry, R.F., and Heaps, N.S. 1976. Storm surges in the southern Beaufort Sea. *Journal of the Fisheries Research Board of Canada* 33:2362-2376.
- Hill, Philip R., Nadeau, Odette C. Storm-dominated sedimentation on the inner shelf of the Canadian Beaufort Sea, *JOURNAL OF SEDIMENTARY RESEARCH* 1989 59: 455-468
- Hudak D. R., J. M. C. Young: 2002: Storm climatology of the Southern Beaufort Sea, *Atmosphere-Ocean*, Volume 40, Number 2, 145-158.
- Hume JD, Schalk M (1967) Shoreline processes near Barrow, Alaska: a comparison of the normal and the catastrophic. *Arctic* 20:86–103
- Hunkins, K. L. 1965. Tide and storm surge observations in the Chukchi Sea. *Limnol. Oceanogr.*, 10, 29-39.
- Kowalik, Z. 1984, Storm surges in the Beaufort and Chukchi Seas. *JGR*, 89(11), 10,570-10,578.
- Kowalik, Z. and Proshutinsky, A., 1994, *The Arctic Ocean Tides*, in *The Polar Oceans and their role in shaping the global environment*, Geophysical Monograph 85, American Geophysical Union.
- Mason, O.K., Jordan, J.W., Plug, L., 1995. Late Holocene storm and sea-level history in the Chukchi Sea, *J. Coastal Res.*, Spec. Issue, 17, 173–180.
- Marsh, P., and T. Schmidt, 1993: Influence of a Beaufort Sea storm surge on a channel levels in the Mackenzie Delta, *Arctic* 46, pp. 35-41.
- Open University Course Team (1989) *Waves, tides and shallow-water processes*. Pergamon Press, 187pp.
- Proshutinsky, A. Yu., 1993. *Arctic Ocean Level Oscillations*. Gidrometeoizdat, St. Petersburg, 216 pp. (in Russian).
- Proshutinsky, A. Yu., and M. Johnson, 1997. Two circulation regimes of the wind driven Arctic Ocean. *Journal of Geophysical Research*, 102, 12,493-12,514.

Reimnitz, E., and Maurer, D.F. 1978. Storm surges in the Alaskan Beaufort Sea. United States Department of the Interior, Geological Survey, Open-File Report 78-593, Menlo Park, California. 26 p.

Reimnitz, E., and Maurer, D.F. 1979. Effects of storm surges on the Beaufort Sea coast. Northern Alaska. *Arctic* 32:329-344.

Rothrock, D. A.. 1975. The mechanical behavior of pack ice, *Annual Review of Earth Planetary Sciences*, 3, 317-342.

Zhou, J-F and Li, J-C (2005). Modeling storm-induced current circulation and sediment transport in a schematic harbor, *J. Waterway, Port, Coastal, and Ocean Engineering*, 131(1), 25-32.

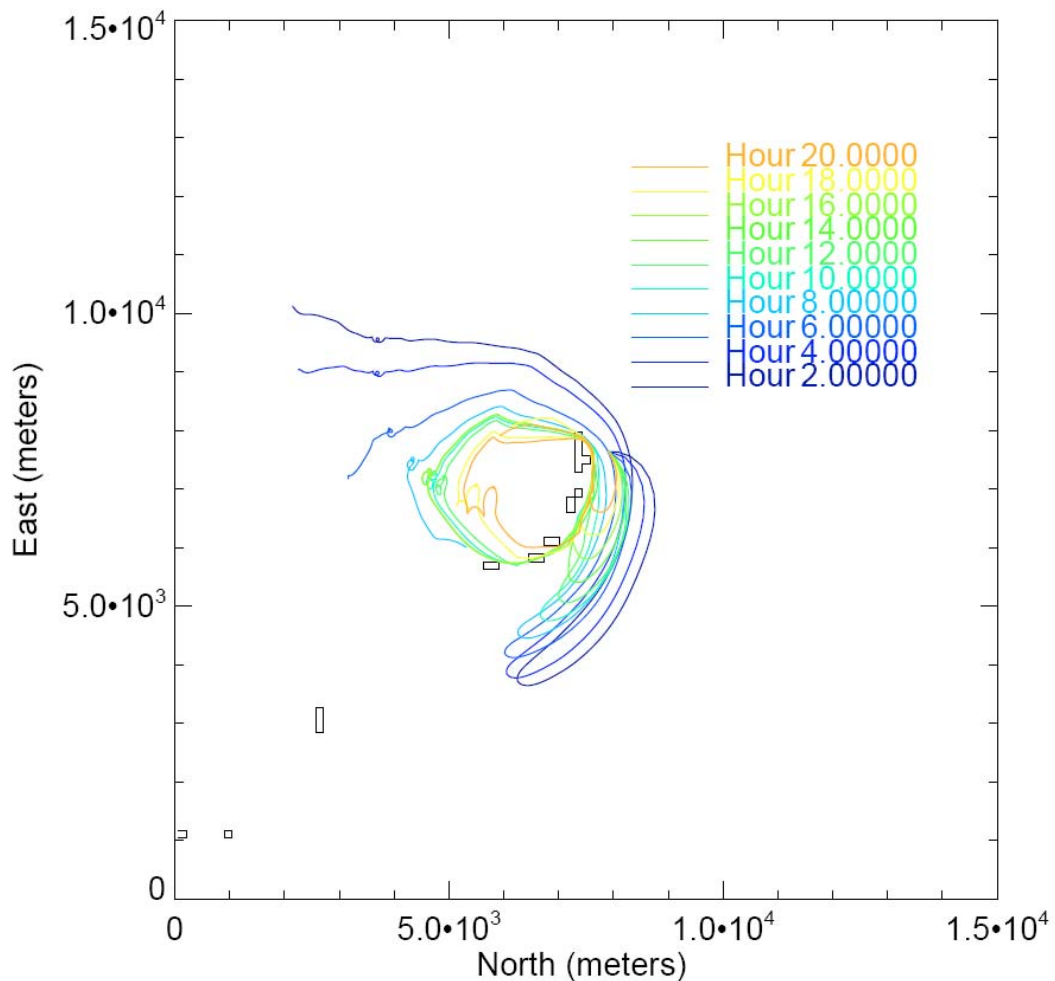


Figure Particle trajectories around McClure Islands during the period of sea level decrease (counter-clockwise circulation) in the region. Shown are trajectories of 10 particles released north of McClure Islands with a 2-hour interval.



### **The Department of the Interior Mission**

As the Nation's principal conservation agency, the Department of the Interior has responsibility for most of our nationally owned public lands and natural resources. This includes fostering sound use of our land and water resources; protecting our fish, wildlife, and biological diversity; preserving the environmental and cultural values of our national parks and historical places; and providing for the enjoyment of life through outdoor recreation. The Department assesses our energy and mineral resources and works to ensure that their development is in the best interests of all our people by encouraging stewardship and citizen participation in their care. The Department also has a major responsibility for American Indian reservation communities and for people who live in island territories under U.S. administration.